UPPSALA UNIVERSITET

Digital Comprehensive Summaries of Uppsala Dissertations from the Faculty of Medicine 1903

Peptide Receptor Radionuclide Therapy in Neuroendocrine Neoplasms

Aspects of tumour characteristics, receptor recycling and peptide mass

ULRIKA JAHN

ACTA UNIVERSITATIS UPSALIENSIS UPPSALA 2023

ISSN 1651-6206
ISBN 978-91-513-1714-4
URN urn:nbn:se:uu:diva-492855

Dissertation presented at Uppsala University to be publicly examined in Skoogsalen, ing 78/79 1 tr, Akademiska Sjukhuset, Uppsala, Friday, 31 March 2023 at 09:00 for the degree of Doctor of Philosophy (Faculty of Medicine). The examination will be conducted in Swedish. Faculty examiner: Docent Mona-Elisabeth Rootwelt-Revheim (Oslo University Hospital, Oslo, Norway).

Abstract

Jahn, U. 2023. Peptide Receptor Radionuclide Therapy in Neuroendocrine Neoplasms. Aspects of tumour characteristics, receptor recycling and peptide mass. *Digital Comprehensive Summaries of Uppsala Dissertations from the Faculty of Medicine* 1903. 96 pp. Uppsala: Acta Universitatis Upsaliensis. ISBN 978-91-513-1714-4.

Neuroendocrine neoplasm (NEN) can arise in any part of the body, but most commonly in the lungs, bronchi, and the gastrointestinal tract including the pancreas. They combine neuroendocrine and tissue-of-origin-specific characteristics; explaining different symptoms depending on the organ of origin. NEN is divided into slow-growing neuroendocrine tumours (NETs) and the rarer aggressive neuroendocrine cancers (NECs). Some hormone producing NETs give rise to symptoms (functioning), generally detected earlier than the non-functioning NETs, which often are larger and metastatic at diagnosis. NETs commonly express an abundance of somatostatin receptors (SSTR). Synthetic copies of somatostatin (somatostatin analogues, SSA), supress hormonal symptoms such as diarrhoea and flush. The SSA-SSTR ligand-receptor complex interaction instantly internalises into the cells, separate, and the SSTR re-surface. Gallium-68 (^{68}Ga)-labelled SSAs are used for PET/CT-camera visualisation of NETs, and SSA labelled with a therapeutic radionuclide, provide a means for internal radiotherapy, peptide receptor radionuclide therapy (PRRT).

The aim of the thesis was to compare the tumour response to PRRT in small intestinal NET (SI-NET) and pancreatic NET (P-NET). Study I, II and IV are retrospective and include patients who underwent PRRT with ^{177}Lu-DOTA-TATE at the Uppsala University Hospital. Study I, quantified and related the radiation dose in 25 SI-NETs to tumour shrinkage using two- and three-dimensional measurements, although no dose-response relationship was demonstrated. A relationship between tumour shrinkage and the total administered activity was however found. Study II compared the tumour response between SI-NETs from study I with P-NETs included in an earlier report, now re-evaluated by adding more tumour parameters, and with longer observation time. There radiation dose in P-NETs was the same as in SI-NETs. The radiation dose in P-NETs was highest at the first PRRT cycles, and then decreased significantly in consecutive cycles, which was not observed in SI-NETs.

The prospective study III, mapped the recirculation time of SSTR in SI-NETs and normal organs. Thirteen tumours were measured at repeated ^{68}Ga-DOTA-SSA-PET examinations. Larger tumours (>4 cm) showed a faster SSTR turn-over rate than small tumours, demonstrating a turnover resembling that in the normal organs. These results open the possibility that pre-treatment could protect normal tissues during PRRT, and probably increase radioactivity tumour uptake and hence, the radiation dose.

The retrospective study IV investigated the effects of various amounts of SSA delivered in the PRRT preparation, although the absorbed radiation dose to tumours and normal tissues, was unrelated to the amount of peptide and to the patient's total tumour burden.

Keywords: Neuroendocrine tumors, Peptide receptor radionuclide therapy (PRRT), Peptide, Small-Intestinal, Pancreatic, Dosimetry, Somatostatin receptor

Ulrika Jahn, Department of Surgical Sciences, Radiology, Akademiska sjukhuset, Uppsala University, SE-75185 Uppsala, Sweden.

© Ulrika Jahn 2023

ISSN 1651-6206
ISBN 978-91-513-1714-4
URN urn:nbn:se:uu:diva-492855 (http://urn.kb.se/resolve?urn=urn:nbn:se:uu:diva-492855)

“It is only in strong winds the kite will fly”

(an old Chinese saying)

Cover picture: Peptide pre-treatment before PRRT. *Ezgi Ilan PhD*

List of Papers

This thesis is based on the following papers, which are referred to in the text by their Roman numerals.

I. Jahn, U., Ilan, E., Sandström, M., Garske-Román, U., Lubberink, M., Sundin, A. (2020) ^{177}Lu-DOTATATE peptide receptor radionuclide therapy: dose response in small intestinal neuroendocrine tumors. *Neuroendocrinology,* 110: 662-670

II. Jahn, U., Ilan, E., Sandström, M., Lubberink, M., Garske-Román, U., Sundin, A. (2021) Peptide receptor radionuclide therapy (PRRT) with ^{177}Lu-DOTATATE; differences in tumor dosimetry, vascularity and lesion metrics in pancreatic and small intestinal neuroendocrine neoplasms. *Cancers* 13: 962-977

III. Jahn, U., Ilan, E., Sandström, M., Velikyan, I., Fröss-Baron, K., Lubberink, M., Sundin, A. Receptor depletion and recovery in small-intestinal neuroendocrine tumors and normal tissues after administration of a single intravenous dose of octreotide measured by ^{68}Ga-DOTATOC PET/CT. *Eur J Nucl Mol Med Reseach*.

IV. Jahn, U., Ilan, E., Garske-Román, U., Sandström, M., Lubberink, M., Sundin, A. Impact of administered amount of peptide on tumor dosimetry at the first cycle of peptide receptor radionuclide therapy (PRRT) in relation to total tumor somatostatin receptor expression (*Submitted*).

Reprints were made with permission from the respective publishers.

Contents

Abbreviations

APUD	Amine precursor uptake and decarboxylation
BIM-23027	Synthetic agonist
BASS	Synthetic antagonist
BL	Baseline
^{11}C-5-HTP	Carbon-11-5-hydroxy-tryptophan
CAF	Cancer associated fibroblasts
CEUS	Contrast-enhanced ultrasound
CgA	Chromogranin A
CR	Complete response
CSC	Cancer stem cell
CT	Computed tomography
CZT	SPECT Scanner
DES	Diffuse endocrine system
DNA	Deoxyribonucleic acid
DOTA	Tetraaza-cyclo-dodecane-tetra-acetic acid
DSB	Double strand break
DTPA	Diethylenetriaminepentaacetic acid
DWI	Diffusion-weighted imaging
EC	Enterochromaffin
ECM	Extra cellular matrix
ENET	European Neuroendocrine Tumour society
EUS	Endoscopic ultrasound
^{18}F-DOPA	Fluorine-18-L-dihydroxy-phenylalanine
^{18}FDG	Fluorine-18-deoxy-glucose
5-FU	5-fluorouracil
5-HIAA	5-hydroxy-indol-acetic acid
5-HT	5-hydroxy-tryptamine
5-HTP	5-hydroxy-tryptophan
FLNA	Filament A
FV	Functional volume
GBq	Giga Becquerel
Gd	Gadolinium
GEP-NET	Gastro-entero-pancreatic NET
GH	Growth hormone
GI	Gastrointestinal

GIST	Gastrointestinal stromal tumour
GLP-1	Glucagon-like peptide-1 (Receptor on insulin producing tumours)
HH_3O^+	Reactive water molecule
h.p.f.	high power field
hSSTR	Human Somatostatin receptor (1–5)
HIF 1A	Hypoxia inducible factor 1A
HIPEC	Hyperthermic perioperative chemotherapy
HU	Hounsfield Units
IARC	International Agency for Research and Cancer
^{131}I-MBG	Iodine-131-meta-iodobenzylguanidine
IOUS	Intraoperative ultrasound
JR11	antagonistic SSTR-binding molecule
JMP	Software for statistical calculations
Ki	Net influx rate
Ki-67	Proliferating protein present at cell division
LET	Linear energy transfer
MDCT	Multi-detector computed tomography
MEHR	Collimator type for SPECT scanner
MEGP	Collimator type for SPECT scanner
MEN	Multiple endocrine neoplasia
MRI	Magnetic resonance imaging
mTOR	mechanistic target of rapamycin
MWA	Microwave ablation
NEC	Neuroendocrine cancer
NEN	Neuroendocrine neoplasms
NET	Neuroendocrine tumour
NIH	National institute of health
OS	Overall survival
PACS	Picture archive and communication system
P-CgA	Plasma Chromogranin A
PD	Progressive disease
PDGF	Platelet growth factor
PET	Positron emission tomography
PET/CT	Positron emission tomography combined with Computed tomography
P-NET	Pancreatic NET
PR	Partial response
PRRT	Peptide receptor radionuclide therapy
PFS	Progression free survival
PVE	Partial volume effect
RECIST	Response evaluation criteria in solid tumours
RCC	Renal cell carcinoma
RFA	Radiofrequency ablation
RIAR	Radiation-induced adaptive response

RIBE	Radiation-induced bystander effect
RIGI	Radiation-induced genomic instability
RIS	Radiological information system
SD	Stable disease
SEER	Surveillance, epidemiology and end results database
SI-NET	Small intestinal NET
SIRT	Selective internal radiation therapy
SPECT	Single-photon emission computed tomography
SPECT/CT	SPECT combined with computed tomography
SRIF	Somatotropin release-inhibiting substance
SSA	Somatostatin analogue
SSTR	Somatostatin receptor (1–5)
STZ	Streptozocin
SUV	Standardized uptake value
TACE	Trans-arterial chemo-embolization
TAE	Trans-arterial embolization
TATE	[Tyr^3]-octreotate
TBR	Tumour-to-blood-ratio
TME	Tumour micro environment
TSSTRE	Tumour somatostatin receptor expression
tTSSTRE	Total tumour somatostatin receptor expression
U-5-HIAA	Urinary 5-hydroxy-indol-acetic acid
US	Ultrasound
VEGF	Vascular-endothelial growth factor
VIP-omas	NET tumour in pancreas
VOI	Volume of interest
WB	Whole body
WDHA	Water, diarrhoea, hypokalaemia and hyper-glycemia
WHO	World Health Organisation

1 Introduction

1.1 Neuroendocrine Tumours

1.1.1 Definition

The current WHO definition of neuroendocrine tumours is: “A tumour made of neoplastic cells of epithelial origin, characterized by structural, phenotypic and functional properties recalling those of normal peptide- or amine-producing endocrine cells” [1]. Hence, these tumours are able to arise in most any organ or tissue of the body, and carry resemblance of both specific NEN traits and traits from the organ of origin.

1.1.2 History in brief

The tumour entity that currently is denoted neuroendocrine neoplasm (NEN) has constituted a challenge ever since the time of its recognition, in the beginning of the 20th century. Two excellent historical reviews by G Klöppel [2] and Modlin et al. [3] depict Siegfried Oberndorfer to be the first pathologist to define these tumours as a separate entity, which he presented at the German Pathological society convention in Dresden 1907. In that report he described the tumours as non-malignant, yet malignant-like, thus naming them “Karzinoide”. Two decades later (1929), he officially admitted that the carcinoids could metastasize, and thus possessed malignant properties [3]. The term carcinoid remained in use for a long time, later being replaced by the expression neuroendocrine tumours (NET), now NEN, with two sub-groups, well differentiated NETs and poorly differentiated NECs, while “carcinoid” is still being applied to lung-NENs.

Before Obendorfer´s presentation at the Dresden pathology conference, there were during the early 19th century occasional reports by F. Merling (1829) and T. Langhans (1839) of autopsy findings of tumours in the appendix and in the intestine that stained differently than the surrounding intestinal cells [2]. At the end of that century O. Lubarsch (1888) and W.B. Ransom (1890) described small gut tumours at autopsy, and Ransome concomitantly described symptoms of flushing, rapid bowel movements /diarrhoea and wheezing [3]. This symptom triad was later denoted the “carcinoid syndrome”.

1.1.3 Pathophysiology

1.1.3.1 Early Pathological Tools

Limited to microscopic identification of stained cells and analysis of chemical compositions of specimens, T. Langhans could 1867 describe a submucosal jejunal tumour lacking evidence of peritumoral invasion, with a cell growth that was glandular-like and arranged in nests with a thick fibrous stroma [3]. At the end of the 19th century, R.P. Heidenhain reported the finding of scattered yellow cells in the small-intestinal mucosa in dogs (after fixation) and called them enterochromaffin cells (EC cells). Two decades later A. Nicolas discovered these cells to be situated in the crypts of Lieberkuhn (1891), a finding that was confirmed by M. Kulchitsky, who called them acidophilic cells [4, 3]. Based on the staining of the Lieberkuhn crypt cells, that was more similar to endocrine cells, and deviated from the staining of the surrounding intestinal cell types, the crypt cells were suggested to be dissimilar in origin to the ordinary lining cells of the intestine. These crypt cells received two different names; the chromaffin cells, by Schmidt (1905), and EC cells by M. Ciaccio (1906). Similar cells were later found in carcinoid tumours and A. Gosset and P. Mason suggest that the carcinoids might arise from the EC cells in the Lieberkuhn crypts (1914). The enterochromaffin cells were later shown to be wildly distributed throughout the body, why the term "diffuse endocrine system" (DES) was suggested by Feyrter 1938. During the 20th century, prominent Swedish medical scientists contributed to the knowledge regarding carcinoids; G. Björk et al. described carcinoid heart disease with pulmonary artery stenoses, tricuspid insufficiency and cyanosis in a young male who at autopsy disclosed hepatic metastases from a carcinoid in the jejunum [5]. In 1952, A. Thorson et al. for the first time described a series of patients with pulmonary stenoses, tricuspid insufficiencies, bronchoconstriction and cyanosis, in combination with carcinoid tumours of the small intestine with liver metastases, all of whom showed increased plasma levels of 5-hydroxy-tryptamin (5-HT) [6], now more commonly called serotonin. In the same year, B. Pernow and J. Waldenström reported that paroxysmal flushing was a major symptom in carcinoid patients [7] and later undeniably proved the connection between the increase of 5-HT in serum and 5-hydroxy-indol-acetic-acid (5-HIAA) in urine, in 33 patients with abdominal carcinoids [8] as mentioned by Modlin et al. [3].

1.1.3.2 Early Biochemical Techniques

Soon after M. Rapport (1948) discovered the serotonin molecule, F. Lembeck (1953) could verify that the carcinoid tumours contained and excreted serotonin, which explained the symptoms in these patients, earlier described by Ransom (1890). The Dutch pathologist A.J. Scholte (1931) was the first to describe the combination of symptoms, diarrhoea, cyanoses, cough, low

extremity oedema, and cutaneous telangiectasia in a patient with a carcinoid, and also the first to report on tricuspid valve thickening in a carcinoid patient. Later the same year, M.A. Cassidy reported flushing and diarrhoea in a patient who at autopsy disclosed an "adenocarcinoma" and cardiac valvular lesions. Based on the typical facial flush on the accompanying picture the finding was regarded to be a carcinoid [3]. During the second half of the 20th century, new methods were developed in the field of pathology, such as immunocytochemistry, autoradiography and molecular techniques that improved the understanding of these heterogenous tumours.

1.1.4 Somatostatin

Somatostatin was first discovered as a growth hormone (GH) inhibiting substance in extracts from the hypothalamus by Krulich et al., who named it somatotropin release-inhibiting substance (SRIF) [9]. It is a cyclic peptide and the product of a single gene that encodes the 116 amino acids as a long pre-pro-somatostatin molecule. This molecule is further processed to the pro-somatostatin (96 amino acids) and spliced into the end product as two/tree separate somatostatins -14 and -28a and 28b [10, 11]. The two forms are distributed broadly in the brain and in multiple tissues throughout the body [12-14] and mainly act in a paracrine fashion. The presence of the somatostatin (SS) in mid-gut carcinoid tumour cells was demonstrated in 6 out of 18 tumours by Lundqvist and Wilander [15].

Somatostatin mainly works in a paracrine fashion, eliciting a multitude of functions, and is rapidly degraded after release (less than 3 minutes half-life). Apart from inhibiting GH, it inhibits the action of multiple other hormones, such as thyrotropin, corticotrophin-releasing factor, adeno-cortico-trophic hormone, insulin, glucagon and secretin. Furthermore, somatostatin reduces the mesenteric blood flow, inhibits gastric motility and the production of gastric acid and bile [14, 16]. It is further able to modulate the immune response [17] and acts on the Ca^{2+} canals and inhibits cell proliferation [14]. Somatostatin is also involved in various brain activities, with effect on motor, sensory and cognitive functions [18, 19].

It was early demonstrated that extracts comprising native somatostatin decreased the symptoms in patients with acromegaly [20]. However, the extracts had to be infused intravenously and the effect only lasted a couple of minutes, due to the rapid degradation of the natural peptide.

1.1.4.1 Somatostatin Analogues

The search for a synthetic somatostatin analogue (SSA) with prolonged action was solved by Sandoz Ltd., the first company to present a more stable SSA, the octapeptide octreotide, the use of which primarily was focused on the release of acromegalic symptoms [21]. Newer, more long-acting somatostatin analogues have since then reached the market, and octreotate and lanreotide

bind with various affinity to the various somatostatin receptors (SSTR) sub-types [22].

Lately, biometric modelling has been tested for the search for effective long -acting SSAs to identify the attachment grove for the agonist on the SSTR [23].

1.1.4.2 Somatostatin Antagonist

By a slight modification of octreotide, Bass et al. could show that the molecule was converted from a receptor agonist to a receptor antagonist, with high affinity for the SSTR [24].

1.1.5 Somatostatin Receptors

A decade after the identification of SRIF, it was demonstrated that somatostatin (14 and 28) showed tissue specific binding [25]. The first SSTR identified 1978, was shown to belong to the G-protein coupled seven transmembrane domains receptor family [26]. The existence of SSTR in various endocrine tumours was later demonstrated by Reubi et al. who, based on their findings, foresaw the possibility that, a new type of classification of the carcinoid tumours would develop [27]. Based on their results from experiments with immunocompetent T- and B-cells, Sreedharan et al. the same time suggested the presence of more than one SSTR type [28]. Later molecular techniques confirmed the existence of five main SSTR sub-types, with SSTR sub-type 2 further divided into 2a and 2b, all of which were products of separate genes ($SSTR_1$/14, $SSTR_2$/17, $SSTR_3$/22, $SSTR_4$/20 and $SSTR_5$/16) [29, 30]. All SSTR were found to be widely spread in the central nervous system and most organs and tissues of the body, however in different combinations.

1.1.6 Agonist Receptor Interaction.

Interaction: In the end of the 20th century, it was known from *in vitro* studies that hormones were internalised into the target cells [31]. Viguerie et al. demonstrated that the same process applied to the coupling between the SSA and the SSTR *in vitro* in pancreatic acini cells [32]. Almost a decade later, this was also confirmed in human carcinoid cells by Anderson et al. [33].

Response to stimulation: Simultaneously, Hukovic et al. verified that chronic treatment with a short-acting SSA agonist, affects the production of the different SSTR sub-types. The $hSSTR_3$ and $hSSTR_5$ were readily internalized without any upregulation, $hSSTR_2$ and $hSSTR_4$ presented a moderate level of internalization with some upregulation, but $hSSTR_1$ failed to internalize, and presented a marked upregulation [34]. It was also demonstrated that radiolabelled agonists, showed slightly lower affinity for the $SSTR_2$ receptor than the native (non-labelled) agonists and that an excess of unlabelled agonists

can displace the radio-ligand receptor binding to SSTR within 10 minutes after injection [35-37].

The intracellular transport: The fate of the radioligand, after internalization was addressed by Koenig et al., who *in vitro* found a dynamic cycling and recycling of the agonist-receptor complex between the cell surface and the intracellular compartments [35]. By using radiolabelled iodine (^{125}I) somatostatin-14 and the SSA (BIM-23027) it was demonstrated that the influx is energy dependent, and occurs via clathrin-coated pits. They could also show that the rate of dissociation and recycling depended on the strength of the agonist-receptor binding and varied for different analogues and radioligands. Alternatively, when identified as non-functional, the receptor can be rerouted to lysosomes for degradation [38]. In cell experiments and in tumour xenografts in rats, Froidevaux et al. could demonstrate, that after withdrawal of peptide stimulation, the total body of receptor types (SSTR 1-4) is restored within 16 to 24 hours, due to either recycling or de novo syntheses [39]. $SSTR_5$ is the only receptor subtype that has an internal receptor pool, which is rapidly activated to restore the membrane pool after depletion [40]. Continuous long-term exposure to agonists, result in $SSTR_2$ receptor up-regulation, more pronounced in tumours than in normal tissues [39], contrary to that for most of the other SSTR sub-types. Internalization and the intracellular progression of the receptor has recently been found dependent on the recruitment of actin fibres from the cytoplasm by the cytoskeleton protein filament A (FLNA) and their migration to the clathrin coated pits. After the internalization process, the receptor signalling is neutralized by the recruitment of the ß-arrestin [41]. FLNA is similarly important for the receptors to progress from the peri-nuclear endoplasmic reticulum back to the outer cell membrane [42]. The C-terminal of the SSTR is shown to be of importance for the intra-cellular progression from early to late endosomes and for the transfer from late endosomes to the perinuclear area in the trans Golgi network [43].

1.1.7 Antagonist Receptor Interaction.

Interaction: The antagonist molecules are considered to engage a variety of receptors, other than the SSTR, and more than one at a time. The antagonists are believed to bind to both active and inactive SSTRs, and mainly remain bound on the surface membrane of the cell for a longer period of time [44]. Thus, even though each antagonist shows a lower affinity than the agonist to the specific $SSTR_2$, they appear to stay connected to the cell surface up to 72 hours [45].

Response to stimulation: In contrast to the agonist, antagonists mostly remain attached to the surface membrane, and does not elicit any internalization [24]. Dalm et al. found that the radiation dose in tumour cells when using ^{177}Lu-antagonists, *in vitro* and *in vivo,* was higher than that of the agonist ^{177}Lu-DOTATATE, and even resulted in 50 to 60 percent more DNA double-

strand breaks (DSB) [46]. Presently, the agonist, JR11 has shown to be the most effective antagonist in preclinical trials, and is tested for imaging by Fani et al. [47]. However, the conundrum with the long-time binding of agonist when used for peptide receptor radionuclide therapy (PRRT), is how sensitive normal tissue, such as the kidneys and bone marrow, can be protected.

1.1.8 Tumour Micro Environment (TME).

Cancerous transformed cells in tissues attract a mixture of supportive cell types, and create a micro-environment consisting of a variation of cell types engaged in cross talks [48]. An extensive review states that: "TME encompass immune cells, blood vessels, extracellular matrix (ECM), transformed fibroblasts, lymphocytes, bone-marrow-derived inflammatory cells, signalling molecules and a multitude of growth factors" [49]. Cancer-associated fibroblasts (CAF) provide the extracellular matrix and the alfa-smooth muscle actin-positive myofibroblasts stimulate growth of tumour cells through paracrine mechanisms [50].

The high demand for oxygenation is a stimulus for rapidly growing faulty tumour vessels, with incompletely formed wall structures, that leak and collapse and thus fail to sufficiently oxygenate the tumour tissue. Consequently, the metabolism turns anaerobic leading to an acidification of the tumour complex. Additionally, the vessel leakage creates a raise in the intra-tumoral pressure, which further reduces the oxygen transport, adding to the acidification [51, 52]. A notable exception from this rule is presented in well-differentiated pancreatic NETs (P-NETs), that demonstrate a strikingly high vessel density of a mature type, that separates them from most other epithelial cancer types, and this is called the neuroendocrine paradox [53].

Although debated, the possible existence of a cancer stem cell (CSC) has been suggested. The CSC is assumed to sustain hypoxia, to survive in a dormant form, and is believed to initially have a multi-potent capacity to migrate and produce metastases [54, 49]. As the low multiplication rate lengthens their time for DNA repair, the CSC is more refractory to conventional radioactive- and chemotherapy [55].

The accumulation of knowledge regarding the tumour microenvironment in NENs is in its beginning, however, compared to most common solid tumours, the infiltration of immunological cells varies between NEN types and among different NEN grades. Major differences between P-NETs and small intestinal NETs (SI-NETs) have been shown; in general, P-NETs, demonstrate a higher density of mature blood vessels [53] while SI-NETs express an increased production of interstitial fibrotic tissue [56, 57]. This discrepancy is likely to result in differences regarding the oxygenation of these two tumour types as well as a difference in the stress and sheer forces created in the TME between these two NET types. Thus, due to the better vascularization and limited degree of fibrosis in P-NETs, their intra-tumoral pressure might be lower

than in SI-NETs, possibly facilitating the access of therapeutic agents in P-NETs. This could be an explanation to the more rapid shrinkage of P-NETs in response to PRRT, than in the more fibrotic and poorly vascularized SI-NETs [58-61].

1.2 Classification of NENs

1.2.1 History in brief

The histo-pathological complexity of the carcinoid cells with the combination of endothelial and neuroendocrine traits has created a challenge to the understanding of their embryonic origin, a conundrum that is still unsolved, although many suggestions have been presented through the century.

During the histochemical era, any of the tree embryonic layers were suggested to be the origin; endodermal (Feyrter 1938), neuroectodermal (Pagés 1956), neuroendocrine-programmed epiblastic ancestors (Pearse 1980), who earlier (1968) had proposed the "amine precursor uptake and decarboxylation" (APUD) cell system concept (Pearse 1980).

A more clinically oriented approach for classification, was based on the embryologic structures from which the affected organs are formed, the foregut, midgut and hindgut. Later, in 1997, J. Soga and Y. Yakuwa initiated a pathological classification based on the specific growth pattern of the carcinoid tumour; insular, trabecular, glandular, mixed or undifferentiated, which is still in use [3].

Soon after the report on an atypical carcinoid tumour of the lungs, by MG Arrigoni (1972), it became clear that carcinoids are not confined to the gastro-entero-pancreatic system only, but can develop in virtually any organ or tissue of the body [62]. The NENs appear as hybrids and simultaneously present typical characteristics of neuroendocrine properties, but also the characteristics of the organ of origin. This made NEN categorization difficult, and in the first classification from World Health Organization (WHO) (1980) the term carcinoid was used for most tumours of the neuroendocrine system, although excluding endocrine tumours of the pancreas, thyroid, paragangliomas, small-cell lung carcinomas and Merkel cell tumours of the skin. Later, WHO based the sub-classification on histo-pathological staining techniques and disregarded the classification founded on the embryonic gut [62]. Based on the new methods in the field of pathology, developed during the second half of the 20th century, it was demonstrated that tumours with endocrine properties represented a larger variation than covered by the specific term carcinoids. Thus, a more appropriate term "neuroendocrine tumours" was suggested by Capella et al. who advocated a new classification based on the specific growth patterns and level of differentiation of the tumours which also could be correlated to

clinical outcomes [62]. These terminological suggestions were then adopted in the 2nd WHO edition of 2000.

1.2.2 Present Time

In the most resent version of the 5th WHO edition and it´s International Agency for Research and Cancer (IARC) edition, a new term "neuroendocrine neoplasm" (NEN) is proposed. This term includes the well-differentiated neuroendocrine tumours (NETs) with a low mitotic activity together with the poorly differentiated neuroendocrine cancers (NECs), characterized by a high mitotic activity. The nomenclature aims to combine tumours that mainly consist of neuroendocrine cells, and excludes tumour types with merely scattered nests of neuroendocrine-like cells and was up-dated by Rindi et al. 2022 [63].

Most NETs are slow growing and heterogenous as regards presentation and prognosis [64, 65]. They are mostly found in the lungs and upper gastro-intestinal tract, and 40 to 60% of the latter give rise to hormonal symptoms [66, 67]. The characteristic carcinoid syndrome (flushing, diarrhoea and bronchoconstriction) derives from serotonin-producing tumours primarily in the SI-NET. The symptoms appear when the hormonal production exceeds the metabolic capacity of the liver, and seldom occur prior to liver metastasis [66, 68]. Only tumours that give rise to hormonal symptoms are called functional, although non-functioning tumours biochemically may show apparent hormonal production, as commonly found in many P-NETs [69, 70].

The NEN classification is currently based on a combination of differentiation and mitotic activity, or the amount of Ki-67 protein as measured by immunohistochemical staining in specific hot spots of a tumour specimen. NENs of the abdomen are divided into four groups, the first three constitute well differentiated NETs; grade 1, G1 (Ki-67 < 3% / mitotic index < 2 mitoses /10 high power fields (hpf); grade 2, G2 (Ki-67 3-20% / mitotic index 2-20 mitoses/hpf); grade 3, G3 (Ki-67 > 20% / mitotic index > 20 mitoses/hpf) and regular growth pattern. The fourth group (G4) constitutes the poorly differentiated neuroendocrine cancers (NECs) (Ki-67 > 20%) with irregular growth pattern. This grading system provides important prognostic information for both SI- and P-NET patients [71, 72]. Well differentiated NET tends with time to migrate from lower (G1) to higher (G3) grades, but do not dedifferentiate. Based on the genetic differences between the well differentiated NETs and the poorly differentiated NECs, the latter are regarded as an entity of its own, and not an end stage of earlier well differentiated NETs [1]. The genuine difference between NET and NEC has recently been further proven through genetic studies by van Riet et al. [73]. They argue that it is possible to distinguish between the largest two well-differentiated NET groups (pancreatic and small intestinal) based on somatic mutation and copy-number profiles [73].

1.3 Characteristics of Pancreatic (P-) and Small Intestinal (SI-) NETs

1.3.1 P-NETs

Well differentiated P-NETs seldom present with hormonal symptoms (90%) in spite of their often biochemically apparent hormonal production, and are consequently classified as non-functioning [74]. Functioning P-NETs give rise to specific hormonal symptoms characteristic for the particular tumour cell types. Insulinomas cause hypoglycaemia, glucagonomas result in hyperglycaemia and VIP-omas give rise to watery diarrhoea, hypokalaemia, achlorhydria (WDHA syndrome) and dehydration, flushing, hypercalcemia and hyperglycaemia. Due to the hormonal symptoms, patients with functional P-NETs often present at an early stage in the tumour development, when the tumours mostly are small, and may be a challenge to visualize. The most common functional P-NET, the insulinomas, are generally semi-malignant (90-95%), and are frequently less than 1 cm in diameter when they give rise to symptoms. The few insulinomas that are malignant, create more severe hypoglycaemia and are mostly larger at diagnosis, when they often have metastasized [75].

The non-functioning P-NETs are usually large at diagnosis, and frequently discovered due to local symptoms of mass effect, and because of overgrowth to adjacent organs. Generally, P-NETs in the early stage metastasize to regional lymph nodes and the liver, and in later stages to bone and lungs. Most P-NETs do not have an active gene for fibrotic tissue production, however there is a recently discovered version of small (< 2 cm) duct-related P-NETs that are actively producing fibrotic tissues, similarly to SI-NETs, and are denoted sclerotic P-NETs [76]. The majority of P-NETs (90%) appear without connection to any genetic disorder [77]. In one report, three genetic subtypes of P-NETs were identified, that corresponded to three typical presentations; the insular/insulinoma variant characterized by a low grade and reduced metastatic activity, the more high-proliferative, metastasizing, P-NET and the intermediate intense version of MEN1-like P-NET, that often is hereditary linked [78]. In sporadic, well-differentiated P-NETs, about half lack genetical changes, indicating that epigenetic changes are thought to play a key part in the cancerous transformation [79]. Recently a whole-exome and whole-genome sequencing of 85 various advanced NENs, revealed a characteristic difference between P-NETs and SI-NETs and underlined the heterogeneity of the NET population [73].

1.3.2 S-I NETs

Primary SI-NETs are situated in the wall of the small intestine, and most likely arise from the enterochromaffin (EC) cells, although by the present WHO

definition (please see 1.1.1) they could possibly arise in any epithelial cell type of the intestinal wall. Often, multiple primary tumours are found in the intestinal wall, raising the unanswered question whether the satellites constitute local metastases from a single primary tumour, or if one single event, with the appearance of multiple synchronous tumours, is the likely explanation. Even though SI-NETs generally are slow-growing they often metastasize to the liver and regional lymph nodes, even at a very small size [50]. The majority of SI-NETs are serotonin producing, giving rise to one or more of the typical carcinoid symptoms (flushing diarrhoea and oedema) (please see 1.1.3.2 and 1.2.2).

Serotonin has further been demonstrated to stimulate the expression of collagen producing genes in mesenchymal tissues and cardiac fibroblasts, that thickens the tricuspid valves [80]. Serotonin furthermore causes a transformation of pulmonary artery adventitial fibroblasts, that promotes a phenotypic change where extra cellular matrix accumulates, which in itself causes pulmonary hypertension. This will in addition lead to the valvular fibrotic thickening, to tricuspid stenosis and heart failure [81]. It has been demonstrated by Cunningham et al. that the gene for fibroses is activated in SI-NETs [57], which may explain why the SI-NET micro-environment comprise more fibrotic tissue than that in most other NEN types, as was appreciated already by T. Langhans in 1867. The SI-NET genetics is not as well comprehended as that of the P-NETs, however loss of chromosome 18 appears to be a common finding (60%-90%), the significance of which is unclear [82]. Further, progressive change in the methylation index between primary tumours and their corresponding metastases, might indicate an epigenetic dysregulation of SI-NETs [83].

1.4 Epedimology

1.4.1 Incidence/ Prevalence

Although still rare, there has been a constantly growing, age adjusted, yearly incidence of NENs from 1.09 per 100,000 inhabitants in 1973 to 6.98 in 2012, as reported by Dasari et.al. from the Surveillance, Epidemiology and End Results database (SEER) covering 39% of the US population. The largest increase in incidence was in the age group > 65 years [84]. However, already 1976 a Swedish autopsy study covering the years 1958-1969 presented a yearly incidence of 5.4/100 000 inhabitants [85]. During the following period (1970-1982) the combination of autopsy findings and clinical cases confirmed a similar rate of incidence of SI-NETs (5.33 per 100,000) in a Swedish population [86]. A study based on a commercial database in the US (Explorys Inc, Cleveland OH) Saleh et al. report a yearly incidence of 9.2/100,000 between 2012-2017, for SI-NETs only, and estimated a yearly rate of new cases to be

14.2/100,000 between the years 2016-2017 [87]. Multiple studies report an increasing NET incidence from several countries and continents, such as Australia [88], Norway [89] and Taiwan [90]. It is nevertheless a challenge to compare NEN incidence over time, due to differences in classification and grading over the decades (please see 1.2.1). Further, it is difficult to separate the true incidence from the influence of improved detection rates because of better diagnostic tools, such as multi-detector computed tomography (MDCT), high field strength magnetic resonance imaging (MRI), diffusion-weighted MRI, endoscopic ultrasound [84, 91] and positron emission tomography (PET). Possible environmental etiological factors have been speculated on, although no consensus has been reached in this regard. In the SEER study 2014, broncho-pulmonary NETs were found most frequent, SI-NETs and rectal NETs were the second most common, followed by P-NETs. However, when SI-NETs and P-NETs were combined into one entity, gastro-entero-pancreatic NETs, (GEP-NETs), these were found most common [84]. The slow tumour growth and improved treatments have resulted in 0.048% prevalence in the US population in 2012, and was anticipated to result in 171 321 cases by 2014 [84]. The existence of a racial difference in the US prevalence is also observed [87].

1.4.2 Risk factors

Few studies comment on risk factors for NET development and, due to heterogeneity and often low statistical power in these studies, the results must be regarded as merely indicative. The majority of NET patients are old, with the largest prevalence (30%) in the age group of 75 to 79 years, and a median age of 63 years [91], which makes old age a classic risk factor [87]. Sporadic P-NENs and SI-NENs seem to have similar risk-factors, and the second most common is to be a first degree relative with a cancer diagnosis, followed by a history of recurrent pancreatitis, especially for P-NETs. Diabetes and/or obesity and the combination of heavy smoking and high alcohol intake are also regarded as risk-factors [92-95, 87]. No environmental risk factors have so far been identified [96].

NETs in the young are regularly associated with a specific genetic disorder, such as multiple endocrine neoplasia (MEN) 1 and 2, mainly in combination with P-NETs [91], von Hipple-Lindau´s disease, Tuberous Sclerosis and Neurofibromatosis (Mb Recklinghausen) [87]. In MEN 1 patients, P-NETs are mostly slow growing, non-functional and multifocal [82, 97]. About 10% of patients with von Hipple-Lindau´s disease [98], and 1% to 5% of those with Tuberous Sclerosis [99] develop P-NETs, whereas in Neurofibromatosis only sporadic cases of P-NETs occur [100].

2 Symptoms

2.1 P-NETs

The majority of P-NETs are non-functional and indolent, in spite of overproduction of hormones. Consequently, most patients seek medical attention at a later stage, primarily due to abdominal symptoms, because of tumour overgrowth and/or local symptoms of mass effect by the tumour (please see 1.3.1). About 10% of the P-NETs present with hormonal symptoms, making the patient prone to seek early medical attention [75]. The insulinomas are the most frequent functional P-NETs, leading to low glucose levels which patients self-medicate by eating. The rest of the P-NETs are rare, and usually present with metastases at diagnoses, such as VIP-oma associated with the WDHA syndrome (please see 1.3.1), glucagonomas causing diabetes and with a characteristic rash, and the gastrinomas often related to MEN 1 [101, 65, 75], followed by about 10 more extremely rare pancreatic NENs.

2.2 SI-NETs

The majority of SI-NETs give rise to subtle, atypical easily misinterpreted discrete symptoms, caused by more common and benign diseases [102]. It takes on average of 5-7 years for diagnosis, from the start of symptoms, due to the combined patient´s and doctor's delay [65], hence there are often metastatic lesions when the diagnosis is finally made [70]. When the carcinoid syndrome appears, with flushing, diarrhoea and wheezing (please see 1.3.2) the capacity of the liver to degrade excessive serotonin production is outgrown and the syndrome may be combined with carcinoid heart disease [103]. Other late symptoms are abdominal pain, because of mesenteric metastasis with intestinal obstruction and/or venous ischemia due to fibrotic strangulation of the intestinal and/or mesenteric veins, and ultimately weight loss [70]. Occasionally, small SI-NETs can be discovered incidentally at the earliest stage, during open surgery e.g., cholecystectomy, or found at the pathological examination following appendectomy, or on CT or MRI performed for other reasons.

3 Diagnosis

3.1 Nuclear Medicine Imaging History

In the middle of the 20th century, low energy γ-emitting iodine was administered to patients to be incorporated in the thyroid, and the radioactive uptake was measured by 2D planar imaging (scintigraphy). The acquisition technique was developed applying single-photon emission computed tomography (SPECT), whereby the detectors were stepwise rotated around the patient, to acquire cross-sectional 3D images.

Later, at the end of the 20th century, clinically applicable positron emission tomography (PET), scanners were developed, with higher spatial resolution than SPECT.

3.1.1 Radioactivity in Medicine

X-rays, γ-rays and ß-rays ($ß^+$ and $ß^-$) all represent "energy packets", although created in different ways and with different wave lengths and penetration. X-rays are produced through the acceleration of electrons to a high energy level before sending them off to a full stop in a heavy target that mostly consists of tungsten or gold. Parts of the incoming energy in this target is converted to X-rays, resulting in a scattered energy bundle of photons with various wave lengths, ranging between 1,24 and 124 keV. By contrast, γ-rays, are emitted from a nucleus with an imbalance between neutrons and protons. Any unbalanced nucleus strives for stability in either of two ways depending on whether the imbalance is due to the excess of neutrons or protons. In case of an extra neutron, it will convert to a proton by the emission of an electron ($ß^-$). Such decay most often results in an exited (instable) daughter nucleus that instantly emits a γ-ray (photon) to regulate the energy surplus. Conversely, an unstable nucleus equipped with an extra proton, accordingly sends out a positron ($ß^+$). This positron has a similar size but a higher energy compared to that of an electron, but with opposite charge. When such positron travers the tissues, it loses energy and starts to interact with any surrounding electron ($ß^-$) with an equal spin. The opposite charges will result in an annihilation of the two different ß-particles. This process results in the emission of two high energy (511 keV) photons (γ-rays) that travel in opposite directions (180°). A PET camera is constructed with several rings of detectors that only register photons which simultaneously (within a few nanoseconds) reach two detectors, a so-called

line of response. All these lines of response, registered during a PET examination, are reconstructed into a 3D image volume of the patient. Any annihilation that sends out their photons with angels apart from 180 degrees may be registered by the PET camera (scatter). Also, photons from two different annihilation processes can create a false line of response (randoms) which result in indistinct imaging and are corrected for in the image reconstruction. Radionuclides emitting photon ($ß^-$) are used for radionuclide therapies (please see 4.2.2.2.2.1).

3.1.2 Biological effects of Photons

Photons exert indirect effects on biomolecules, and give rise to one of two processes, the Compton process or the photoelectric absorption process, and they are both able to damage biomolecules.

The Compton effect occurs when the incoming energy is absorbed by a loosely bound electron in the outer shell, which is converted to a *fast electron* that leaves its position while simultaneously emitting a photon with a long wave-length with low energy.

The photoelectric absorption process occurs when the incoming photon energy interacts with an electron in one of the inner electron shells (K, L or M), releasing an electron from its orbit and converting it to a *fast electron* and emitting a long-wave photon. The remaining vacancy in the inner shell is promptly filled, either by an electron from any of the outer shells of the same atom, or by an electron from outside. This filling in process, of an electron traversing from a higher to a lower energy level also reduces a surplus energy of the electron by emitting a low energy photon.

The *fast electrons*, are the ones that cause biological damage, and they act similar regardless of the source. Water, comprising about 60% of the body, offers the *fast electron* the most abundant molecule to engage with. When this happens, the water molecule becomes ionized and converts to a free radical (H_3O^+), which instantaneously reacts with a neighbouring water molecule (H_2O) to create a free hydroxyl radical (OH^-). The OH-radical is able to diffuse in a volume with a radius of about 1 nm, and may react with a DNA molecule, to create DNA strand breaks. Single strand DNA brakes are usually reparable, while the double strand breaks are lethal to the cell, either momentarily or in the long run.

3.2 Nuclear Medicine NET Imaging

3.2.1 History

Nuclear medicine imaging utilises radiolabelled molecules (and sometimes a radionuclide alone) which are administered to the patient, usually

intravenously, to engage with a specific cellular receptor, substances or biological process within the body. Their distribution in the body is registered by using a gamma-camera or a PET-camera.

Inspired by Sisson et al. [104] who showed that the radio-iodinated amine precursor analogue (^{131}I-meta-iodobenzylguanidine, ^{131}I-MIBG) could be incorporated in tumour cells with neurosecretory capacity in the adrenal medulla and in pheochromocytomas, Hoefnagel et al. demonstrated that this was true also for certain NETs, and performed the first clinical functional imaging of carcinoid tumours with ^{131}I-MIBG scintigraphy. [105].

Parallel in time, the Krenning group in Rotterdam developed a radio-iodinated somatostatin analogue ([Tyr3]-octreotide) focusing on the SSTR overexpression in most carcinoids [106]. Shortly thereafter, they switched radioiodine to using Indium-111 (^{111}In) as the label, to create ^{111}In-DTPA-octreotide with longer half-life, more favourable excretion pattern and less liver toxicity [107]. Similar in time, the PET group in Uppsala reported the results from a study using the newly developed PET tracer ^{11}C-5-hydroxy-tryptophan (^{11}C-5-HTP), thus exploring the APUD concept in carcinoids, i.e., their capacity for amine precursor uptake and decarboxylation. ^{11}C-5-HTP-PET showed higher detection rate than CT and ^{111}In-DTPA-octreotide scintigraphy in several different NET types [108]. Because of the complicated radiosynthesis, ^{11}C-5-HTP-PET have been restricted in availability, and used in merely two European centres. The further development of the hybrid PET/CT systems improved the diagnostic precision and confidence. The major step in PET/CT imaging of NETs was the development of the gallium-68 (^{68}Ga)-labelled somatostatin analogues, ^{68}Ga-DOTATOC, ^{68}Ga-DOTATATE and ^{68}Ga-DOTANOC. The use of gallium-68 became widely available and have the advantage of being produced locally in a generator, without the dependence of an in-house cyclotron [108].

3.2.2 Present time

PET/CT with ^{68}Ga-DOTA-somatostatin analogue (SSA) is currently the most used nuclear medicine method for diagnosing well-differentiated NENs, the majority of which show an abundance of SSTR. PET/CT has almost totally replaced scintigraphy with indium-111 pentetreotide previously used to select patients for PRRT, whereby the uptake in the tumours in relation to that in normal liver parenchyma was assessed according to the Krenning score [109], for which now instead ^{68}Ga-DOTA-SSA-PET/CT is employed. Apart from being superior in NEN detection, with a diagnostic sensitivity and specificity ranging between 92-100% [109], PET/CT substantially reduces the time from tracer injection to examination from 24 to 1 hours [110, 111].

For NENs that lack sufficient SSTR expression, alternative PET-tracers, available in some specialized centres, are ^{18}F-labelled L-dihydroxy-phenylalanine (^{18}F-DOPA) and ^{11}C-labelled 5-hydroxy-tryptophan (^{11}C-5-HTP).

Increased metabolic activity in tissues, of any cause can be visualized by ^{18}F-labelled deoxy-glucose PET (^{18}FDG-PET). A higher NET grade is often combined with less SSTR expression, and increased metabolic activity, usually in high G2 and G3 NETs and NECs. Because of the heterogenic characteristics of NETs, even low G2-NETs may be FDG-positive. Thus, the combination of receptor imaging with ^{68}Ga-DOTATOC-PET/CT and metabolic imaging with ^{18}FDG-PET/CT is increasingly employed, to provide prognostic information also on the presence of tumour cell clones with a higher degree of malignancy [112, 113].

3.2.3 Radiolabelled Agonists for diagnosis

It has long been debated whether the tumour uptake of ^{111}In-DTPA-octreotide and ^{68}Ga-DOTA-SSAs can be influenced by competitive binding, through administration of unlabelled "cold" SSA, and whether patients therefore should discontinue their medication of long-acting somatostatin analogues before diagnostic imaging [114]. Dörr et al. demonstrated that five patients who continued their daily medication of 600 µg short-acting octreotide, on ^{111}In-pentetreotide scintigraphy exhibited significant lower tracer uptake in the normal abdominal organs, resulting in better tumour visualization. They suggested that, the cold peptide depleted the normal tissue receptors, thus enhancing tumour detection, and even suggested a potential advantage of administering a "protective" load of cold peptide at PRRT [115]. Their conclusion was that the number of tumour receptors outnumbered those in the normal tissues, thus the radioligand uptake in the tumours was not affected by the short-acting cold SSA. The impact on radioligand uptake in tumours and normal tissue by adding intravenous (i.v.) cold peptide in conjunction with ^{68}Ga-DOTATOC PET/CT, was studied by Velikyan et al. [116] who showed decreased uptake in the normal tissues when 50µg and 500µg cold octreotide were administered 10 minutes before ^{68}Ga-DOTATOC. The tumours showed an increased tracer uptake of at the lower amount (50µg) but not at the higher dose (500µg), except in a large P-NET with very high SSTR-expression. These findings of competitive receptor blocking have been confirmed in two later studies [117, 118].

Insulinomas often show low or no $SSTR_2$ expression, and therefore are difficult to detect on ^{68}Ga-DOTA-SSA-PET/CT [119, 120]. As they usually express the GLP-1 receptor, PET/CT instead using the ^{68}Ga-radiolabeled GLP-1 receptor agonists ^{68}Ga-exendin-4 have shown promising results in the detection of insulinoma [121, 122].

3.3 Radiological NET Imaging Techniques with X-rays

3.3.1 History

Röntgen´s discovery during the late 19th century, that low energy X-rays sent through the body could be captured on an ordinary photographic film to produce anatomical images, was within a few years implemented in the clinical medical practice. The method favoured imaging of bone and air, and was initially used to diagnose skeletal and lung pathologies. Later, with the development and administration of various contrast agents, the technique was extended to other applications. The registration of X-rays is, since the last couple of decades, digitalized and the data are stored on servers and the images are reviewed on computer monitor screens.

During the 1970th G. Hounsfield and A. Mac Leold Cormack created a scanner, computed tomography (CT) (Nobel Prize 1979) in which both the X-ray source and the X-ray detector revolved around the patient, who was positioned on a bed. By stepwise moving the patient through the tunnel (gantry), which held the X-ray tube and detector, information of the X-ray attenuation in serial transverse sections of the body, was collected and reconstructed into cross-sectional images. To improve the CT image contrast, an intravenous iodine-based contrast medium is usually administered.

3.3.2 Computed Tomography

Currently, CT is the preferred imaging method for patients with abdominal discomfort, and has formed the basis for NET imaging. This requires i.v. contrast-enhanced multi-phase CT with a pre-contrast examination of the liver followed by i.v. contrast-enhancement in the late arterial and in the venous phase [123, 111]. Due to difficulties in identifying hypo-vascular (low blood flow) lesions, CT shows 64-81% sensitivity [124] and 86% specificity for NETs [111]. The downside of CT is the high radiation dose and the nephrotoxicity of the contrast media in patents with renal impairment [125], for whom MRI is better suited.

3.4 Imaging Techniques without X-rays

3.4.1 Magnetic Resonance Imaging (MRI)

MRI in medicine is based on the hydrogen nucleus (protons) and the way they react to radiofrequency signals, depending on the macro-molecule into which they are integrated. When the patient is positioned in the MR gantry, comprising a high field strength electromagnet, all protons in the body are aligned with or against the magnetic field. The minor exceeding fraction of protons

aligned in the direction of the magnetic field are those utilized for the MRI acquisition. By sending combinations of radio frequency (energy) signals "MRI sequences" by means of a radio transmitter to an antenna in the gantry (tunnel) of the magnet, the protons become excited to higher energy levels. When the radiofrequency transmission stops, these protons return to their normal energy level and in turn emit a characteristic relaxation signal that is registered by the antenna and converted to MR images.

Standard MR sequences are based on the specific relaxation signals from protons, depending on in which molecule they are integrated, such as water, fat or bone. An enhanced signal can be achieved by means of intra venous contrast media, usually Gadolinium (Gd) based, which changes the magnetic forces locally in the tissues. By diffusion-weighted imaging (DWI), the movements of the water molecules in the tissues are registered to show whether these are free, as in urine or cysts, or restricted as in dens cellular tissues, like in tumours, in which the abundance of cell membranes will restrict the molecule´s diffusion.

The spatial resolution on MRI (about 0.5 mm) is less than that of CT (about 0.1 mm), and an MRI examination regularly requires 0,5-1h, or more for some whole-body acquisitions, as compared to CT 5-15 min. However, MRI offers better tissue contrast and provides vastly superior imaging of the liver, bone and CNS compared to CT. Further, MRI can supply more imaging information than CT without the use of contrast media, and is therefore better suited in patients with kidney impairment and those with severe adverse reactions to CT contrast media. Since MRI does not expose the patients to radiation, it is advantageous in the younger, especially in those who undergo long-term follow-up.

The most serious limitation of MRI is with the existence of magnetic metals implants in a person, that can create image artefacts and sometimes be displaced by the strong magnet field. Also, some medical devices may be sensitive to the magnetic fields, such as older types of pacemakers. Problems with claustrophobia, that requires management, are usually more pronounced in the longer and narrower MRI gantry than in the shorter and wider CT gantry.

3.4.2 Ultrasound

Ultrasound (US) utilizes high frequency sound to create images. The applied frequency interval is approximately 3 to 15 MHz, i.e., far above the upper audible limits of human hearing (20 kHz). The ultrasound transducer both transmits the sound wave pulses into the body, and subsequently registers the reflected sound waves of the target tissues. These echoes are then converted through data processing to create an image. US is thus a type of sonar technique, based on the time laps for the ultrasound pulse to return from the tissue of interest, that provides evidence regarding the distance and type of tissue, and offers anatomical and structural information. The flow of fluids (direction

and velocity) can be visualized by using Doppler technique. Traditional abdominal non-contrast US has its limitations when diagnosing small primary NETs, but in metastatic disease US is useful to visualize enlarged abdominal and retroperitoneal lymph nodes and liver metastases. Contrast-enhanced abdominal ultrasound (CEUS), using intravenous microbubbles, has greatly improved the detection and characterization of liver lesions. US is also extensively used for image guiding of needle biopsies.

Endoscopic ultrasound (EUS) is outstanding to visualize P-NETs with higher detection rate than both CT and MR. EUS also offer the possibility for simultaneous needle biopsies. A major draw-back of EUS is that it is invasive, and with frequent need for sedation and/or anaesthesia [126]. Further, intraoperative US (IOUS) is of great value for localizing small liver metastases and P-NETs, especially in the head of the pancreas, and is mandatory at surgery in MEN-1 patients [127].

3.4.3 Conclusions on Imaging Techniques

In spite of all reports on imaging results and improved detections rates for tumours and metastases, one has to be aware of the limitations of each of these techniques, as excellently illustrated in a study using ex vivo thin slice pathology following hemi-hepatectomy in NET patients, where MRI as the most superior method yet detected less than half of the metastases identified with the microscope [128].

3.5 Texture analysis

Recent imaging research has focused on extraction of imaging information, beyond what can be provided by conventional reading and measurements of CT attenuation, MRI signal intensity, PET tracer uptake etc. By the use of specialized computer software, spatial information may be extracted on how the image voxels are interrelated, in for instance tumour tissue, so called texture analysis, applicable to both CT, PET and MRI. Metrics for some of these different components have been found to provide prognostic information on progression free survival (PFS) [129]. Especially entropy, at the base line PET/CT examination before PRRT, has been shown to differentiate between high-risk and low-risk P-NETs and the patients´ response to treatment [130]. Many studies have also been focused on predicting tumour grade in GEP-NETs [131].

3.6 Chemical diagnoses with biomarkers

3.6.1 Chromogranin A

Chromogranin A (CgA) is a water-soluble acidic glycoprotein and a secretory product that frequently is elevated in NEN patients. Historically, it was suggested to be a specific secretion product of the NENs [132], but was later found to be elevated in a multitude of diseases such as atrophic gastritis, and in patients treated with proton-pump inhibitors [133], in inflammatory bowel disease, and renal failure [134] and in liver and heart failure. CgA is a secretory product and as such, it does not conform to any of the eight hallmarks of cancer, and is an unsuitable tool for evaluating such a heterogenous entity as NENs [48, 135]. Furthermore, the CgA measurements are performed with different assays and numerous commercially available kits, preventing direct comparisons between studies performed at various centres [136]. CgA thus fails to comply with the National Institutes of Health (NIH) criteria for a clinical biomarker, that should objectively measure and evaluate a pathological process (Biomarkers Definitions Working 2001). Accordingly, a recent prospective multicentre study merely showed a weak association between the changes in CgA levels and tumour burden [136] and one study concluded that CgA alone is inadequate to predict tumour progression [137].

3.6.2 5-hydroxy-indole acetic acid

5-hydroxy-indole acetic acid (5-HIAA) is the metabolite of serotonin (5-hydroxy-tryptamine), which is converted in the platelets and tumour tissue and excreted through the kidneys, and is primarily found in patients with functioning SI-NETs. Since the serotonin production varies during the day and night, the most reliable measurements are achieved by 24-hour urinary collection.

3.6.3 Upcoming biomarkers Genetics.

The genetic mapping of NENs has developed substantially over the years, and circulating gene products from NENs can now be identified in blood samples (liquid biopsy) using gene expression assays, showing 90% sensitivity and specificity for NETs [138, 139]. The NETest constitutes of a battery of gene products that represent growth factors (growth factor signalome) and metabolic factors (tumour metabolome). An elevation of these gene products has been noted almost a year before any sign of tumour progression can be identified by imaging [140]. The NETest has also been found to correlate with the outcome of therapeutic interventions such as surgery and PRRT. Recently, the genomic exploration of P-NETs has revealed new possible biomarkers regarding the stage of dedifferentiating of the tumours that might be useful as upcoming biomarkers [141].

As the genetics methods develop, more insight is gained regarding the development of NETs and their tumour environment. This is especially the case for P-NETs, and a recent work demonstrated the genetic basis for the dedifferentiation responsible for the metastatic capacity in P-NET type [142]. This is just a beginning, or the beginning of the beginning, and in the future, we are likely to see new biomarkers and even new grounds for NET classification, more related to prognosis and outcome [143].

3.7 Pathology Examinations

3.7.1 Histology and Immunohistochemistry

The grading of NENs is based on biopsy from a tumour specimen or a needle biopsy, to determine the tumour differentiation either by the number of mitoses (mitotic index), or the Ki-67 index. The Ki-67 is a nuclear protein associated with cellular proliferation, and is present in all active cell cycle phases except the quiescent (G0) (please see 1.2.2). It is measured by immunohistochemistry techniques using a specific mouse antibody [144] and the fraction (%) of stained cells is counted in a hot spot of 500 tumour cells [144]. The mitotic index is defined as the percentage of mitotic cells in a hot-spot area of 10, non-overlapping, consecutive high-power fields. Furthermore, the characteristic growth pattern of the tumour, such as acinar, insular, trabecular type, or undifferentiated growth is also analysed for the classification.
The presence of synaptophysin, a glycoprotein stored in the synaptic vesicles, in the tumour is also detected by immunohistochemistry, and constitute a strong indication of a NEN.

3.8 Tumour grade and tumour staging

Apart from NEN differentiation and grade (G1-G3) the primary tumour is staged based on specimens from surgery and/or imaging, according to the local growth of the tumour (TX-T4) in relation to their organ of origin, the number of regional metastatic lymph nodes (NX-N1) and metastatic spread to distant organs (M0-M1). Locally growing NENs (TX) are often accidentally identified on imaging or at open surgery, performed for other causes, or are found because of hormonal symptoms, typically with benign insulinomas and pituitary adenomas. Because of the generally discrete symptoms from NENs, they have in about half of the patients already metastasized at the time of presentation, often to regional lymph nodes and the liver in about half of the number of patients.
The TNM staging varies for different organs, as listed in Table 1.

Table 1. TNM classification for abdominal NENs adapted from the Swedish national treatment recommendations for neuroendocrine tumours of the abdomen.

Primary Tumour	(T)	
Pancreas	TX	The primary tumour cannot be evaluated
	T0	The primary tumour cannot be found
	Tis	Carcinoma in situ
	T1	The tumour is constrained to pancreas and $\leq$ 2 cm
	T2	The tumour is constrained to pancreas and $\geq$ 2 cm
	T3	The tumour growth is beyond the pancreas but does not engage the celiac artery or the superior mesenteric artery
	T4	The tumour involves the celiac artery or the superior mesenteric artery

Primary Tumour	(T)	
Small Intestine	TX	The primary tumour cannot be evaluated
	T0	The primary tumour cannot be found
	T1	The tumour invades the lamina propria and submucosa and is $\leq$ 1 cm
	T2	The tumour invades the lamina propria and submucosa or is $\geq$1 cm
	T3	The tumour penetrates the muscular propria and into the subserosa but not through it.
	T4	The tumour penetrates the serosa entirely and invades other organs.

The N and M classification is similar for all organs and NENs

NX	Regional lymph nodules cannot be evaluated
N0	No regional lymph node metastases
N1	Nodular lymph node metastases

M0	No distant metastases
M1	Distant Metastases

The combinations of the TNM stages identifies the overall tumour stage (Table 2).

Table 2. Disease staging for endocrine tumours of the abdomen, [145].

Stage	Primary tumour	N-regional node	M-distant metastases
I	T1	N0	M0
IIA	T2	N0	M0
IIB	T3	N0	M0
IIIA	T4	N0	M0
IIIB	Any T	N1	M0
IV	Any T	Any N	M1

4 Treatments

4.1 Surgery

4.1.1 Primary tumour

Surgery is the only curative NEN-treatment, provided the tumour is discovered at an early stage. Occasionally small primary SI-NENs are found and resected at open surgery for other causes, or found at pathological examination of a resected appendix. The treatment of small (< 2cm), low-grade, non-functional P-NETs are controversial although the ENET guidelines allows for a "watch-and-wait" approach [96]. Non-metastasizing insulinomas and pituitary adenomas are the few NETs for which surgery always offers curative treatment.

4.1.2 Tumour debulking procedures

Decreasing the tumour burden by cytoreductive surgery have proven favourable results for relieving symptom in SI-NETs, reducing 5-HIAA levels and prolonging PFS [146, 147] and possibly over-all survival (OS).

4.1.2.1 Surgical debulking strategies mainly of liver metastasis.

Surgical debulking of liver metastatic growth, such as hemi-hepatectomy and metastasis enucleation, has proven to be a therapeutic possibility for patients with well-differentiated NENs and considered to improve the OS [148, 149]. In carefully selected patients, tumour reduction can also include surgical treatment of peritoneal carcinomatoses and hyperthermic perioperative chemotherapy (HIPEC) and has improved the 5-year survival [128, 150].

4.1.2.2 Non-surgical

4.1.2.2.1 Trans-arterial liver embolization

NEN patients with suitable blood vessel anatomy can be offered selective trans-arterial treatment of liver metastases. These are exclusively supplied by the hepatic artery, in contrast to the liver parenchyma which is mainly supplied by the portal vein.

Embolization can be accomplished by intraarterial injection of gel-foam (trans-arterial embolization, TAE) or by adding a chemotherapeutic agent

(trans-arterial chemo-embolization, TACE). The process of selectively introducing an internal radiation compound to liver metastases is called selective internal radio-therapy (SIRT), whereby ^{90}Y imbedded microspheres are injected intraarterially to deliver focused radiation to the selected metastasis [151]. SIRT is presently regarded as a standard procedure in selected NEN patients and mainly focus on larger metastases [149]. Selective intra-arterial treatment of the liver with radiolabelled SSA agonists, such as ^{111}In-DTPA-octreotide and ^{177}Lu-DOTATATE, has also been tried, and demonstrated a higher degree of response in the ^{177}Lu-group than with ^{111}In-DTPA-octreotide, however, the radioactivity was mainly transferred into the systemic circulation and not contained in the liver [152].

4.1.2.2.2 Percutaneous Cryo- and Radiofrequency ablation

Radiofrequency ablation (RFA) and cryo-ablation are procedures, guided by ultrasound or CT, used to treat focal liver metastases. It is usually performed as a percutaneous intervention but also intra-operatively. Microwave ablation (MWA) offering a larger ablation area has lately replaced RFA because of its limitation of being confined to treatment of smaller metastasis < 3-4 cm in diameter [149].

4.2 Systemic treatments

Prior to the discovery of the somatostatin molecule there was little to offer patients with carcinoid symptoms, and NET patients suffering from non-functioning tumours were mostly diagnosed at operation or autopsy.

Soon after the discovery of somatostatin, extracts from peptide rich tissues was tested as therapy for patients with acromegaly and those with the carcinoid symptoms. However, the therapy presented difficulties due to the extremely short half-life of the peptide (< 3min). The introduction of a synthetic analogue octreotide in the 1980th (please see 1.1.4.1) offered a treatment opportunity to low grade tumours and control of the carcinoid symptoms. This treatment was initially regarded to prolong the over-all survival compared to non-treated patients [153, 154], an insight that has lately been revised [155]. Currently, the management of NEN patients is a multi-disciplinary task engaging surgeons, oncologists, gastro-enterologists pathologists, radiologists, nuclear medicine physicians and physicists, which has improved the treatment outcome and over-all survival for these patients. A vast challenge for cancer treatment is the tendency of tumour cells to develop resistance to treatments by developing alternative pathways for growth.

4.2.1 Non-targeted

4.2.1.1 Chemotherapy

5-fluorouracil (5-FU), developed in the middle of 20th century, was the first chemotherapeutic agent developed, and tested on pancreatic and gastrointestinal NETs with questionable results [56]. During the coming decades innumerable combinations of assorted chemotherapeutical drugs were tested as regards combinations, administration forms, toxicity and end points. P-NETs, even low-grade tumours, were found to demonstrate a sensitivity to 5-fluorouracil (5-FU) in combination with streptozocin (STZ) or termozolomide. Presently, in the US, STZ, approved by FDA in 1982, is the only chemotherapeutic agent accepted specifically for treatment of progressive pancreatic NEC:s [156].

In Europe, however, the ENET guidelines recommend chemotherapy as a second line therapy for P-NETs in the form of the combination of streptozotocin and 5-FU or doxorubicin. However, in case of tumour-related local symptoms, high liver burden or rapid progression these combinations can even be considered as a first line treatment [157]. The Swedish national guidelines on chemotherapy closely follows the ENET recommendations but adding the termozolomide separately or in combination with capicetabine to any P-NET.

4.2.1.2 Interferon-alpha.

During the decades before and around the turn of the century interferon-alpha was considered beneficial in treating neuroendocrine tumours [158, 22]. At this time interferon-alpha was further shown to result in growth inhibition when tested *in vitro* on neuroendocrine cells [159, 160]. Later, a prospective, randomized, multicentre trial demonstrated comparable results for either SSA, interferon-alpha or the combination [161]. Due to the high rate of negative side-effects and low anti-tumoral effect, the treatment with interferon-alpha is no longer in use [162].

4.2.2 Targeted therapy

4.2.2.1 Non-Radioactive

4.2.2.1.1 Somatostatin Analogues (SSAs)

4.2.2.1.2 History

Immediately after the release of the synthetic SSA (please see 1.1.4.1), initially developed for patients with acromegaly, it was successfully tested on NEN patients with carcinoid symptoms and, as expected, decreased their hormonal symptoms. Although the early synthetic SSA had longer biological half-life than the natural peptide, further work resulted in the development of long-acting SSAs that could be administered monthly as a slow-release

preparation, and further improved the patients´ every-day life. The comparison between the two synthetic SSAs octreotide (administered s.c. every 8 h) and lanreotide (i.m. monthly) showed similar long term symptom control in most studies [162].

4.2.2.1.3 Present time

The synthetic SSAs primarily binds to the $SSTR_2$ and to a lesser extent to $SSTR_3$ and $SSTR_5$, but hardly at all to $SSTR_1$ or $SSTR_4$. The PROMID trial (SI-NET patients) and the CLARINET trial (gastro-entero-pancreatic NEN patients) demonstrated longer PFS for long-acting SSAs than placebo, but did not affect OS [163, 164, 155]. SSA treatment can cause abdominal side effects, such as nausea, diarrhoea, steatorrhea and bloating and a risk for biliary stone and sludge [96], and therefore prophylactic cholecystectomy can sometimes be considered.

4.2.2.1.4 mTOR inhibitor

With biological macro molecules, it is possible to target dysfunctional processes in cancer cells and specific factors that promote excessive tumour growth, without adversely affecting the processes of normal cells. Currently, the most successful targets are the tyrosine kinas domains and various growth factor receptors, together with the dysregulated mTOR molecule.

Through the discovery of the rapamycin molecule (from a soil bacteria) during the mid 21st century [165], the mTOR function in cells was mapped and shown to be dysregulated and upregulated in many cancers. The mTOR signalling acts as a serine/threonine and tyrosine protein kinase that drive cell growth by its stimulating effect on protein syntheses and inhibition on autophagy [166]. There are also indications that mTOR supply oxygen to tumour cells by increasing the hypoxia inducing factor 1A (HIF 1A) translation [167]. *In vivo*, the mTOR inhibitor Everolimus prolongs PFS in many cancer patients including those with NENs [168]. The drug has been approved for P-NETs since 2011 and for advanced well-differentiated, non-functional gastrointestinal (GI) and lung NENs since 2016.

4.2.2.1.5 Anti-angiogenic therapy

Sunitinib, a tyrosine kinase inhibitor that targets the platelet derived growth factor (PDGF) receptor and the vascular-endothelial growth factor (VEGF) was initially approved for renal cell carcinoma (RCC) and gastrointestinal stroma tumour (GIST). Later, an extended application for unresectable or metastatic well-differentiated P-NETs was approved in November 2010 by the European Commission, followed by the United States Food and Drug Administration may 2011. Sunitinib blocks the tyrosine kinase signalling and reduce the maturation of tumour vessels [169], and significantly improves the PFS and OS in unresectable or metastatic well-differentiated P-NET patients as compared to placebo [170].

4.2.2.1.6 Immunotherapy

Immunotherapies have so far shown disappointing results in regards to well differentiated NETs of the abdomen, as contrasted to the encouraging results for skin NEN and the small cell lung cancer [171].

4.2.2.2 Radionuclide Therapy

4.2.2.2.1 Internal Radiation

In contrast to external radiotherapy with high Linear Energy Transfer (LET), radionuclide therapy applies its effect through low LET by radionuclides with a short-range decay. The exact mechanisms for the low LET effects on the tumours are still not completely understood [172]. Low LET radiation presents specific aspects such as the radiation-induced bystander effect (RIBE), the radiation-induced genomic instability (RIGI), the radiation-induced adaptive response (RIAR) and the low dose hyper-radiosensitivity that have to be further explored. The RIBE, describe the lethal or semi-lethal influence from a targeted cell to its neighbour cells, involving tumour cells and normal cells, a process that might be working both ways [173]. The RIGI, refers to the increase of spontaneous/stress-induced genetic lesions that can be found in later generations of cells to those parental generations that survived irradiation of non-toxic doses [174, 175]. Such cells will either experience a late apoptosis or develop a secondary malignancy. The RIAR encounters the effect of radioresistance, which is shown in some biological systems, after being pre-exposed to a low amount of radioactivity before a higher amount of radioactivity. This is a situation often occurring in the clinical setting when an imaging session precedes the therapy session [172, 176]. As opposed to external radiotherapy, the fraction of the administered radioactivity taken up by the tumours during radionuclide therapy, depend not only of the number of receptors on the tumour cells, but also on the tumour size, the cells in the surrounding micro environment, the tumour´s vascular supply, and the radioactivity in the normal tissues. Furthermore, external radiotherapy delivers the radiation dose at a short moment of exposure, whereas the highest tissue accumulation of the radiolabelled preparation is found a few hours after start of radionuclide therapy, and then with a decline, over the following days in parallel with the cellular processing of the preparation and formation of metabolites [172].

4.2.2.2.2 Radiolabelled Somatostatin Receptor Agonists for treatment and Peptide Receptor Radionuclide Therapy (PRRT).

4.2.2.2.2.1 History

Radionuclides can be used for both diagnostic imaging and/or therapeutic purposes after being coupled to a targeting molecule that engages with a specific cell structure or enters a biochemical pathway. In the case of SSTR targeting of NENs, whether for imaging or treatment purposes, the radiolabelled SSA

is immediately internalized in tumour cells after engaging with the membrane bound SSTRs [33]. After the introduction of [^{111}In-DTPA-d-Phe1]-octreotide for scintigraphy of NENs [107] the same compound, although administered in substantially higher amounts, was tested for a possible treatment effect. A 55-year-old female with a non-functional P-NET showing increased levels of glucagon and a high SSTR expression was the first patient to receive therapeutic doses of [^{111}In-DTPA-d-Phe1]-octreotide. The experiment turned out positively with reduction of the patient´s symptoms and this treatment was denoted peptide receptor radionuclide therapy (PRRT). Rather soon the ^{111}In isotope was found to be suboptimal as a therapeutic radionuclide, due to its major decay of γ-photons and short-range of Auger electrons (nano-to micrometres) [177] and excretion through the liver, with the risk of liver failure. Instead, the more effective β-emitter Yttrium-90 (^{90}Y) was suggested for therapy [178]. However, this isotope showed to dissociated from the DTPA chelate and engaged with bone. By switching the chelate to DOTA, the ^{90}Y was, however, stabilized [179]. ^{90}Y is a high-energy β-emitter (934.8 keV), with a long range in water of 3-11 mm (mean 2,5 mm in soft tissue) and a short half-life (2.67 days) but without γ-photons in its decay. Parallel in time, Lutetium-177 (^{177}Lu) was tested and found a more suitable alternative for therapy, due to its shorter range, less kidney toxicity and with an additional emission of γ-photons, allowing schintigraphic imaging of the tissue uptake during the treatment [109].

^{177}Lu is a low-energy β-emitter (133.1 keV) with a medium range in tissue of 0.5-2 mm (medium 0.67 mm) and a longer half-life (6.64 days) and with emission of γ-photons [180, 181].

Radio Metal	Energy/decay	Range	Half-life (days)	γ-emission
^{111}Indium	Auger	µm-nm	2.8	Yes
^{90}Yttrium	(β^-) 934.8 keV	3-11 mm	2.67	No
^{177}Lutetium	(β^-) 133.1 keV	0.5-2 mm	6.64	Yes

Multiple groups have, in cell cultures and *in vivo*, analysed various combinations of SSTR agonists and chelates, to improve the binding and affinity to the SSTRs, and the treatment outcome [182-184, 38, 185]. In order to improve the detection of small tumours in the vicinity of the kidneys on scintigraphy with ^{111}In-pentetreotide, Hammond et al. suggested a simultaneous intravenous administration of arginin-lycin, which was shown to minimized the kidney uptake by blocking the renal tubular reabsorption. This was adopted to PRRT, and amino acid infusion for renoprotection is currently an important part of the PRRT administration protocol [186].

It was estimated that human carcinoid tumours, cultured *in vitro*, retained about 50% of the internalized ^{111}In-DTPA-octreotide while the rest was metabolized and released by the cells. The remaining intracellular activity was found in close vicinity of the nucleus within 6 hours, a localization also

described in tumour specimens analysed post operatively after seven SI-NET patients received injection of 200 MBq ^{111}In-DTPA-octreotide two days before operation [187] . With ^{177}Lu-DOTATATE, there is also a newly discovered systemic metabolization in plasma, whereby less than half of the original molecules remained at 24h post infusion [188]. The radio-metabolites have not yet been identified, nor whether they have any binding capacity to the SSTRs.

4.2.2.2.2.2 Recent Time

^{177}Lu is nowadays the most frequently used radionuclide for PRRT, especially after the favourable results by the Rotterdam group [189] and more recently, the prospective NETTER-1 trial [190]. There have been arguments that ^{90}Y with its longer beta-range would be more favourable for the treatment of large metastases [191]. It has also been suggested that the combination of ^{177}Lu and ^{90}Y for PRRT would provide a synergistic effect, and be superior to each radionuclide alone [192]. However, an extensive retrospective analysis of PRRT with either ^{177}Lu, ^{90}Y or the combination of both, confirmed that ^{177}Lu-based PRRT was less toxic than any ^{90}Y containing treatment, in regard to both haematological and renal adverse effects [193]. The traditional and most frequently administered PRRT is the so called “empiric regime” with 4 cycles of 7.4 GBq ^{177}Lu-DOTA-TATE/TOC, administered to all patients regardless of NET type, tumour load, body-weight, age or gender. At Uppsala University Hospital a personalized treatment was developed whereby 7.4 GBq of ^{177}Lu-DOTATATE per cycle was administered with close dosimetric monitoring. The maximum number of cycles were given until 23 Gy accumulated absorbed dose to the kidneys was reached and/or 2 Gy to the bone marrow [60]. In this study, half of the patients were able to receive more than 4 cycles, and with survival benefits (PFS and OS) for those who reached 23 Gy absorbed dose to the kidneys, as compared to those who did not [60].

4.2.2.2.2.3 Present Time.

Since the registration of Lutathera® in 2017, PRRT with ^{177}Lu-DOTATATE is given according to the empiric regime. There are ongoing studies assessing the notion of improving the PRRT by increasing the radio-sensitivity of the tumours by co-treatment with tyrosine kinase inhibitors and immunotherapeutic agents to improve the therapeutic outcome of PRRT [194].

4.2.2.2.3 Radiolabelled Antagonists

Initial *in vitro* studies showed promising results regarding the binding capacity of SSTR antagonistic to NENs [45] and the first SPECT study in NET patients, compared the distribution of one of the early antagonists ^{111}In-DOTA-BASS to ^{111}In-DOTA-octerotide, and reported a 4 times higher tumour uptake and lower kidney uptake of the antagonists [195]. For PET/CT, ^{68}Ga-DOTA-JR11 was tested [47] and in a recent phase 1/2 study, showed higher tumour-to-

normal tissue ratio than ^{68}Ga-DOTATOC, and with less kidney and bone marrow uptake [196]. As the antagonists possibly occupy multiple binding sites, and to a much lesser extent are internalized into the cell, they exert their effect from the outer membrane. In a therapeutic mice model, ^{177}Lu-DOTA-JR11 showed longer attachment to the cells compared to the agonists, which were internalized and metabolized [46]. Unfortunately, the radiation effects on kidneys and bone marrow presents a major challenge.

4.2.2.2.4 Eligibility

The patients´ eligibility to receive PRRT depends on their tumour SSTR expression. This was initially evaluated based on SSTR scintigraphy with indium-111 pentetreotide and estimated according to the Krenning score as described earlier (please see 3.2.2.) [109]. When scintigraphy was replaced by ^{68}Ga-DOTA-SSA-PET/CT, the Krenning score has been adapted accordingly, but differently in various centres and thus, without an established standard.

4.2.3 Safety monitoring

4.2.3.1 Dosimetry

Dosimetry is the method to calculate the absorbed energy from all primary and secondary ionizing processes occurring in biological tissues after radiation exposure. The basic requirements are; that the absorbed radioactivity can send out measurable photons and that the medium is homogenous and of a regular shape. As this is seldom the case in biological tissues, approximations are required. A major difference of PRRT, as compared to external radiation therapy, is the continuous internal radiation lasting for days or weeks instead the of iterative, short radiation pulses per day. To master this anomaly, various adapting techniques have been developed, one of which is to perform repeated measurements during PRRT for an extended time e.g., on days 1, 4 and 7, as performed at Uppsala University Hospital.

Dosimetry during PRRT was initially based on measurements from low-resolution antero-posterior 2D planar scintigraphy images, with low spatial resolution. Presently, dosimetry is based on 3D single-photon emission computed tomography (SPECT), with better resolution, and combined with CT for attenuation correction of the measurements, yielding considerably better results. Although still with its limitations, SPECT-based dosimetry provides estimates of the absorbed dose in various normal organs and/or tumours, although the method hitherto has not been fully developed and its accuracy not completely appreciated [189, 197]. Initially, the safety limits for the kidneys, was adopted from those set by the external beam radiation therapy (23 Gy) [198], and for the bone marrow, this was based on the earlier experiences with radioiodine therapy (2 Gy) [199]. However, an accumulated body of evidence, based on experiences from PRRT with ^{177}Lu-DOTATATE, has shown that the

upper limits for the kidneys is probably set too low and absorbed doses to kidneys up to 40 Gy BED have merely shown grade I-II side effects [200].

4.2.3.2 Local Practice of Dosimetry.

Dosimetry at our institution is performed as follows: For solid organs, the dosimetry is based on the small volume method, on SPECT/CT examination of the abdomen, and on one whole body scan [201]. A complete protocol is always performed at the first cycle with SPECT/CT examination on day 1, day 4 and day 7 after therapy start. Every second to third cycle, a shorter protocol is used with SPECT performed at 24 h only, and applying the same effective half-life estimate as in the earlier 7 days measurement. For bone marrow dosimetry, the complete protocol is based on an integrated blood activity curve (self-dose) resulting from blood samples taken at 0.5, 1, 2.5, 4, 8 and 24 h from therapy start. The total bone marrow dose is calculated by adding the self-dose from blood, to the photon dose from local activity in tumours, and the remainder of the body including organs. The photon dose is calculated from consecutive whole-body scans at 1,4 and 7 days after the therapy. The kidney, liver, spleen and tumours are delineated with regions of interest, and the whole body is calculated from the geometrical mean images at 24 h and are transferred to the 4- and 7-days images. The complete 7-days protocol is always achieved at the first treatment cycle and every third or fourth treatment cycle, but also when the tumour volume has changed substantially, on the suspicion of decreasing kidney function, and after extended delay between cycles.

4.2.3.3 Biochemistry

Before and after every PRRT cycle, the bone marrow and kidney functions are checked biochemically, verifying sufficient number of thrombocytes, acceptable white blood cell count and plasma creatinine.

4.2.4 The influence of cold somatostatin analogues in PRRT

There has been a concern regarding PRRT, that an excess amount of cold peptide may block the radiolabelled SSA from interacting with the SSTRs. As a consequence, ever since the introduction of PRRT, the recommendation is to perform both imaging and therapy just prior to the next SSA injection [114, 202]. This recommendation has prevailed in spite of the findings on SSTR scintigraphy by Dörr et al in 1993 (please see 3.2.3) [115], which is supported by studies performing ^{68}Ga-DOTA-SSA-PET/CT before and after the start of long-acting SSAs, and before and after repeated dose of long-acting SSA [117, 118, 203].

5 Treatment monitoring

5.1 History

At the appearance of cytotoxic drugs, it became obvious that specific criteria were necessary to monitor tumour response in phase II-IV trails. To meet this requirement, WHO presented a system of regulations and criteria on how to standardize the tumour response in 1981 [204]. As it turned out, these standards ("WHO criteria") were used differently among various centres and between different studies and thus a stricter standardization was called for. The result was the development of "response criteria in solid tumours, the RECIST 1.0," presented and published in 2000 [205]. A later revision, the RECIST 1.1, was presented in 2009, simplifying the therapy monitoring by including fewer tumours for size measurements (a maximum of 5 instead of 10) [206].

5.2 RECIST 1.1 and other criteria for therapy monitoring

The RECIST 1.1 version, still in use, is based on changes of the sum of target lesion diameters, measured by their largest transversal diameter, except for lymph nodes, measured by their short-axis (> 15 mm), and taking the appearance of new tumour lesions into account. The target lesions should consist of a maximum of five of the largest tumours/metastases (> 10 mm). Only two tumours per organ and a maximum of 2 metastatic lymph nodes are included. The same target lesions should be measured throughout the study. The RECIST 1.1 version does not specify the slice thickness for CT/MRI (as was the case in RECIST 1.0) due to the current high resolution multidetector CT and modern MRI scanners.

For assessments of regression, the sum of diameters is to be compared to that of the baseline examination (BL) by CT or MRI, while progression is compared to the examination when the sum was the smallest (nadir). When new lesions appear the RECIST 1.1 result is always progressive disease (PD) despite the response of the target lesions. RECIST 1.1 denotes four groups of response; complete response (CR) when there is no remaining tumour, partial response (PR) when the sum of the diameters has shrunk by < 30% of the base line value, progressive disease (PD) when the sum of lesion diameters

increases ≥ 20% compared to nadir, and/or the appearance of new lesions. Stable disease (SD) is defined as non- CR, PR or PD, i.e., when the sum of the diameters is within ≥ 20% of nadir and < 30% of BL and there are no new lesions. The tumours other than the target lesions, the "non-target lesions" are also assessed, but not measured. Occasionally, these alone are clearly seen to progress, "unequivocal progression of non-target lesions" resulting in PD. Enlarged lymph nodes included as target lesions need to be measured and registered even after normalization of their size (< 10mm). Thus, the sum of lesion diameters in a patient with CR can still be > 0 mm.

The RECIST criteria have been rightfully criticized for assessing size changes as the only indication of antitumour activity [207, 208].

One should bear in mind that the RECIST 1.1 criteria were developed for testing new cytotoxic drugs for treatment of solid tumours within general oncology. Thus, when used to evaluate other treatments and tumour types, the RECIST criteria may be less well suited, for example for treatment monitoring of slow-growing NETs, which also respond late with tumour shrinkage, or not at all, and instead merely stabilize. Cell death may result in extended tumour necrosis, and because of osmosis this may further lead to tumour enlargement, a pseudo-progression. None of these phenomena are accounted for by RECIST 1.1, both of which are of importance for evaluation of NEN therapies, and especially of PRRT. It should further be noted that RECIST 1.1 is tailored for comparing treatment results in dedicated study protocols.

Apart from RECIST 1.1, there is a variety of other criteria, suggested for assessing tumour response, such as the Choi criteria for GIST, incorporating changes in tumour CT attenuation, [209], the PERSIST criteria for therapy monitoring by FDG-PET [210], and the Deauville grading in lymphoma [211]. There are attempts to predict and monitor treatment effects in NETs with ^{68}Ga-DOTA-SSA-PET/CT, whereby tumour uptake has shown predictive of PRRT outcome [212, 213]. However, changes in tumour SUV have not correlated to response to PRRT [214, 215]. In studies on dynamic ^{68}Ga-DOTATOC/TATE-PET, the net influx rate Ki as a measure of tumour SSTR expression, has been shown to correlate to tumour SUV, but not for high values (> 25), The tumour-to-blood ratio, compensating for the saturation of tumour SSTRs, by contrast showed perfect correlation to Ki, and changes in the tumour-to-blood ratio is therefore currently evaluated in a clinical study for monitoring of PRRT (Weber MM, Pettersson O et al. Submitted manuscript).

A novel NET grading scheme, "NET-PET-score", was proposed by Chan et al. based on the combined findings from ^{68}Ga-DOTA-SSA-PET and FDG-PET [216] thus taking two aspects of cell biology into account, SSTR-expression and metabolic activity, for tumour characterization. In their retrospective study, they could show that this grading system correlated significantly to the patient outcome, whereas histological NET grade, age and presence of extra hepatic disease, did not.

6 Prognosis

Due to the scarcity of NENs and their heterogeneity, there are a limited number of studies with long-time follow up of separate NEN types. Thus, in most reports, especially from the early times, the cohorts included various NET types, making it difficult to draw conclusions concerning any specific NET type. The majority of NEN trials are observational, evaluating treatments in regards to progression free survival (PFS) and over-all survival (OS), and side effects for specific NEN types [193, 60]. The first prospective study to focus on a specific type of NEN was the NETTER-I trial focusing on PRRT outcome in SI-NET patients [190]. Further, the placebo-controlled, double-blind, prospective, randomized PROMID study investigated the effect of octreotide LAR in patients with metastatic neuroendocrine midgut tumours (SI-NET) [163, 155]. P-NETs, in particular, are more often studied, in separate cohorts, possibly depending on their more rapid response to treatment. By way of example, a resent long-term study on the outcome of a well-differentiated, locally advanced P-NETs in 99 patients treated with extensive surgery showed a 5-year survival of 91% and 5-year disease free survival of 61% [217].

7 Background to the thesis

PRRT constitutes an internal, targeted radionuclide therapy that provides prolonged survival in many patients suffering from progressive well-differentiated, disseminated, and/or non-resectable SSTR-positive NENs, whereby 7,4 GBq of ^{177}Lu-DOTATATE is administered intravenously in four cycles. There are two major philosophies regarding the PRRT treatment protocol. One is the "one size fits all" treatment comprise of 4 x 7,4 GBq of ^{177}Lu-DOTATATE, administered to everybody, with no regard to the NEN type, tumour burden, body-weight, or other individual characteristics, with a high risk of undertreatment but with minimal risks for adverse effects. The other, the so called "personalized" strategy, is an individually customised PRRT protocol, where the number of PRRT cycles and/or the amount of administered activity are adjusted, based on kidney and bone marrow reaction to the treatment measured by dosimetry for each patient and cycle. In Uppsala, the latter method was implemented and patients received between 2 to 10 PRRT cycles, tailored by dosimetry and kidney and bone marrow function until September 2018 [60].

P-NETs and SI-NETs, have, until recently been often regarded as one entity the so-called gastro-entero-pancreatic NETs (GEP-NETs), despite the knowledge that P-NETs for instance responded faster to PRRT with tumour shrinkage than SI-NETs [218, 219, 60]. This might have been due to the scarcity of patients, and possibly because of little knowledge and/or awareness of detail regarding differences between the two NET types. With the use of dosimetry-tailored PRRT whereby absorbed doses to organs and tumours were measured, a dose-response relationship was established for P-NETs [220].

The influence of the amount of cold peptide on the biodistribution of imaging radioligands (^{111}In-DTPA-octreodide and ^{68}Ga-DOTA-SSAs) has been investigated in several studies [115, 116, 203], but has not yet been thoroughly explored in the context of PRRT. There are concerns that i.v. administration of cold peptide may diminish the tumour uptake of the radiolabelled peptide, as was demonstrated *in vitro* and *in vivo* studies with ^{111}In-DTPAoctreodide [221].

8 Aims of the thesis

The general aim of this study was two-fold; firstly, to explore differences and similarities between well-differentiated and disseminated P-NETs and SI-NETs in their response to PRRT with ^{177}Lu-DOTATATE. The second aim was to analyse the influence of peptide mass, both on receptor behaviour (internalization and re-cycling), and on the absorbed doses in tumours and normal tissues.

8.1.1 Paper I

To investigate a possible dose-response relationships in small intestinal neuroendocrine tumours (SI-NET) during and after the treatment of peptide receptor radionuclide therapy (PRRT) with ^{177}Lu-DOTATATE.

8.1.2 Paper II

To evaluate and compare tumour-related and patient-associated parameters between well-differentiated progressive pancreatic and small intestinal neuroendocrine tumours in the context of PRRT with ^{177}Lu-DOTATATE.

8.1.3 Paper III

To assess the time-dependent effect of somatostatin receptor depletion and recirculation in small intestinal neuroendocrine tumour (SI-NET) metastases and normal tissues (liver, spleen, kidney and bone marrow), following a single intravenous high dose of short-acting somatostatin agonist (400µg octreotide) by means of ^{68}Ga-DOTA-TOC PET/CT during 7 hours.

8.1.4 Paper IV

To assess the possible impact of administered peptide at the first cycle of PRRT on the absorbed dose in selected pancreatic and small intestinal neuroendocrine tumours and normal organs, in relation to the patients´ total tumour somatostatin receptor expression.

9 Materials and Methods

9.1 Study population

All patients in this thesis suffered from locally advanced and disseminated, well-differentiated NETs of the pancreas (P-NETs) or the small intestine (SI-NETs) confirmed by histopathology. They were eligible for PRRT or had undergone PRRT at Uppsala University Hospital. The first paper (Paper I) includes twenty-five SI-NET patients who had completed PRRT with ^{177}Lu-DOTATATE according to the personalized treatment regime, administered at Upsala University Hospital. Paper II includes twenty-four SI-NET patients from Paper I together with twenty-tree P-NET patients earlier reported by Ilan et al. [220]. Paper III includes four SI-NET patients who underwent the experiment one day prior to PRRT, and Paper IV includes 62 patients with P-NET and 141 patients with SI-NET, for whom data collected in connection to their first cycle of PRRT were evaluated. The patients in Paper I, II and IV were retrieved from the list of patients receiving PRRT by compassionate use, and later from the cohort in the prospective PRRT study EudraCT nr 2009-012260-14. All patients demonstrated sufficient tumour expression of SSTR on somatostatin receptor scintigraphy, according to the Krenning score for PRRT [109].

9.2 Data acquisition

9.2.1 Paper I and II

All patients´ data in Paper I and II were retrieved from the patients´ digital medical records and the digital radiological information system (RIS) and picture archive and communication system (PACS) at Uppsala University Hospital. The patients´ eligibility for receiving PRRT was evaluated on somatostatin receptor scintigraphy with OctreoScan™, according to the Krenning score. The individual number of PRRT cycles for each patient was guided by the accumulated absorbed doses to the kidneys and bone marrow. All patients (n=25) included in Paper I, suffered from SI-NETs, and underwent PRRT with 3-7 cycles of ^{177}Lu-DOTATATE. Most of these patients received 7,4 GBq ^{177}Lu-DOTATATE at each cycle (n=20) and out of 124 cycles, ten cycles (12%) in five patients, the administered activity was reduced (to 6 or 5,5 GBq).

In Paper II twenty-four of the patients described in Paper I were included together with twenty-three pancreatic P-NET patients, who had undergone 2-6 cycles of PRRT as earlier reported by Ilan et al. [220] , but were re-evaluated and compared to the SI-NET patients. Most of the P-NET patients were infused with 7,4 GBq ^{177}Lu-DOTATATE at each cycle (n=16) and out of 102 cycles eleven cycles (11%) in seven patients were reduced (to 6 or 5,5 GBq). In Paper I and II the selected tumours were all larger than 2.2 cm in order to apply to the requirements of the dosimetric method used [197]. Furthermore, the selected lesions were sufficiently isolated from other tumours, and normal-tissue accumulations, in order to minimize scatter. Suitable tumours in Paper I, were identified by the author on the baseline CT examinations. All P-NET patient in study II, earlier reported, were revaluated by the author in the second study.

In both Paper I and II, imaging after start of PRRT was performed on an Infinia Hawkeye SPECT/CT system (GE healthcare) with MEGP collimators. In both papers, a phantom was used to measure partial volume effect (PVE) correction. In a NEMA IQ phantom, six hollow spheres were filled with ^{177}Lu-DOTATATE and scanned using the same SPECT/CT scanner with identical imaging parameters as for patients. Tumour response was evaluated with clinical routine CT/MR of the abdomen employed pre-therapy, between cycles and post-therapy at ordered intervals.

Plasma chromogranin A (P-CgA) and urinary 5-hydroxy-indol-acetic acid (U-5-HIAA) was measured at scheduled follow-up visits during and after PRRT.

9.2.2 Paper III

Four patients participated in the study the day before their first cycle of PRRT. A base line ^{68}Ga-DOTATOC PET/CT (whole-body) (WB 0), was performed 1–3.5 months earlier. The study day was initiated by the intravenous infusion of 400μg, after which three consecutive dynamic PET/CT examinations were performed with three hours intervals. Each scan started simultaneous with intravenous injection of ^{68}Ga-DOTATOC and lasted for 45 minutes. Scan number 2 and 3 was preceded by a static acquisition for 5-minutes including the patients' upper abdomen, to account for the remaining activity. The dynamic scans were reconstructed into 22-time frames (6x10, 3x20, 3x60, 5x180, 5x300 s). Each dynamic scan was followed by a whole-body PET/CT examination, one hour after tracer injection; 1 h (WB 1), 4 h (WB 2), and 7 h (WB 3). The same scanner (GE Discovery MI PET/CT) was used for all patients. A graphic representation of the study design is given in (Figure 1).

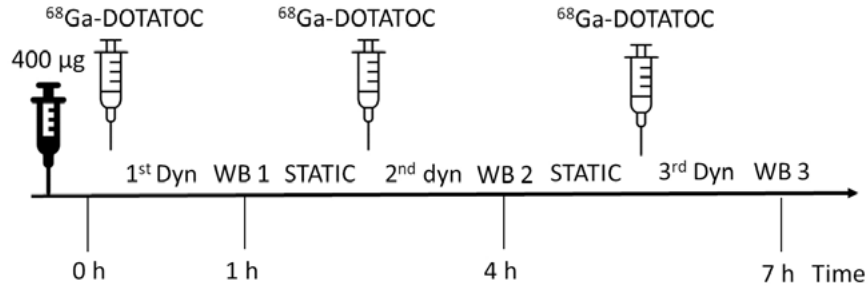

Figure 1. *Schematic overview of the study design for study III.*

9.2.3 Paper IV

In Paper IV, only the first cycle of the PRRT was assessed in the eligible SI-NETs and P-NETs patients (n=203). In the cohort of more than 800 NEN patients, undergoing PRRT with the ^{177}Lu-DOTATATE inhouse preparation, at Uppsala University Hospital between 2006 to 2018, 510 SI-NET and P-NET patients were identified and 203 (40%) of them were suitable for assessment. All study patients had undergone SPECT/CT with indium-111 pentetreotide for the Krenning evaluation of eligibility for PRRT, and received 7,4 GBq ^{177}Lu-DOTATATE at their first PRRT cycle. For tumour-absorbed-dose estimations the dosimetry method as described in Paper I and II was used. Because data were retrospectively collected from PRRT performed over a decade, the SPECT imaging utilized four types of gamma cameras; Millenium VG, Infinia, Discovery 670 and SPECT/CT CZT (General Electric Medical Systems), all equipped with a CT scanner used for attenuation correction. The VG camera applied 60 angles with 60 s for each frame for the imaging, and 120 angles with 30 s for each frame was used in the other three systems. In the CZT camera the energy window was 208 keV (±6%), and 113keV (±10%) and 208 (±10%) windows were summed for the VG camera. Both for the Infinia and Discovery 670 cameras the energy windows were 208 (±10%). For the CZT camera the collimators were MEHR and for the other tree systems it was MEGP.

The administered amount of peptide in each PRRT cycle was retrieved from analogue data sheets and the patients´ body-weight from digital medical records. The patients´ total tumour somatostatin receptor expression (tTSS-TRE) was assessed from the 24h SPECT examination, performed for dosimetry, by using a non-commercial research version of Affinity Viewer 3.0 (HERMES Medical Solutions AB., Stockholm, Sweden). As the SPECT images represented counts, an Excel sheet was prepared with a function to recalculate a pre-defined SUV to counts for each patient, in order to apply a SUV-based cut-off volume of interest (VOI) for the tumour delineation. The function was taking into account the amount of administered activity (7,4 GBq),

the patient´s weigh, and the respective calibration factor to correct for the different sensitivities (counts/Bq) for each of the four gamma camera types

9.3.1 Volume Measurements

In the first two studies (Paper I and II) the assessments of the clinical SPECT/CT examinations and those of the phantom utilized a Hermes workstation (Hybrid PDR, version 1.4B, Hermes medical solutions). An automated 42% threshold iso-contour VOI was applied for the measured tumours and phantom spheres, and all the tumours included in the study were larger than 2.2 cm throughout the course of the study. In Paper I both tumour and liver volume at each examination was measured by using the semi-automated software offered by the vendor (Carestream Vue PACS, version 12.0.0.7; Lesion Management) and manually corrected to fit the outer border of the tumours and livers. In Paper II all selected tumours were re-evaluated, by the first author, according to their largest transversal diameter as well as tumour volume (calculated using the semi-automated soft-ware and with manual corrections), time to best response, time to progression and the over-all survival of each patient.

Paper III, calculating the receptor reactivation, used Hermes (Hybrid viewer PDR, version 5.1.1, Hermes Medical Solutions) to evaluate the PET/CT examinations. All measured tumours were larger than 1 cm in diameter and the VOIs were delineated by using a 50% iso-contour threshold.

In Paper IV, dosimetry was performed for the patient´s two to three largest tumours with the highest uptake on 24 h SPECT. The total somatostatin tumour receptor expression (tTSSTRE) of the tumour load for each patient was assessed on the SPECT acquired 24h after start of PRRT, by using a non-commercial research version of Affinity Viewer 3.0 (HERMES Medical Solutions AB., Stockholm, Sweden). From an Excel sheet with a function to transform SUV to counts, the calculated pre-defined “cut-off” count number for the individual patient was entered into the threshold VOI tool of the Affinity Viewer software. Semiautomated VOIs were then generated to outline all tumours within the field-of-view of the SPECT examination. For tumour conglomerates, a software “splitter” tool allowed for larger VOIs to be split into smaller VOIs, representing single tumours and/or more homogenous tumour areas (Figure 2). In the next step, a 42% cut-off of the highest activity in each VOI was applied, and the resulting functional volume (FV) of each VOI was registered, together with their respective number of counts. By again using the Excel sheet, now instead entering the number of counts for each VOI, the reverse recalculation provided their the respective SUVmeans. For each VOI, the SUVmean was multiplied by the FV to achieve its tumour somatostatin receptor expression (TSSTRE). In the final stage, the TSSTRE for all tumour VOIs were added to form the patient´s tTSSTRE. The intention was to apply an identical SUV cut-off value for the tumour VOI measurements in all

patients. However, when performing a pilot test on P-NETs (n=48) and SI-NETs (n=73), it was found necessary to adapt separate SUV cut-off values for patients with high tumour load (SI-NETs SUV 5,5 and P-NETs SUV 7,1) but the same for all patients with low tumour burden (SUV 3,5).

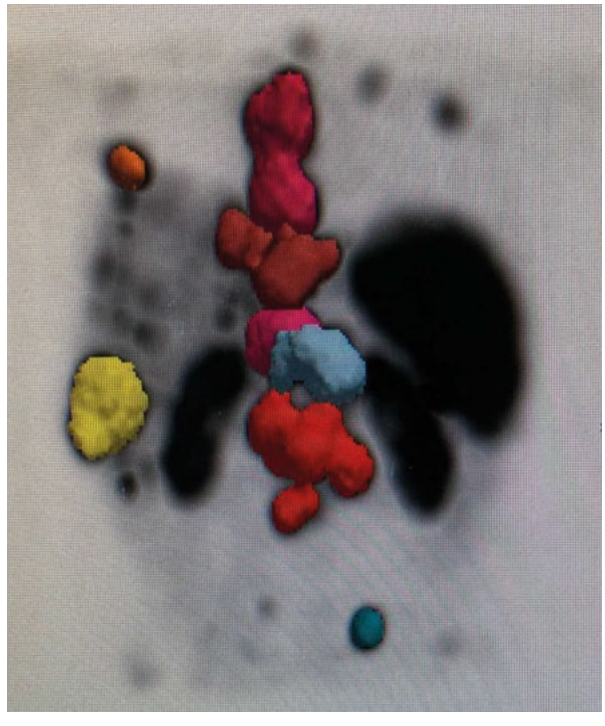

Figure 2. *"Semiautomated VOIs were generated to outline all tumours within the field-of-view of the SPECT examination"*

9.3.2 PET measurements in normal organs

PET measurements of normal organs (liver, kidneys, spleen, pancreas and bone marrow) utilized a spherical 1.5 cm diameter VOI. The blood measurements in the left ventricle of the heart and in the descending aorta were performed with 1 cm diameter VOIs.

9.3.3 Dosimetry

Full dosimetry calculations (the absorbed dose in tumours) after start of PRRT with ^{177}Lu-DOTATATE requires SPECT/CT readings at 24, 96, and 168 h at the first, third and fifth cycle. The time-integrated-activity concentration was assessed from the area under the curve of a single exponential fit. The phantom studies provided the recovery coefficients used for correcting the partial volume effect (PVE) when calculating the activity concentrations for each

SPECT scanning time point. At the interceded cycles, a 24h SPECT was used based on the effective half-life presented at the previous full dosimetry protocol thus presumed to be unaffected between the two cycles.

9.3.4 Best response

In Paper I and II the shrinkage of the selected tumours, named the best response, was calculated from the baseline to when progression of the disease appeared, and was determined as changes in both selected tumour transverse diameters and change in the selected tumour volumes compared to base line. Best response was also assessed according to RECIST 1.1.

9.3.5 Statistical Methods

In **Paper I**, the JMP 12.0.1 software package (SAS Institute Inc., Cary, NC, USA), was used for calculations of correlations and linear regression. A p-value less than 0.05 was regarded statistically significant, in combination with an explanation value of r^2 larger or equal to 25%.

In **Paper II**, the Kaplan–Meier analysis was used to calculate the PFS from the first PRRT cycle until any progression based on CT/MR was found according to RECIST 1.1 or death. The JMP 12.0.1 software package (SAS Institute Inc., SAS Campus Drive, Cary, North Carolina 27513, USA) was employed for reckoning the linear regressions, Kaplan–Meier analysis, the Wilcoxon signed-rank test and creating the box plots. A p-value less than 0.05 with an explanation value of r^2 larger or equal to 25% was required for the linear regression to be regarded statistically significant. Microsoft Excel was used for analysing the descriptive statistics and paired t-tests, and the differences within groups were anticipated to be significant at 95% level using the independent t-test and manually calculated confidence intervals; to illustrate correlations and confidence intervals the GraphPad Prism, Version 6.07 was utilised.

In **Paper III** the Wilcoxon matched- pairs test was exercised (Prism, version 6.07; GraphPad Software, Inc.) when assessing the tumours and whole-blood SUV (and normalised SUV) and comparing between all whole-body images. For significance the level was set to p-value less than 0.05. For calculating the three dynamic PET scans regarding K_i the same test was used. Linear regression and the square of Pearson correlation was utilised when evaluating the relationship between K_i and tumour to blood ratio and the relationship between K_i and SUV

In **Paper IV** the injected amount of peptide, and the median absorbed dose in tumours and normal tissues, in relation to the tTSSTRE was calculated using the Speaman´s Rank test.

10 Results

10.1 Paper I

Paper I, failed to show any dose-response relationship in the 25 SI-NET lesions in regards to either the transverse diameter or the volume of the tumours, during the mean 26 months follow-up time. This result was in contrast to what was earlier reported for P-NETs in a study from our department [220]. However, for the analysed SI-NET lesions, there was a correlation between the amount of administered activity and tumour volume shrinkage ($r^2 = 0.25$, $p = 0.01$) and tumour shrinkage when measured according to RECIST 1.1. ($r^2 = 0.28$, $p = 0.01$) although with a fairly low explanation of both values (Figure 3, 4).

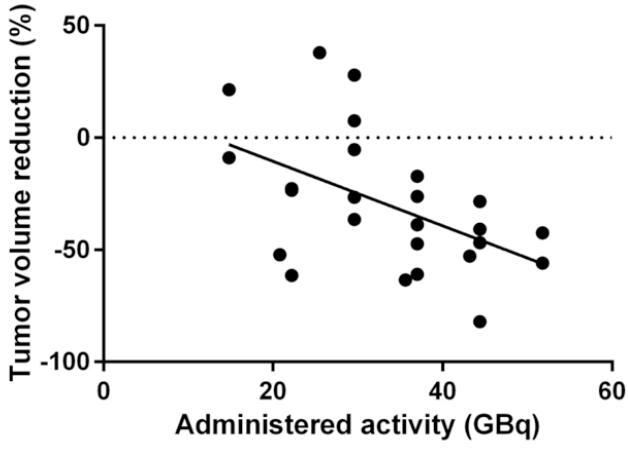

***Figure 3**. Tumour volume shrinkage ($r^2 = 0.25$, $p = 0.01$)*

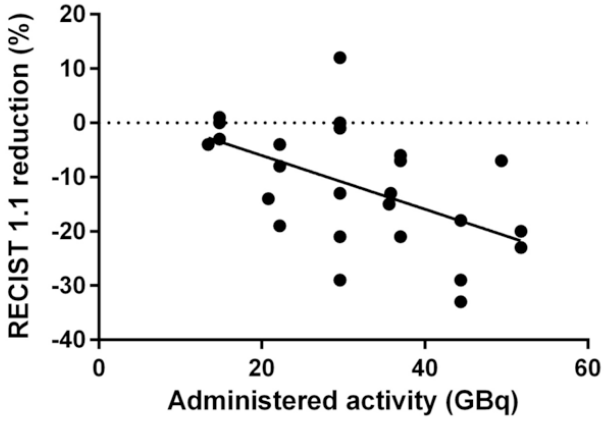

Figure 4. *Tumour response according to RECIST 1.1 versus administered radioactivity (r^2 = 0.28, p = 0.01).*

10.2 Paper II

With the longer follow-up in Paper II (mean 49 months), as compared to in Paper I (mean 26 months), a weak dose-response relationship was found in the SI-NET lesions between absorbed dose and tumour diameter shrinkage (r^2= 0.29, p= 0.001) and between absorbed dose and tumour volume shrinkage (r^2= 0.26, p= 0.02), although not as strong as the corresponding correlations for the P-NET lesions (r^2= 0.37, p= 0.004 and r^2= 0.31, p= 0.03, respectively) (Figure 5, 6). The correlation between administered activity and SI-NET lesion shrinkage, noted in Paper I, was strengthened by the longer follow-up (r^2= 0.28 to r^2= 0.33). No such correlation, between administered activity and tumour shrinkage, was found in the P-NET group (Figure 7).

Further, a significant decrease of the absorbed dose in the P-NETs between consecutive cycles, was demonstrated (Figure 8), and could be related to a corresponding decrease in tumour-to-aorta ratio between cycles, as measured on contrast-enhanced CT (Figure 9). In the SI-NETs a corresponding, although non-significant, decline was seen. Furthermore, in the native phase of the at BL CT examination, the tumour attenuation (Hounsfield Units, HU) of the 25 SI-NET lesions was higher than that in the 23 P-NET lesions, indicating a denser tissue in the former group. As assessed on contrast-enhanced CT in the late arterial contrast-enhancement phase of the same BL CT examination the 23 P-NET lesions demonstrated a higher degree of vascularization compared to that of the 25 SI-NETs.

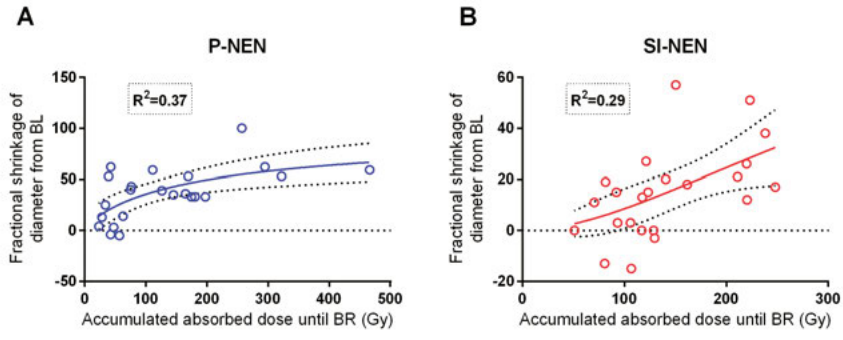

Figure 5. *Comparison between tumour dose (Gy) and diameter shrinkage in P-NENs versus SI-NENs. Accumulated absorbed dose (Gy) to the tumour versus maximum fractional diameter shrinkage in P-NEN lesions (A) (n = 23) and SI-NEN lesions (B) (n = 24). P-NEN (p = 0.004), SI-NEN (p = 0.001). BL; baseline.*

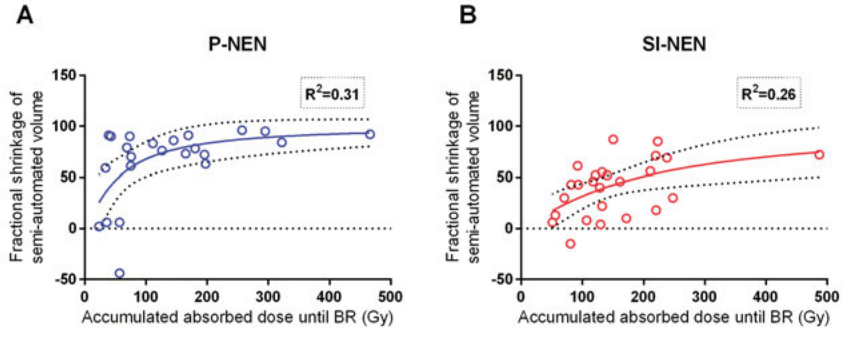

Figure 6. *Comparison between tumour dose (Gy) and semi-automated volume (cm^3) shrinkage in P-NENs versus SI-NENs. Accumulated absorbed dose (Gy) to the tumour versus the maximum fractional shrinkage of semi-automated volume (cm^3) in P-NENs (A) (n = 23) and SI-NENs (B) (n = 25). P-NEN (p = 0.03), SI-NEN (p = 0.02). BR: best response.*

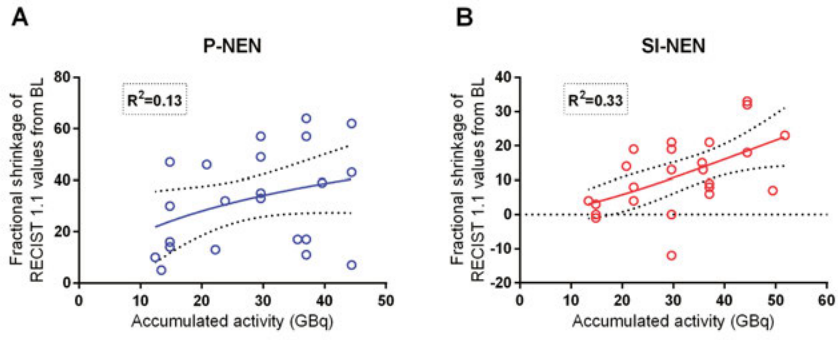

Figure 7. *Correlation between accumulated activity (GBq) and RECIST 1.1 values. Accumulated activity (GBq) versus RECIST 1.1 values. (A) P-NENs (n = 23) and (B) SI-NENs (n = 25). P-NENs (p = 0.1) SI-NENs (p < 0.01). Two patients in each group have identical values. BL; baseline.*

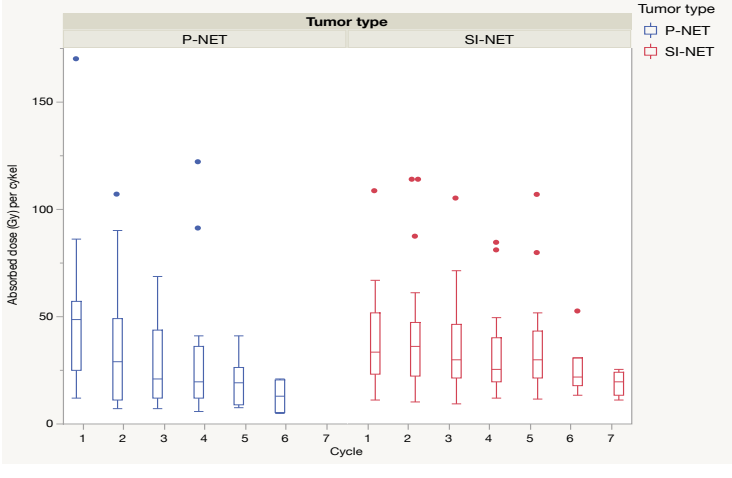

Figure 8. *Tumour dose at each dosimetry estimates. Median absorbed dose (Gy) in the measured tumours at each cycle. Full seven-day dosimetry cycles are shown together with 24h dosimetry results. The absorbed doses showed a continual decrease during the course of PRRT in both P-NETs (blue) (n=23) and SI-NETs (red) (n=25).*

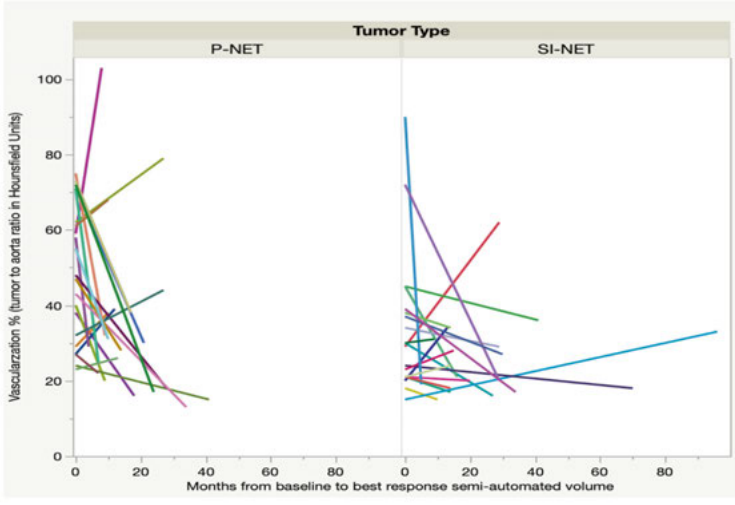

Figure 9. *Fractional change (Δ%) of the tumour to aorta ratio (as an indication of tumour vascularization) from CT at base line to best response, as regards fractional semi-automated volume. Each line represents one tumour*

10.3 Paper III

All measurements of tumour SUV at the three whole-body (WB 1-3) PET examinations during the study day were normalised against the tumour SUV at the baseline PET WB0. Immediately after the intravenous injection of 400µg short-acting octreotide, the receptor activity (and uptake of ^{68}Ga-DOTA-TATE) decreased in tumours (ratio < 1). This study shows a tumour receptor recovery of the normalised SUV from base line levels already at four and seven hours (WB2 and WB3) (Figure 10 A-D). Thus, for the tumours there is a prompt and significant (p<0.05) recovery to base line values and even above, for the normalised SUV in each step from WB1 to WB2, from WB2 to WB3 and from WB1 to WB3. Regarding the net influx rate, K_i, determined in the dynamic scans, a significant increase between the first and second and the first and third scan was disclosed (p<0.05), although not between the second and third scan (p >0.05) (Figure 11). Pearson correlation (square) used for comparison between the K_i values to both the SUV and TBR demonstrated a linear correlation of 0.96 and 0.97, respectively.

The normalized SUV continued to stay low in all normal organs, apart from the kidneys and bone marrow (Figure 12 A-C), and only the kidneys and the bone marrow reached base line values (Figure 12 D-F).

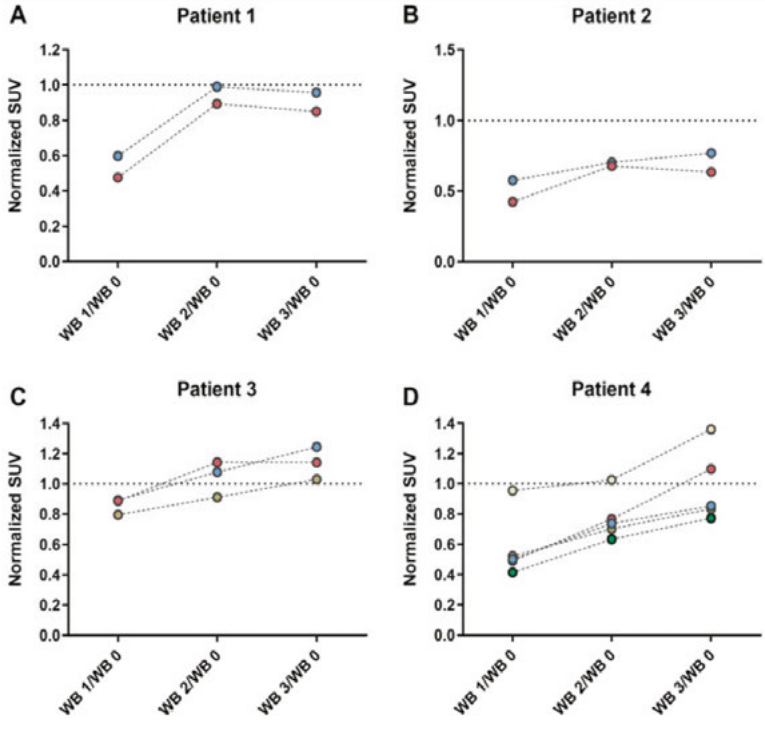

***Figure 10**. Normalized tumour SUV for patients in Paper III where SUV in whole-body (WB) 1,2 and 3 is normalized against WB 0 (baseline scan)*

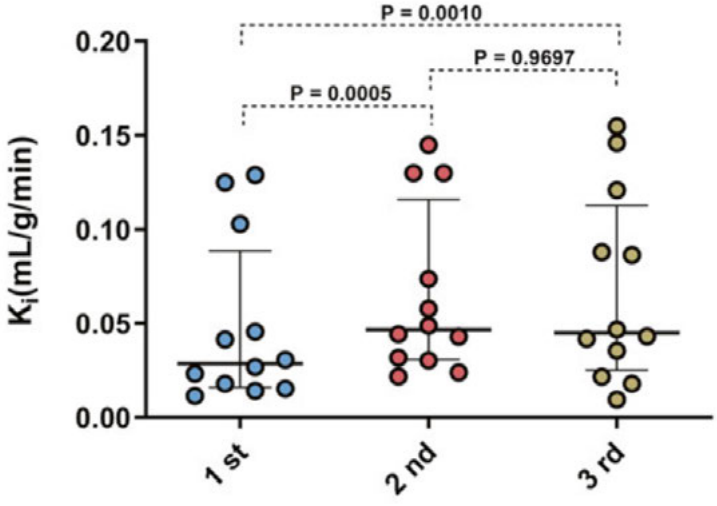

Figure 11. *Scatter dot plots of K_i at the first, second, and third dynamic scan (0, 4, and 7 h). Between the first and the second dynamic scan, a significant increase was found in tumour K_i. This was also seen between the first and third dynamic scans but not between the second and third. Solid horizontal lines show median and interquartile range.*

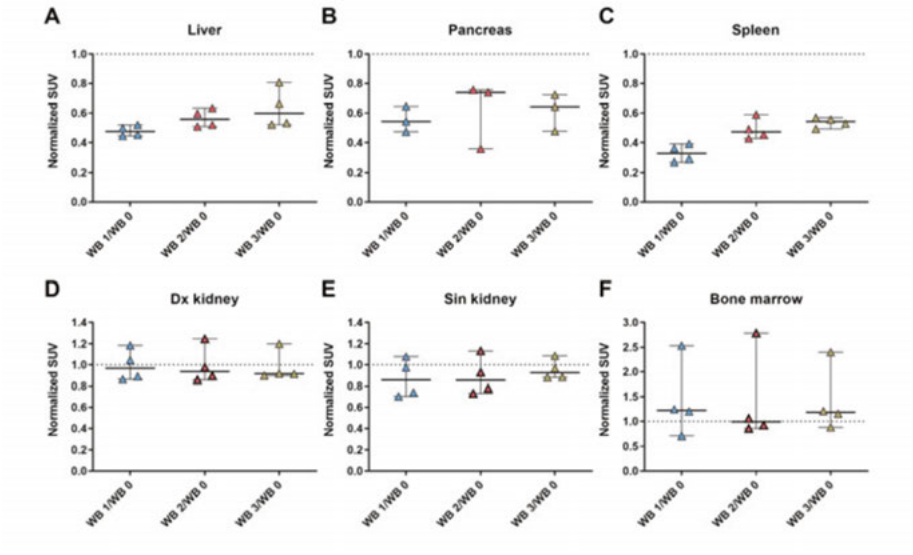

Figure 12. *Scatter dot plots of normalized SUV in the liver (A), pancreas (B), spleen (C), dexter and sinister kidney (D and E), and bone marrow (F) where SUV in whole-body (WB) 1, 2 and 3 is normalized against SUV at WB 0 (baseline scan). Solid horizontal lines show median and interquartile range.*

10.4 Paper IV

No influence of the amount of peptide (µg) in the PRRT preparation could be seen regards any of the tested entities in relation to tTSSTRE, when using the Spearman's Rank correlation. In the separate regression analyses no influence of the administered amount of peptide (µg) was found when tested separately in subgroups of tTSSTRE (low, median and high) (Figures 13).

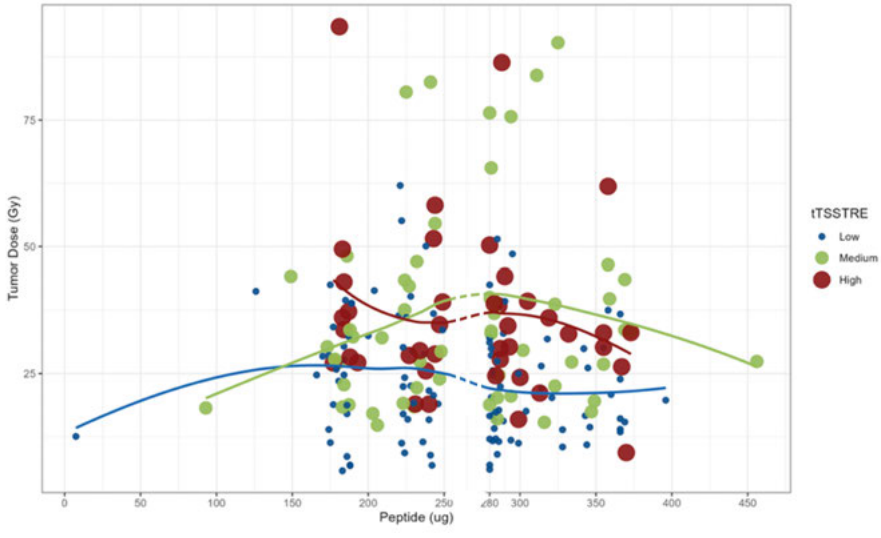

Figure 13. *Regression analyses whereby the mean tumor dose (Gy) is plotted against the administered amount of peptide (µg) at the first PRRT cycle in respect to the patient`s total tumor somatostatin receptor expression (tTSSTRE). The blue dots (the smallest) represent the patients in the lowest tTSSTRE group (values <5000, (SUV x mL) n=106), the green dots (slightly larger) represent the patients in the medium tTSSTRE group (values 5000 – 15000, (SUV x mL) n=56) and the brown dots (the largest) represent the patients in the largest tTSSTRE (SUV x mL) group (values >15000, (SUV x mL) n=41). The blue, green and red lines represent the fitted line for the peptide values of each tTSSTRE group.*

11 Discussion

The first two retrospective studies focus on the relationship between the tumour dose at PRRT and the treatment effects in well-differentiated SI-NETs and P-NETs, with the aim to improve the understanding of significant factors that may influence the outcome of PRRT. Paper I, found a lack of dose-response in the SI-NET lesions, between absorbed dose in the tumours and largest tumour diameter and the tumour volume, respectively, during mean 26 months follow-up. Contrariwise, a correlation was discovered between the amount of administered activity and the tumour volume shrinkage, as well as RECIST 1.1. results. The lack of dose-response in SI-NET lesions contrasted to the earlier reported dose-response found for P-NET lesions [220]. The lack of morphological response in the SI-NETs during the early period post PRRT is believed to, at least partly, be explained by a high content of fibrotic tissue, preventing apparent tumour shrinkage on CT/MRI. Another explanation, may be the low mitotic activity in the SI-NETs, with few dividing tumour cells, and therefore less sensitivity to radiation.

Paper II, allowed for a longer follow-up period, median 49 months, at which time a dose-response was found in the SI-NET lesions. Otherwise, this study could report findings that separate the two NET types in a basic way. At the BL CT/MR examinations the P-NETs demonstrated higher contrast-enhancement of TBR in the late arterial phase, interpreted as an effect of better vascularization in P-NETs. The SI-NET lesions, conversely, demonstrated higher attenuation HU on non-enhanced (native) sequence at BL, indicating a more compact tissue, consistent with high fibrotic content in SI-NETs [57]. The standard deviation of the tumour attenuation measurement (HU) in the non-enhanced CT at BL, however, were the same in SI-NETs and P-NETs, indicating similar degree of heterogeneity in the two NET-type lesions. While the accumulated absorbed dose of the assessed tumours was similar in the two NET groups, the absorbed dose in the P-NETs for individual PRRT cycles declined significantly between the first and the last cycles. This reduction in consecutive cycles was further paralleled by a decrease in the blood supply, from the first to the last cycle. The better vascularization in primary P-NETs than in solid tumours is known from earlier reports and was found to correlate to survival [222, 223]. It is also known that better tumour vascularization improves the cellular oxygenation and makes them more susceptible to ionizing radiation [172]. The reduced absorbed dose in the P-NETs during the course

of PRRT can only be speculated on. One reason could be the reduced vascularization, due to radiation damage to the vessels, with decreased delivery of both ^{177}Lu-DOTATATE and oxygen, and the reduction of oxygen will further diminish the effect of the radiation. It is also possible that the radiation damage reduces the receptor capacity of the tumour cells, hampering the influx of the ^{177}Lu-DOTATATE preparation. Further, with subsequent tumour shrinkage the dosimetric calculations will become less precise, because of increased PVE, possibly underestimating the radioactivity concentration [220]. Additionally, the reduced absorbed dose in consecutive cycles could be an influence of the so called low LET radiation-induced adaptive response (RIAR) [172]. Results from *in vitro* studies on cancer cell lines, also indicate the existence of transportable microparticles, that create antitumor effects through the death of immunological cells in the tumour micro environment that might add to the negative factors [224].

The longer observation time after PRRT disclosed a dose-response in SI-NETs, indicating that change in size is slower for this NET type, which is well known regarding tumour growth of SI-NETs [58, 225, 226, 60]. One possible explanation for this could be the higher degree of fibrosis, with restricted capacity to change in size (shrinkage and growth), in spite of the decreasing/increasing number tumour cells. An alternative explanation is that with the lower mitotic activity in G1 tumours, dominating the SI-NET group in our study, fewer tumour cells are radiosensitive to PRRT. Thus, based on these differences between P-NETs and SI-NETs, it would be reasonable to regard the two NET types as separate entities. The prevailing practice in many studies, is to lump P-NETs and SI-NETs, together with other gastrointestinal NETs, into a broader NET category, GEP-NETs. This will, however, emphasis similarities rather than explore differences between the NET-types, and prevent discovery of individual NET-type-specific factors, that may constrain the development of more effective treatments. Despite differences in appearance at BL and behaviour during PRRT, the mean time to best response was similar for P-NETs and SI-NETs, with a tendency to be on the slow side in the SI-NET group. The median PFS was similar for P-NETs and SI-NETs, which is in line with an earlier report [60] and the reason for this can only be speculated on.

In the third study (Paper III), the influence of amount of administered peptide on the receptor turnover, and specifically the depletion and reappearance of SSTRs in SI-NETs as compared to normal organs, was addressed. A single intravenous injection of 400µg octreotide (equivalent to a large peptide amount at PRRT) was followed by three dynamic sessions and whole body (WB) of ^{68}Ga-DOTATOC (2 MBq/kg) during seven hours, to register the timing of SSTR reappearance in SI-NET tumours and normal tissues. In this study also the rest activity before the next tracer injection was accounted for. It was found that compared to the BL examination (WB0), the SSTR expression in most tumours (and in liver, spleen and pancreas) dropped significantly

following octreotide injection on the first whole body ^{68}G-DOTATOC PET/CT (WB1). Over time (in WB2 and 3), tumour SUV was, however, restored to the baseline level in most of the tumours (7/12); but in the liver, spleen and pancreas, only partial recovery was seen at WB3, the last point of measurement (7h). The five non-responding tumours (from different individuals), had all a functional volume between 1 and 4 mL, and responded with a pattern more resembling that of the normal tissues. For SI-NETs, this might resemble the different behaviour between small and large NETs earlier described for P-NETs by Ilan et al. pointing out the more pronounced effect of PVE in small lesions compared to larger tumours [220]. Regrettably, the reduction of receptors after the single bolus of peptide was not obvious in the two most radiosensitive organs, the kidneys and bone marrow, which for the former probably was masked by the radioactivity excreted in the urine. This knowledge, not earlier described *in vivo*, opens the possibility to partially spare normal organs from radiation exposure in the initial phase of PRRT, thus allowing for more activity to be available for the reappearing tumour receptors, which might improve the absorbed dose in the larger (> 4cm), responding tumours. However, the total somatostatin receptor expression of the tumours will always be the ultimate limitation.

A major drawback of Papers I-III, is the small number of patients, and consequently with low statistical power. In paper I and II, both retrospective, this was owing to the requirements of the dosimetric method, leading to a strict selection of tumours to be included in the study. It may be well debated to what extent the selected tumours can be regarded as representative of the patient´s total tumour load, or even representative for a larger study cohort. Yet, the differences between the SI- and P-NEN types, as regards volume change, degree of vascularization, and tissue density, seem to be larger between these two types than within each NET type, despite their individual heterogeneity.

Paper IV**,** also retrospective, assessed 40% of all SI-NET and P-NET patients treated with PRRT at Uppsala University Hospital, without finding any influence of the amount of peptide in the ^{177}Lu-DOTATATE preparation, on the absorbed dose in tumours, normal organs or the tumour-to-normal-tissue ratios, in relation to the patient´s total tumour load, expressed as its tTSSTRE. The tTSSTRE is based on the assumption that the number of counts registered in the tumours with the highest ^{177}Lu-DOTATATE uptake at 24 hours after start of PRRT, represents the receptor activity of the tumours. In a prospective study, the optimal time point for SPECT to quantify tTSSTRE would instead be at approximately 3h following ^{177}Lu-DOTATATE administration [227]. At the time point of 24h it is uncertain what the remaining radioactivity in the tumours represent; considering *in vitro* studies stating that only 50% of the initially incorporated radioactivity remain in the cells after 12 hours [33, 37], and that analysis of radiolabelled metabolites in blood, shows that at 24h less than 50% of the administered ^{177}Lu-DOTATATE is intact [188]. These metabolites have so far not been characterized, and their potential SSTR binding

capacity is unknown. Given the sparse evidence in the literature of the impact of the administered peptide mass at PRRT on NETs, in relation to the total tumour load, our findings warrant further investigation.

12 Conclusions

Paper I. It was not possible to identify any dose-response relationship in SI-NETs, although a positive correlation was found between the administered amount of activity and tumour volume shrinkage and RESIST 1.1 results.

Paper II. In P-NETs a subsequent decline of the absorbed dose was found in consecutive cycles, paralleled by a decline in the tumour vascularization on contrast-enhanced CT, but not in the SI-NETs. The correlation between administered amount of activity and tumour response according to RECIST 1.1 in SI-NETs was corroborated, but no such correlation was disclosed in the P-NET group. With the longer observation time, a weak dose-response relationship appeared in the SI-NETs.

Paper III After a large pre-load (400 µg) of i.v. short acting octreotide, prior to serial ^{68}Ga-DOTATOC-PET/CT examinations during 7h, faster recycling of SSTRs was found in larger (> 4cm) SI-NET than in smaller tumours (< 4 cm) and in normal organs, apart from kidney and bone marrow. This might open the possibility to partially protect normal tissues by pre-administering a single dose of cold peptide before start of PRRT, and thus allow for better tumour-to-normal tissue ^{177}Lu-DOTATATE uptake ratios.

Paper IV. No influence of the amount of administered peptide at PRRT could be demonstrated, on the absorbed dose in tumours or normal organs, in relation to the patients´ total tumour SSTR expression.

13 Future perspectives

In spite of two decades of PRRT to patients with well-differentiated and progressive NETs, there are still aspects of this treatment that need to be further investigated to improve the therapy outcome.

By considering the basic differences between P-NETs and SI-NETs, as identified in Paper II, and adjusting the PRRT protocol according to NET-type and mitotic status (G1, G2 or G3), the effects of PRRT might improve. Therapy monitoring by assessing changes in tumour volume, instead of transverse lesion diameter, will probably provide more accurate information.

Further, a redistribution of the amount of administered radioactivity between cycles in P-NET patients, would probably improve the accumulated absorbed dose in the tumours, and possibly minimizing the effect of radiation-induced adaptive response (RIAR).

The identified differences in the recycling time of SSTRs between large SI-NET tumours (> 4 cm) and normal organs opens the possibility to provide a protection of normal tissues at PRRT by adding a five to seven hours preload with short acting octreotide to the PRRT protocol. This might be especially useful in PRRT using SSTR antagonists, as these have shown more radiation to normal organs and tissues.

One day, it might be possible to evaluate the total receptor volume of the patient´s tumours at the time of treatment, without the use of radionuclide-based imaging, that triggers the RIAR, and administer individualized amounts of radioactivity to the tumours at each PRRT cycle, while spearing normal tissue.

14 Populärvetenskaplig sammanfattning

Neuroendokrin neoplasi (NEN) utgör ett samlingsnamn för en sällsynt tumörform som utgår från en unik typ av endokrina celler, spridda i alla vävnader, vilket gör att NEN kan uppstå var som helst i kroppen. Tumörerna uppvisar blandformer genom att de kombinerar egenskaper från ursprungsvävnaden med specifika neuroendokrina egenskaper, vilket gör att symptomen varierar beroende på vilket organ tumören startade i. Det karakteristiska neuroendokrina inslaget är tumörcellernas förmåga att producera specifika hormoner, samt en oreglerad överproduktion av receptorer (en sorts mottagarstrukturer på cellytan) för hormonet somatostatin (SS). NEN innefattar dels långsamväxande, välstrukturerade neuroendokrina tumörer (NET), och dels mer sällsynt aggressivt växande neuroendokrin cancer (NEC). Den vanligaste lokalisationen av NET är lungor och bronker, på andra plats kommer tunntarmen, inklusive första delen av tjocktarmen, och den fjärde vanligaste är NET i bukspottkörteln. Tumörtypen har ökat i incidens under de senaste decennierna, vilket till dels kan förklaras av förbättrade undersökningstekniker som datortomografi (DT) och magnetkamera (MR). Andra orsaker till ökningen är inte ännu klarlagda men hög ålder kan vara en faktor. Vissa tumörer, främst i tunntarmen, producerar symptomgivande hormoner, och kallas funktionella NET, medan många tumörer, särskilt i bukspottkörteln, kan ha överproduktion av hormoner utan att patienten har känningar av det. De symptomgivande tumörerna i bukspottkörteln tenderar att diagnosticeras i ett tidigt skede, medan tunntarmstumörerna och de icke funktionella tumörerna endast ger diskreta symptom, vilket fördröjer diagnosen. Man har beräknat att det tar cirka fem till sju år för exempelvis NET i tunntarmen att diagnosticeras, varför de vid diagnostillfället oftast är stora och redan har metastaserat. Majoriteten av de väldifferentierade NET har ett överflöd av de specifika somatostatin-receptorerna (SSTR) på sin yta. När hormonet binds till receptorn, innesluts hela komplexet i cellen, där hormonet och receptorn separeras, varvid receptorn återvänder till cellytan. Hela proceduren tar omkring 16 till 24 timmar enligt tidigare studier på möss. Syntetiska hormonkopior av somatostatin (somatostatinanaloger) (SSA) används för behandling och dämpar de typiska hormonella symptomen, såsom diarré och värmevallningar. SSA kan även kopplas till radionuklider som när de injiceras i blodbanan tas upp av tumörernas receptorer, och kan utnyttjas för både diagnostik och intern strålbehandling. Vid diagnostik används radionukliden Gallium-68 (^{68}Ga), som har en kort

halveringstid (60 min) för att skapa bilder med en PET-kamera, hopkopplad med en datortomograf (PET/DT). Vid intern strålbehandling, så kallade peptid-receptor radionuklid terapi (PRRT), används oftast radionukliden Lutetium-177 (^{177}Lu) med 6 dagars halveringstid, som dels avger behandlande beta-strålar (β^-), men också gamma-strålar (γ) som kan användas för att skapa bilder med en gammakamera kopplad till en datortomograf (SPECT/DT).

På grund av tumörernas sällsynthet har det varit svårt att kartlägga olika NET-typernas särarter, och många studier har genom åren kombinerat behandlingsresultat från flera skilda typer av NET. Detta gäller särskilt de vanligaste förekommande tumörerna i buken, tunntarms-NET (SI-NET) och bukspottkörtel-NET (P-NET) vilka ofta omnämnts sammantaget som gastointestinala-pancreatiska, GEP-NETs.

Målet med avhandlingen är att jämföra reaktionssättet hos SI-NET och P-NET under och efter intern strålbehandlingen med PRRT, samt att utröna vilka möjliga faktorer som kan ha effekt på behandlingsresultaten. Ett delmål var att utröna om de två tumörtyperna beskriver ett likartat reaktionssätt på strålbehandlingen, eller om deras behandlingssvar är så pass skilda att de bör anses som åtskilda entiteter och behandlas separat. Under sådana förutsättningar kan ett sammanförande till en enhetlig GEP-NET grupp leda till att samma behandling för hela gruppen blir ineffektiv. Studierna genomfördes bakåtblickande, baserat på arkivmaterial bestående av DT och MR undersökningar utförda i samband med PRRT behandlingar vid Akademiska sjukhuset i Uppsala. I det första arbetet analyserades det radioaktiva tumörupptaget i en tumör vardera hos 25 SI-NET patienter. Tumörerna undersöktes under och efter PRRT avseende förändring av tre tumörmått; den största tumördiametern, samt tumörvolymen beräknad på två sätt; dels med hjälp av datormjukvara och dels beräknad baserad på största manuellt uppmätta tumördiametern. Studien visade att det hos SI-NET inte fanns någon korrelation mellan tumörstorleksminskningar och mängden absorberad dos (dos-respons). Detta skiljer sig från vad som tidigare rapporterats för P-NET. För SI-NETs förelåg däremot, ett samband mellan mängden given radioaktivitet och storleksminskning av tumörerna. Minskningen var även signifikant enligt standardmetoden för utvärdering av tumörbehandling, det så kallade RECIST 1.1 måttet. Fokus i studie två var att jämföra det specifika svaret på PRRT hos de P-NET och SI-NET tumörer som rapporterats i tidigare studier. Vid denna studie gjordes en förnyad, mer omfattande utvärdering med uppmätning av fler tumörparametrar, och med längre observationstid. Studien visade att trots att den totala absorberade dosen var densamma, förelåg påtagliga skillnader i absorberad dos mellan de två tumörsorterna vid de olika behandlingstillfällena under PRRT. I P-NETs var radioaktivitetsupptaget högst vid de första behandlingstillfällena och minskade därefter signifikant senare under PRRT. En sådan variation sågs ej för SI-NETs. Med den nu längre observationstiden påvisades ett svagt dos-respons samband mellan absorberad dos i SI-NET och minskning av tumörernas storlek, vilket inte noterats vid den första studien. Alltjämt fanns

emellertid ett samband mellan mängden given radioaktivitet och krympning av SI-NETs, men inte för P-NETs.

De påvisade olikheterna i beteendet hos P-NETs och SI-NETs uppfattas vara av sådan art att tumörtyperna bör betraktas som enskilda entiteter, och genom att separat anpassa PRRT-protokollet till deras respektive särarter finns förutsättningar att kunna förbättra behandlingsresultaten.

I arbete tre studeras receptorsvaret hos SI-NETs och normalvävnad efter en injektion av korttidsverkande SSA. Studien hade till syfte att kartlägga recirkulationstiden för somatostatinreceptorerna i tumörer och olika normalvävnader. Studien innefattade fyra SI-NET patienter (tretton tumörer) vilka genomgick upprepade ^{68}Ga-SSA-PET/CT undersökningar. Resultatet visade att större tumörer (>4 cm) har en snabbare cirkulationshastighet på sina receptorer, jämfört med små tumörer vars receptoromsättning mer liknar normalorganens (lever, mjälte och bukspottkörtel). Dessa resultat ger en helt ny kunskap, och öppnar möjligheten att genom förbehandling med kortverkande SSA kunna skydda normalvävnader vid PRRT, och därigenom öka radioaktivitetsupptaget i tumörerna. Alternativt kan man genom att minska mängden given aktivitet efter förbehandling, uppnå bibehållet radioaktivitetsupptag i tumörerna.

Arbete fyra, utforskar om mängden omärkt SSA, i PRRT preparationen, påverkar stråldosen till P-NETs, SI-NETs och normalvävnader, ställt i relation till patientens hela tumörbörda. Från gruppen av 510 tidigare behandlade P- och SI-NET patienter mellan åren 2006 och 2018, återfanns 141 SI-NET och 46 P-NET patienter som var analyserbara. Varje patients totala tumörbörda skattades med hjälp av en ny mjukvara från Hermes Solution AB med en extra funktion som kan avgränsa områden med varierande aktivitet i ett större tumörkonglomerat, vilket ger mer homogen information jämfört med tidigare system.

Studien har inte kunnat påvisa någon effekt av mängden omärkt SSA på det radioaktiva upptaget vare sig i tumörer eller normalvävnader, och ingen relation till den totala tumörbördan. Eftersom data baserades på undersökningar insamlade under ett drygt decennium finns det sannolikt osäkerheter i resultatet, såsom att flera olika gamakameratyper användes under tidsperioden, och att tidpunkten för undersökning inte var anpassad för optimera studiens mätningar.

15 Acknowledgement

First and foremost, I want to express my deepest gratitude to Prof. Per Hellman, who on the behalf of Uppsala University and the Institution for Surgical Sciences accepted my application for doctoral studies, and allowed me to embark on this developmental journey. It has been an astonishing excursion and I am ever so grateful to have been allowed to experience it.

From my heart, I wish to thank my main supervisor Prof. Anders Sundin for your boundless patients, positivity and respectful guidance throughout this journey of my scientific achievements. Your knowledge is immense and yet you listen openly to alternative thoughts and ideas for which I am so obliged.

With a deeply felt appreciation to my co-supervisors Prof. Mark Lubberink for your unhesitating support in assisting me to insights about perspectives in radionuclide therapy, and for sharing your vast expertise and knowledge.

To Ulrike Garske-Román for your engaging and enthusiastic guidance showering me with your immense knowledge in neuroendocrine tumours and nuclear therapy and generously sharing your data from radionuclide therapies making this thesis possible. Thanks for your encouraging pep-talks as a colleague who has become a dear and respected friend.

Thank you Mattias Sandström, my furtive co-supervisors for enlightening me about the secrets of dosimetry at many instances by the white board, and our engaging discussions on shared thoughts about day-to-day goings-on, and to Irina Velikyan and Katarzyna Fröss-Baron, for your engagement and well-advised support.

A big thanks to all fellow researchers and friends and co-authors at Glunten (14B), heightening the spirit of the day with humorous lunch time jokes blended with enlightening discussions, how I will miss you all. A special thanks to Charlie and Adrian for the assistance with the secrets of the Hermes program, my “room-mates” Elin, Narech, Ram and Ali, and the “extra roomies” My and especially Ezgi, my co-author, for all our scientific discussions in exploring the world of PRRT and to whom I am in total dept with gratitude for your tireless assistance of my ignorance in the present world of digital reality, I could never have managed without you.

To all remarkable colleges, patients and co-workers, who supported and contributed to this thesis I am most grateful, and especially to the PET centre managers Per-Arne and Jonathan who together with the supporting staff found PET/CT time for the studies and took wonderful care of our patients. The

administrative staff at the department of Surgical Sciences: Elin, Carina, Karin and Birgitta who supported and saved me in administrative matters and Anna and Monika at the Nuclear Medicine department, who patiently and kindly supported and helped through the years. To the IT-guys Mats and Mårten for always taking your time to help with a smile be it hard- or software problems.

A warm felt thanks to my former supervisor Prof. Marin Ritzén, and co-supervisor Mikael Holst who gave me the first introduction to academic studies. And heartly thanks to my two supervisors from the training years in radiology Mats Beckman and Per Grybäck and my co-student Michael Torkzad who later became a much-appreciated colleague at Uppsala. Heaps of thanks to the incredible group of abdominal radiologists at Sahlgrenska Hospital; Kjell, John, Kerstin, Fredrik, Farida, Paul, Mats, Barbara, Henrik, Johanna, Mikael, Lilian and Peter who with open arms welcomed me into your amazing group and made me change my focus to abdominal radiology, a necessity for this thesis to come about.

A warm-hearted thanks to all my friends past and present, with a special gratitude to Johan af Klint who by setting an example encouraged me to dare this endeavor and pursue my goal, as age never will be an issue. Heaps of thankfulness to my dear friend Margareta Ihse for sharing so many thoughts and knowhows from her broad academic experience, giving me valuable insights and stimulating forth-baring discussions to the academic world. To my long-time saunter friends Eva, since our first-borne, and Gunilla, sharing bits and pieces of life ever since fifth grade and my regained student friend Helena thank you for all our refreshing and invigorating strolls with pleasant edifying chats, that made the days.

To my sister Marina and cousin Jesper for being supportive in so many ways, and Mariana introducing me to the fascinating culture of Bulgaria sharing our wonderful grandsons and Carina sharing grandmother-hood of our delightful grand-daughters.

Last but not least I want to thank my wonderful two doctorate children, Harald and college Ingegerd, who lovingly have guided me into contemporary life together with their wonderful families; Harald´s wife Amina, my co PhD-student mate, always helpful with digital matters and their lovely girls Isabel and Dalia and Ingegerd´s husband George and their three wonderful boys Marc, Henry and Valter. You are all the sparkling diamonds of my life and I love you beyond words.

16 References

1. Rindi G, Klimstra DS, Abedi-Ardekani B, Asa SL, Bosman FT, Brambilla E, et al. A common classification framework for neuroendocrine neoplasms: an International Agency for Research on Cancer (IARC) and World Health Organization (WHO) expert consensus proposal. Mod Pathol. 2018 Dec;31(12):1770-86.
2. Kloppel G. Oberndorfer and his successors: from carcinoid to neuroendocrine carcinoma. Endocr Pathol. 2007 Fall;18(3):141-4.
3. Modlin IM, Shapiro MD, Kidd M. Siegfried Oberndorfer: origins and perspectives of carcinoid tumors. Hum Pathol. 2004 Dec;35(12):1440-51.
4. Lechago J. The endocrine cells of the digestive tract. General concepts and historic perspective. Am J Surg Pathol. 1987;11 Suppl 1:63-70.
5. Biorck G, Axen O, Thorson A. Unusual cyanosis in a boy with congenital pulmonary stenosis and tricuspid insufficiency. Fatal outcome after angiocardiography. Am Heart J. 1952 Jul;44(1):143-8.
6. Thorson A, Biorck G, Bjorkman G, Waldenstrom J. Malignant carcinoid of the small intestine with metastases to the liver, valvular disease of the right side of the heart (pulmonary stenosis and tricuspid regurgitation without septal defects), peripheral vasomotor symptoms, bronchoconstriction, and an unusual type of cyanosis; a clinical and pathologic syndrome. Am Heart J. 1954 Jun;47(5):795-817.
7. Pernow B, Waldenstrom J. Paroxysmal flushing and other symptoms caused by 5-hydroxytryptamine and histamine in patients with malignant tumours. Lancet. 1954 Nov 6;267(6845):951.
8. Pernow B, Waldenstrom J. Determination of 5-hydroxytryptamine, 5-hydroxyindole acetic acid and histamine in thirty-three cases of carcinoid tumor (argentaffinoma). Am J Med. 1957 Jul;23(1):16-25.
9. Krulich L, Dhariwal AP, McCann SM. Stimulatory and inhibitory effects of purified hypothalamic extracts on growth hormone release from rat pituitary in vitro. Endocrinology. 1968 Oct;83(4):783-90.
10. Brazeau P, Vale W, Burgus R, Ling N, Butcher M, Rivier J, et al. Hypothalamic polypeptide that inhibits the secretion of immunoreactive pituitary growth hormone. Science. 1973 Jan 5;179(4068):77-9.

11. Pradayrol L, Jornvall H, Mutt V, Ribet A. N-terminally extended somatostatin: the primary structure of somatostatin-28. FEBS Lett. 1980 Jan 1;109(1):55-8.
12. Patel YC, Reichlin S. Somatostatin in hypothalamus, extrahypothalamic brain, and peripheral tissues of the rat. Endocrinology. 1978 Feb;102(2):523-30.
13. Keast JR, Furness JB, Costa M. Somatostatin in human enteric nerves. Distribution and characterization. Cell Tissue Res. 1984;237(2):299-308.
14. Polak JM, Bloom SR. Somatostatin localization in tissues. Scand J Gastroenterol Suppl. 1986;119:11-21.
15. Lundqvist M, Wilander E. Somatostatin-like immunoreactivity in mid-gut carcinoids. Acta Pathol Microbiol Scand A. 1981 Jul;89(4):335-7.
16. Patel YC. Somatostatin and its receptor family. Front Neuroendocrinol. 1999 Jul;20(3):157-98.
17. ten Bokum AM, Hofland LJ, van Hagen PM. Somatostatin and somatostatin receptors in the immune system: a review. Eur Cytokine Netw. 2000 Jun;11(2):161-76.
18. Epelbaum J, Dournaud P, Fodor M, Viollet C. The neurobiology of somatostatin. Crit Rev Neurobiol. 1994;8(1-2):25-44.
19. Schindler M, Humphrey PP, Emson PC. Somatostatin receptors in the central nervous system. Prog Neurobiol. 1996 Sep;50(1):9-47.
20. Hall R, Besser GM, Schally AV, Coy DH, Evered D, Goldie DJ, et al. Action of growth-hormone-release inhibitory hormone in healthy men and in acromegaly. Lancet. 1973 Sep 15;2(7829):581-4.
21. Bauer W, Briner U, Doepfner W, Haller R, Huguenin R, Marbach P, et al. SMS 201-995: a very potent and selective octapeptide analogue of somatostatin with prolonged action. Life Sci. 1982 Sep 13;31(11):1133-40.
22. de Herder WW, Hofland LJ, van der Lely AJ, Lamberts SW. Somatostatin receptors in gastroentero-pancreatic neuroendocrine tumours. Endocr Relat Cancer. 2003 Dec;10(4):451-8.
23. Kumar Nagarajan S, Babu S, Sohn H, Devaraju P, Madhavan T. Toward a better understanding of the interaction between somatostatin receptor 2 and its ligands: a structural characterization study using molecular dynamics and conceptual density functional theory. J Biomol Struct Dyn. 2019 Aug;37(12):3081-102.
24. Bass RT, Buckwalter BL, Patel BP, Pausch MH, Price LA, Strnad J, et al. Identification and characterization of novel somatostatin antagonists. Mol Pharmacol. 1996 Oct;50(4):709-15.
25. Srikant CB, Patel YC. Somatostatin receptors: identification and characterization in rat brain membranes. Proc Natl Acad Sci U S A. 1981 Jun;78(6):3930-4.

26. Schonbrunn A, Tashjian H, Jr. Characterization of functional receptors for somatostatin in rat pituitary cells in culture. J Biol Chem. 1978 Sep 25;253(18):6473-83.
27. Reubi JC, Maurer R, von Werder K, Torhorst J, Klijn JG, Lamberts SW. Somatostatin receptors in human endocrine tumors. Cancer Res. 1987 Jan 15;47(2):551-8.
28. Sreedharan SP, Kodama KT, Peterson KE, Goetzl EJ. Distinct subsets of somatostatin receptors on cultured human lymphocytes. J Biol Chem. 1989 Jan 15;264(2):949-52.
29. Kluxen FW, Bruns C, Lubbert H. Expression cloning of a rat brain somatostatin receptor cDNA. Proc Natl Acad Sci U S A. 1992 May 15;89(10):4618-22.
30. Yamada Y, Post SR, Wang K, Tager HS, Bell GI, Seino S. Cloning and functional characterization of a family of human and mouse somatostatin receptors expressed in brain, gastrointestinal tract, and kidney. Proc Natl Acad Sci U S A. 1992 Jan 1;89(1):251-5.
31. Carpentier JL. Receptor-mediated endocytosis of polypeptide hormones: mechanism and significance. Mol Immunol. 1984 Dec;21(12):1157-9.
32. Viguerie N, Esteve JP, Susini C, Vaysse N, Ribet A. Processing of receptor-bound somatostatin: internalization and degradation by pancreatic acini. Am J Physiol. 1987 Apr;252(4 Pt 1):G535-42.
33. Andersson P, Forssell-Aronsson E, Johanson V, Wangberg B, Nilsson O, Fjalling M, et al. Internalization of indium-111 into human neuroendocrine tumor cells after incubation with indium-111-DTPA-D-Phe1-octreotide. J Nucl Med. 1996 Dec;37(12):2002-6.
34. Hukovic N, Panetta R, Kumar U, Patel YC. Agonist-dependent regulation of cloned human somatostatin receptor types 1-5 (hSSTR1-5): subtype selective internalization or upregulation. Endocrinology. 1996 Sep;137(9):4046-9.
35. Koenig JA, Kaur R, Dodgeon I, Edwardson JM, Humphrey PP. Fates of endocytosed somatostatin sst2 receptors and associated agonists. Biochem J. 1998 Dec 1;336 (Pt 2):291-8.
36. Slooter GD, Breeman WA, Marquet RL, Krenning EP, van Eijck CH. Anti-proliferative effect of radiolabelled octreotide in a metastases model in rat liver. Int J Cancer. 1999 May 31;81(5):767-71.
37. Hofland LJ, Lamberts SW. The pathophysiological consequences of somatostatin receptor internalization and resistance. Endocr Rev. 2003 Feb;24(1):28-47.
38. Liu Q, Cescato R, Dewi DA, Rivier J, Reubi JC, Schonbrunn A. Receptor signaling and endocytosis are differentially regulated by somatostatin analogs. Mol Pharmacol. 2005 Jul;68(1):90-101.
39. Froidevaux S, Hintermann E, Torok M, Macke HR, Beglinger C, Eberle AN. Differential regulation of somatostatin receptor type 2 (sst

2) expression in AR4-2J tumor cells implanted into mice during octreotide treatment. Cancer Res. 1999 Aug 1;59(15):3652-7.
40. Stroh T, Jackson AC, Sarret P, Dal Farra C, Vincent JP, Kreienkamp HJ, et al. Intracellular dynamics of sst5 receptors in transfected COS-7 cells: maintenance of cell surface receptors during ligand-induced endocytosis. Endocrinology. 2000 Jan;141(1):354-65.
41. Treppiedi D, Jobin ML, Peverelli E, Giardino E, Sungkaworn T, Zabel U, et al. Single-Molecule Microscopy Reveals Dynamic FLNA Interactions Governing SSTR2 Clustering and Internalization. Endocrinology. 2018 Aug 1;159(8):2953-65.
42. Treppiedi D, Mangili F, Giardino E, Catalano R, Locatelli M, Lania AG, et al. Cytoskeleton Protein Filamin A Is Required for Efficient Somatostatin Receptor Type 2 Internalization and Recycling through Rab5 and Rab4 Sorting Endosomes in Tumor Somatotroph Cells. Neuroendocrinology. 2020;110(7-8):642-52.
43. Olsen C, Memarzadeh K, Ulu A, Carr HS, Bean AJ, Frost JA. Regulation of Somatostatin Receptor 2 Trafficking by C-Tail Motifs and the Retromer. Endocrinology. 2019 May 1;160(5):1031-43.
44. Perrin MH, Sutton SW, Cervini LA, Rivier JE, Vale WW. Comparison of an agonist, urocortin, and an antagonist, astressin, as radioligands for characterization of corticotropin-releasing factor receptors. J Pharmacol Exp Ther. 1999 Feb;288(2):729-34.
45. Ginj M, Zhang H, Waser B, Cescato R, Wild D, Wang X, et al. Radiolabeled somatostatin receptor antagonists are preferable to agonists for in vivo peptide receptor targeting of tumors. Proc Natl Acad Sci U S A. 2006 Oct 31;103(44):16436-41.
46. Dalm SU, Nonnekens J, Doeswijk GN, de Blois E, van Gent DC, Konijnenberg MW, et al. Comparison of the Therapeutic Response to Treatment with a 177Lu-Labeled Somatostatin Receptor Agonist and Antagonist in Preclinical Models. J Nucl Med. 2016 Feb;57(2):260-5.
47. Fani M, Braun F, Waser B, Beetschen K, Cescato R, Erchegyi J, et al. Unexpected sensitivity of sst2 antagonists to N-terminal radiometal modifications. J Nucl Med. 2012 Sep;53(9):1481-9.
48. Hanahan D, Weinberg RA. Hallmarks of cancer: the next generation. Cell. 2011 Mar 4;144(5):646-74.
49. Arneth B. Tumor Microenvironment. Medicina (Kaunas). 2019 Dec 30;56(1).
50. Cives M, Pelle E, Quaresmini D, Rizzo FM, Tucci M, Silvestris F. The Tumor Microenvironment in Neuroendocrine Tumors: Biology and Therapeutic Implications. Neuroendocrinology. 2019;109(2):83-99.
51. Jain RK, Baxter LT. Mechanisms of heterogeneous distribution of monoclonal antibodies and other macromolecules in tumors:

significance of elevated interstitial pressure. Cancer Res. 1988 Dec 15;48(24 Pt 1):7022-32.
52. Stylianopoulos T, Munn LL, Jain RK. Reengineering the Physical Microenvironment of Tumors to Improve Drug Delivery and Efficacy: From Mathematical Modeling to Bench to Bedside. Trends Cancer. 2018 Apr;4(4):292-319.
53. Couvelard A, O'Toole D, Turley H, Leek R, Sauvanet A, Degott C, et al. Microvascular density and hypoxia-inducible factor pathway in pancreatic endocrine tumours: negative correlation of microvascular density and VEGF expression with tumour progression. Br J Cancer. 2005 Jan 17;92(1):94-101.
54. Maccalli C, Rasul KI, Elawad M, Ferrone S. The role of cancer stem cells in the modulation of anti-tumor immune responses. Semin Cancer Biol. 2018 Dec;53:189-200.
55. Skvortsova I, Debbage P, Kumar V, Skvortsov S. Radiation resistance: Cancer stem cells (CSCs) and their enigmatic pro-survival signaling. Semin Cancer Biol. 2015 Dec;35:39-44.
56. Moertel CG, Sauer WG, Dockerty MB, Baggenstoss AH. Life history of the carcinoid tumor of the small intestine. Cancer. 1961 Sep-Oct;14:901-12.
57. Cunningham JL, Tsolakis AV, Jacobson A, Janson ET. Connective tissue growth factor expression in endocrine tumors is associated with high stromal expression of alpha-smooth muscle actin. Eur J Endocrinol. 2010 Oct;163(4):691-7.
58. Kwekkeboom DJ, de Herder WW, Kam BL, van Eijck CH, van Essen M, Kooij PP, et al. Treatment with the radiolabeled somatostatin analog [177 Lu-DOTA 0,Tyr3]octreotate: toxicity, efficacy, and survival. J Clin Oncol. 2008 May 01;26(13):2124-30.
59. Bodei L, Cremonesi M, Grana CM, Fazio N, Iodice S, Baio SM, et al. Peptide receptor radionuclide therapy with (1)(7)(7)Lu-DOTATATE: the IEO phase I-II study. Eur J Nucl Med Mol Imaging. 2011 Dec;38(12):2125-35.
60. Garske-Roman U, Sandstrom M, Fross Baron K, Lundin L, Hellman P, Welin S, et al. Prospective observational study of (177)Lu-DOTA-octreotate therapy in 200 patients with advanced metastasized neuroendocrine tumours (NETs): feasibility and impact of a dosimetry-guided study protocol on outcome and toxicity. Eur J Nucl Med Mol Imaging. 2018 Mar 1.
61. Jahn U, Ilan E, Sandstrom M, Lubberink M, Garske-Roman U, Sundin A. Peptide Receptor Radionuclide Therapy (PRRT) with (177)Lu-DOTATATE; Differences in Tumor Dosimetry, Vascularity and Lesion Metrics in Pancreatic and Small Intestinal Neuroendocrine Neoplasms. Cancers (Basel). 2021 Feb 25;13(5).

62. Capella C, Heitz PU, Hofler H, Solcia E, Kloppel G. Revised classification of neuroendocrine tumours of the lung, pancreas and gut. Virchows Arch. 1995;425(6):547-60.
63. Rindi G, Mete O, Uccella S, Basturk O, La Rosa S, Brosens LAA, et al. Overview of the 2022 WHO Classification of Neuroendocrine Neoplasms. Endocr Pathol. 2022 Mar;33(1):115-54.
64. Reubi JC, Lang W, Maurer R, Koper JW, Lamberts SW. Distribution and biochemical characterization of somatostatin receptors in tumors of the human central nervous system. Cancer Res. 1987 Nov 1;47(21):5758-64.
65. Modlin IM, Oberg K, Chung DC, Jensen RT, de Herder WW, Thakker RV, et al. Gastroenteropancreatic neuroendocrine tumours. Lancet Oncol. 2008 Jan;9(1):61-72.
66. Schnirer, II, Yao JC, Ajani JA. Carcinoid--a comprehensive review. Acta Oncol. 2003;42(7):672-92.
67. Strosberg J. Neuroendocrine tumours of the small intestine. Best Pract Res Clin Gastroenterol. 2012 Dec;26(6):755-73.
68. Schimmack S, Svejda B, Lawrence B, Kidd M, Modlin IM. The diversity and commonalities of gastroenteropancreatic neuroendocrine tumors. Langenbecks Arch Surg. 2011 Mar;396(3):273-98.
69. Kaltsas G, Rockall A, Papadogias D, Reznek R, Grossman AB. Recent advances in radiological and radionuclide imaging and therapy of neuroendocrine tumours. Eur J Endocrinol. 2004 Jul;151(1):15-27.
70. Modlin IM, Kidd M, Latich I, Zikusoka MN, Shapiro MD. Current status of gastrointestinal carcinoids. Gastroenterology. 2005 May;128(6):1717-51.
71. Strosberg JR, Cheema A, Weber J, Han G, Coppola D, Kvols LK. Prognostic validity of a novel American Joint Committee on Cancer Staging Classification for pancreatic neuroendocrine tumors. J Clin Oncol. 2011 Aug 1;29(22):3044-9.
72. Strosberg JR, Weber JM, Feldman M, Coppola D, Meredith K, Kvols LK. Prognostic validity of the American Joint Committee on Cancer staging classification for midgut neuroendocrine tumors. J Clin Oncol. 2013 Feb 1;31(4):420-5.
73. van Riet J, van de Werken HJG, Cuppen E, Eskens F, Tesselaar M, van Veenendaal LM, et al. The genomic landscape of 85 advanced neuroendocrine neoplasms reveals subtype-heterogeneity and potential therapeutic targets. Nat Commun. 2021 Jul 29;12(1):4612.
74. Oberg K, Astrup L, Eriksson B, Falkmer SE, Falkmer UG, Gustafsen J, et al. Guidelines for the management of gastroenteropancreatic neuroendocrine tumours (including bronchopulmonary and thymic neoplasms). Part II-specific NE tumour types. Acta Oncol. 2004;43(7):626-36.

75. Guilmette JM, Nose V. Neoplasms of the Neuroendocrine Pancreas: An Update in the Classification, Definition, and Molecular Genetic Advances. Adv Anat Pathol. 2019 Jan;26(1):13-30.
76. Johnson A, Wright JP, Zhao Z, Komaya T, Parikh A, Merchant N, et al. Cadherin 17 is frequently expressed by 'sclerosing variant' pancreatic neuroendocrine tumour. Histopathology. 2015 Jan;66(2):225-33.
77. Falconi M, Eriksson B, Kaltsas G, Bartsch DK, Capdevila J, Caplin M, et al. ENETS Consensus Guidelines Update for the Management of Patients with Functional Pancreatic Neuroendocrine Tumors and Non-Functional Pancreatic Neuroendocrine Tumors. Neuroendocrinology. 2016;103(2):153-71.
78. Sadanandam A, Wullschleger S, Lyssiotis CA, Grotzinger C, Barbi S, Bersani S, et al. A Cross-Species Analysis in Pancreatic Neuroendocrine Tumors Reveals Molecular Subtypes with Distinctive Clinical, Metastatic, Developmental, and Metabolic Characteristics. Cancer Discov. 2015 Dec;5(12):1296-313.
79. Scarpa A, Chang DK, Nones K, Corbo V, Patch AM, Bailey P, et al. Corrigendum: Whole-genome landscape of pancreatic neuroendocrine tumours. Nature. 2017 Oct 26;550(7677):548.
80. Dees C, Akhmetshina A, Zerr P, Reich N, Palumbo K, Horn A, et al. Platelet-derived serotonin links vascular disease and tissue fibrosis. J Exp Med. 2011 May 9;208(5):961-72.
81. Chen C, Han X, Fan F, Liu Y, Wang T, Wang J, et al. Serotonin drives the activation of pulmonary artery adventitial fibroblasts and TGF-beta1/Smad3-mediated fibrotic responses through 5-HT(2A) receptors. Mol Cell Biochem. 2014 Dec;397(1-2):267-76.
82. Thakker RV. Multiple endocrine neoplasia type 1 (MEN1) and type 4 (MEN4). Mol Cell Endocrinol. 2014 Apr 5;386(1-2):2-15.
83. Karpathakis A, Dibra H, Pipinikas C, Feber A, Morris T, Francis J, et al. Progressive epigenetic dysregulation in neuroendocrine tumour liver metastases. Endocr Relat Cancer. 2017 Feb;24(2):L21-L25.
84. Dasari A, Shen C, Halperin D, Zhao B, Zhou S, Xu Y, et al. Trends in the Incidence, Prevalence, and Survival Outcomes in Patients With Neuroendocrine Tumors in the United States. JAMA Oncol. 2017 Oct 1;3(10):1335-42.
85. Berge T, Linell F. Carcinoid tumours. Frequency in a defined population during a 12-year period. Acta Pathol Microbiol Scand A. 1976 Jul;84(4):322-30.
86. Eriksson J, Norlen O, Ogren M, Garmo H, Ihre-Lundgren C, Hellman P. Primary small intestinal neuroendocrine tumors are highly prevalent and often multiple before metastatic disease develops. Scand J Surg. 2021 Mar;110(1):44-50.

87. Abou Saleh M, Mansoor E, Anindo M, Isenberg G. Prevalence of Small Intestine Carcinoid Tumors: A US Population-Based Study 2012-2017. Dig Dis Sci. 2019 May;64(5):1328-34.
88. Luke C, Price T, Townsend A, Karapetis C, Kotasek D, Singhal N, et al. Epidemiology of neuroendocrine cancers in an Australian population. Cancer Causes Control. 2010 Jun;21(6):931-8.
89. Boyar Cetinkaya R, Aagnes B, Thiis-Evensen E, Tretli S, Bergestuen DS, Hansen S. Trends in Incidence of Neuroendocrine Neoplasms in Norway: A Report of 16,075 Cases from 1993 through 2010. Neuroendocrinology. 2017;104(1):1-10.
90. Tsai HJ, Wu CC, Tsai CR, Lin SF, Chen LT, Chang JS. The epidemiology of neuroendocrine tumors in Taiwan: a nation-wide cancer registry-based study. PLoS One. 2013;8(4):e62487.
91. Sackstein PE, O'Neil DS, Neugut AI, Chabot J, Fojo T. Epidemiologic trends in neuroendocrine tumors: An examination of incidence rates and survival of specific patient subgroups over the past 20 years. Semin Oncol. 2018 Aug;45(4):249-58.
92. Haugvik SP, Hedenstrom P, Korsaeth E, Valente R, Hayes A, Siuka D, et al. Diabetes, smoking, alcohol use, and family history of cancer as risk factors for pancreatic neuroendocrine tumors: a systematic review and meta-analysis. Neuroendocrinology. 2015;101(2):133-42.
93. Leoncini E, Carioli G, La Vecchia C, Boccia S, Rindi G. Risk factors for neuroendocrine neoplasms: a systematic review and meta-analysis. Ann Oncol. 2016 Jan;27(1):68-81.
94. Rinzivillo M, Capurso G, Campana D, Fazio N, Panzuto F, Spada F, et al. Risk and Protective Factors for Small Intestine Neuroendocrine Tumors: A Prospective Case-Control Study. Neuroendocrinology. 2016;103(5):531-7.
95. Haugvik SP, Basim Ibrahim I, Hedenstrom P, Valente R, Hayes AJ, Siuka D, et al. Smoking, alcohol and family history of cancer as risk factors for small intestinal neuroendocrine tumors: a systematic review and meta-analysis. Scand J Gastroenterol. 2017 Aug;52(8):797-802.
96. Cives M, Strosberg JR. Gastroenteropancreatic Neuroendocrine Tumors. CA Cancer J Clin. 2018 Nov;68(6):471-87.
97. Pea A, Hruban RH, Wood LD. Genetics of pancreatic neuroendocrine tumors: implications for the clinic. Expert Rev Gastroenterol Hepatol. 2015;9(11):1407-19.
98. Ebeling T, Vierimaa O, Kytola S, Leisti J, Salmela PI. Effect of multiple endocrine neoplasia type 1 (MEN1) gene mutations on premature mortality in familial MEN1 syndrome with founder mutations. J Clin Endocrinol Metab. 2004 Jul;89(7):3392-6.
99. Kaelin WG, Jr. The von Hippel-Lindau tumour suppressor protein: O2 sensing and cancer. Nat Rev Cancer. 2008 Nov;8(11):865-73.

100. Rogers A, Wang LM, Karavitaki N, Grossman AB. Neurofibromatosis Type 1 and pancreatic islet cell tumours: an association which should be recognized. QJM. 2015 Jul;108(7):573-6.
101. Kaltsas GA, Besser GM, Grossman AB. The diagnosis and medical management of advanced neuroendocrine tumors. Endocr Rev. 2004 Jun;25(3):458-511.
102. Kidd M, Modlin I, Oberg K. Towards a new classification of gastroenteropancreatic neuroendocrine neoplasms. Nat Rev Clin Oncol. 2016 Nov;13(11):691-705.
103. Modlin IM, Champaneria MC, Chan AK, Kidd M. A three-decade analysis of 3,911 small intestinal neuroendocrine tumors: the rapid pace of no progress. Am J Gastroenterol. 2007 Jul;102(7):1464-73.
104. Sisson JC, Frager MS, Valk TW, Gross MD, Swanson DP, Wieland DM, et al. Scintigraphic localization of pheochromocytoma. N Engl J Med. 1981 Jul 2;305(1):12-7.
105. Hoefnagel CA, Voute PA, de Kraker J, Marcuse HR. Radionuclide diagnosis and therapy of neural crest tumors using iodine-131 metaiodobenzylguanidine. J Nucl Med. 1987 Mar;28(3):308-14.
106. Krenning EP, Bakker WH, Breeman WA, Koper JW, Kooij PP, Ausema L, et al. Localisation of endocrine-related tumours with radioiodinated analogue of somatostatin. Lancet. 1989 Feb 4;1(8632):242-4.
107. Krenning EP, Bakker WH, Kooij PP, Breeman WA, Oei HY, de Jong M, et al. Somatostatin receptor scintigraphy with indium-111-DTPA-D-Phe-1-octreotide in man: metabolism, dosimetry and comparison with iodine-123-Tyr-3-octreotide. J Nucl Med. 1992 May;33(5):652-8.
108. Orlefors H, Sundin A, Garske U, Juhlin C, Oberg K, Skogseid B, et al. Whole-body (11)C-5-hydroxytryptophan positron emission tomography as a universal imaging technique for neuroendocrine tumors: comparison with somatostatin receptor scintigraphy and computed tomography. J Clin Endocrinol Metab. 2005 Jun;90(6):3392-400.
109. Kwekkeboom DJ, Bakker WH, Kam BL, Teunissen JJ, Kooij PP, de Herder WW, et al. Treatment of patients with gastro-entero-pancreatic (GEP) tumours with the novel radiolabelled somatostatin analogue [177Lu-DOTA(0),Tyr3]octreotate. Eur J Nucl Med Mol Imaging. 2003 Mar;30(3):417-22.
110. Merola E, Pavel ME, Panzuto F, Capurso G, Cicchese N, Rinke A, et al. Functional Imaging in the Follow-Up of Enteropancreatic Neuroendocrine Tumors: Clinical Usefulness and Indications. J Clin Endocrinol Metab. 2017 May 1;102(5):1486-94.
111. Sundin A, Arnold R, Baudin E, Cwikla JB, Eriksson B, Fanti S, et al. ENETS Consensus Guidelines for the Standards of Care in

Neuroendocrine Tumors: Radiological, Nuclear Medicine & Hybrid Imaging. Neuroendocrinology. 2017;105(3):212-44.
112. Nilica B, Waitz D, Stevanovic V, Uprimny C, Kendler D, Buxbaum S, et al. Direct comparison of (68)Ga-DOTA-TOC and (18)F-FDG PET/CT in the follow-up of patients with neuroendocrine tumour treated with the first full peptide receptor radionuclide therapy cycle. Eur J Nucl Med Mol Imaging. 2016 Aug;43(9):1585-92.
113. Alevroudis E, Spei ME, Chatziioannou SN, Tsoli M, Wallin G, Kaltsas G, et al. Clinical Utility of (18)F-FDG PET in Neuroendocrine Tumors Prior to Peptide Receptor Radionuclide Therapy: A Systematic Review and Meta-Analysis. Cancers (Basel). 2021 Apr 10;13(8).
114. Bozkurt MF, Virgolini I, Balogova S, Beheshti M, Rubello D, Decristoforo C, et al. Guideline for PET/CT imaging of neuroendocrine neoplasms with (68)Ga-DOTA-conjugated somatostatin receptor targeting peptides and (18)F-DOPA. Eur J Nucl Med Mol Imaging. 2017 Aug;44(9):1588-601.
115. Dorr U, Rath U, Sautter-Bihl ML, Guzman G, Bach D, Adrian HJ, et al. Improved visualization of carcinoid liver metastases by indium-111 pentetreotide scintigraphy following treatment with cold somatostatin analogue. Eur J Nucl Med. 1993 May;20(5):431-3.
116. Velikyan I, Sundin A, Eriksson B, Lundqvist H, Sorensen J, Bergstrom M, et al. In vivo binding of [68Ga]-DOTATOC to somatostatin receptors in neuroendocrine tumours--impact of peptide mass. Nucl Med Biol. 2010 Apr;37(3):265-75.
117. Cherk MH, Kong G, Hicks RJ, Hofman MS. Changes in biodistribution on (68)Ga-DOTA-Octreotate PET/CT after long acting somatostatin analogue therapy in neuroendocrine tumour patients may result in pseudoprogression. Cancer Imaging. 2018 Jan 24;18(1):3.
118. Aalbersberg EA, de Wit-van der Veen BJ, Versleijen MWJ, Saveur LJ, Valk GD, Tesselaar MET, et al. Influence of lanreotide on uptake of (68)Ga-DOTATATE in patients with neuroendocrine tumours: a prospective intra-patient evaluation. Eur J Nucl Med Mol Imaging. 2019 Mar;46(3):696-703.
119. Sharma P, Arora S, Karunanithi S, Khadgawat R, Durgapal P, Sharma R, et al. Somatostatin receptor based PET/CT imaging with 68Ga-DOTA-Nal3-octreotide for localization of clinically and biochemically suspected insulinoma. Q J Nucl Med Mol Imaging. 2016 Mar;60(1):69-76.
120. Nockel P, Babic B, Millo C, Herscovitch P, Patel D, Nilubol N, et al. Localization of Insulinoma Using 68Ga-DOTATATE PET/CT Scan. J Clin Endocrinol Metab. 2017 Jan 1;102(1):195-99.
121. Luo Y, Pan Q, Yao S, Yu M, Wu W, Xue H, et al. Glucagon-Like Peptide-1 Receptor PET/CT with 68Ga-NOTA-Exendin-4 for

Detecting Localized Insulinoma: A Prospective Cohort Study. J Nucl Med. 2016 May;57(5):715-20.
122. Sowa-Staszczak A, Trofimiuk-Muldner M, Stefanska A, Tomaszuk M, Buziak-Bereza M, Gilis-Januszewska A, et al. 99mTc Labeled Glucagon-Like Peptide-1-Analogue (99mTc-GLP1) Scintigraphy in the Management of Patients with Occult Insulinoma. PLoS One. 2016;11(8):e0160714.
123. Sundin A, Wills M, Rockall A. Radiological Imaging: Computed Tomography, Magnetic Resonance Imaging and Ultrasonography. Front Horm Res. 2015;44:58-72.
124. Kim JH, Eun HW, Kim YJ, Lee JM, Han JK, Choi BI. Pancreatic neuroendocrine tumour (PNET): Staging accuracy of MDCT and its diagnostic performance for the differentiation of PNET with uncommon CT findings from pancreatic adenocarcinoma. Eur Radiol. 2016 May;26(5):1338-47.
125. Nijssen EC, Rennenberg RJ, Nelemans PJ, Essers BA, Janssen MM, Vermeeren MA, et al. Prophylactic hydration to protect renal function from intravascular iodinated contrast material in patients at high risk of contrast-induced nephropathy (AMACING): a prospective, randomised, phase 3, controlled, open-label, non-inferiority trial. Lancet. 2017 Apr 1;389(10076):1312-22.
126. Lee L, Ito T, Jensen RT. Imaging of pancreatic neuroendocrine tumors: recent advances, current status, and controversies. Expert Rev Anticancer Ther. 2018 Sep;18(9):837-60.
127. Law JK, Singh VK, Khashab MA, Hruban RH, Canto MI, Shin EJ, et al. Endoscopic ultrasound (EUS)-guided fiducial placement allows localization of small neuroendocrine tumors during parenchymal-sparing pancreatic surgery. Surg Endosc. 2013 Oct;27(10):3921-6.
128. Elias D, Lefevre JH, Duvillard P, Goere D, Dromain C, Dumont F, et al. Hepatic metastases from neuroendocrine tumors with a "thin slice" pathological examination: they are many more than you think. Ann Surg. 2010 Feb;251(2):307-10.
129. Werner RA, Lapa C, Ilhan H, Higuchi T, Buck AK, Lehner S, et al. Survival prediction in patients undergoing radionuclide therapy based on intratumoral somatostatin-receptor heterogeneity. Oncotarget. 2017 Jan 24;8(4):7039-49.
130. Werner RA, Ilhan H, Lehner S, Papp L, Zsoter N, Schatka I, et al. Correction to: Pre-therapy Somatostatin Receptor-Based Heterogeneity Predicts Overall Survival in Pancreatic Neuroendocrine Tumor Patients Undergoing Peptide Receptor Radionuclide Therapy. Mol Imaging Biol. 2018 Dec;20(6):1068.
131. Staal FCR, Aalbersberg EA, van der Velden D, Wilthagen EA, Tesselaar MET, Beets-Tan RGH, et al. GEP-NET radiomics: a systematic review and radiomics quality score assessment. Eur Radiol. 2022 Oct;32(10):7278-94.

132. Eriksson B, Arnberg H, Oberg K, Hellman U, Lundqvist G, Wernstedt C, et al. Chromogranins--new sensitive markers for neuroendocrine tumors. Acta Oncol. 1989;28(3):325-9.
133. Sanduleanu S, De Bruine A, Stridsberg M, Jonkers D, Biemond I, Hameeteman W, et al. Serum chromogranin A as a screening test for gastric enterochromaffin-like cell hyperplasia during acid-suppressive therapy. Eur J Clin Invest. 2001 Sep;31(9):802-11.
134. Molina R, Alvarez E, Aniel-Quiroga A, Borque M, Candas B, Leon A, et al. Evaluation of chromogranin A determined by three different procedures in patients with benign diseases, neuroendocrine tumors and other malignancies. Tumour Biol. 2011 Feb;32(1):13-22.
135. Marotta V, Zatelli MC, Sciammarella C, Ambrosio MR, Bondanelli M, Colao A, et al. Chromogranin A as circulating marker for diagnosis and management of neuroendocrine neoplasms: more flaws than fame. Endocr Relat Cancer. 2018 Jan;25(1):R11-R29.
136. Gut P, Czarnywojtek A, Fischbach J, Baczyk M, Ziemnicka K, Wrotkowska E, et al. Chromogranin A - unspecific neuroendocrine marker. Clinical utility and potential diagnostic pitfalls. Arch Med Sci. 2016 Feb 1;12(1):1-9.
137. Malczewska A, Kos-Kudla B, Kidd M, Drozdov I, Bodei L, Matar S, et al. The clinical applications of a multigene liquid biopsy (NETest) in neuroendocrine tumors. Adv Med Sci. 2020 Mar;65(1):18-29.
138. Bodei L, Kidd M, Modlin IM, Prasad V, Severi S, Ambrosini V, et al. Gene transcript analysis blood values correlate with (6)(8)Ga-DOTA-somatostatin analog (SSA) PET/CT imaging in neuroendocrine tumors and can define disease status. Eur J Nucl Med Mol Imaging. 2015 Aug;42(9):1341-52.
139. Malczewska A, Oberg K, Kos-Kudla B. NETest is superior to chromogranin A in neuroendocrine neoplasia: a prospective ENETS CoE analysis. Endocr Connect. 2021 Jan;10(1):110-23.
140. Bodei L, Kidd MS, Singh A, van der Zwan WA, Severi S, Drozdov IA, et al. PRRT neuroendocrine tumor response monitored using circulating transcript analysis: the NETest. Eur J Nucl Med Mol Imaging. 2020 Apr;47(4):895-906.
141. Saghafinia S, Homicsko K, Di Domenico A, Wullschleger S, Perren A, Marinoni I, et al. Cancer Cells Retrace a Stepwise Differentiation Program during Malignant Progression. Cancer Discov. 2021 Oct;11(10):2638-57.
142. Janson ET, Knigge U, Dam G, Federspiel B, Gronbaek H, Stalberg P, et al. Nordic guidelines 2021 for diagnosis and treatment of gastroenteropancreatic neuroendocrine neoplasms. Acta Oncol. 2021 Jul;60(7):931-41.
143. Pastorino L, Grillo F, Albertelli M, Ghiorzo P, Bruno W. Insights into Mechanisms of Tumorigenesis in Neuroendocrine Neoplasms. Int J Mol Sci. 2021 Sep 25;22(19).

144. Gerdes J, Schwab U, Lemke H, Stein H. Production of a mouse monoclonal antibody reactive with a human nuclear antigen associated with cell proliferation. Int J Cancer. 1983 Jan 15;31(1):13-20.
145. Rindi G, Kloppel G, Couvelard A, Komminoth P, Korner M, Lopes JM, et al. TNM staging of midgut and hindgut (neuro) endocrine tumors: a consensus proposal including a grading system. Virchows Arch. 2007 Oct;451(4):757-62.
146. Eriksson J, Stalberg P, Nilsson A, Krause J, Lundberg C, Skogseid B, et al. Surgery and radiofrequency ablation for treatment of liver metastases from midgut and foregut carcinoids and endocrine pancreatic tumors. World J Surg. 2008 May;32(5):930-8.
147. Norlen O, Stalberg P, Zedenius J, Hellman P. Outcome after resection and radiofrequency ablation of liver metastases from small intestinal neuroendocrine tumours. Br J Surg. 2013 Oct;100(11):1505-14.
148. Sarmiento JM, Panneton JM, Nagorney DM. Reconstruction of the hepatic artery using the gastroduodenal artery. Am J Surg. 2003 Apr;185(4):386-7.
149. D'Souza D, Golzarian J, Young S. Interventional Liver-Directed Therapy for Neuroendocrine Metastases: Current Status and Future Directions. Curr Treat Options Oncol. 2020 May 23;21(6):52.
150. Wong LCK, Li Z, Fan Q, Tan JW, Tan QX, Wong JSM, et al. Cytoreductive surgery (CRS) with hyperthermic intraperitoneal chemotherapy (HIPEC) in peritoneal sarcomatosis-A systematic review and meta-analysis. Eur J Surg Oncol. 2022 Mar;48(3):640-48.
151. Barbier CE, Garske-Roman U, Sandstrom M, Nyman R, Granberg D. Selective internal radiation therapy in patients with progressive neuroendocrine liver metastases. Eur J Nucl Med Mol Imaging. 2016 Jul;43(8):1425-31.
152. Limouris GS, Poulantzas V, Trompoukis N, Karfis I, Chondrogiannis S, Triantafyllou N, et al. Comparison of 111In-[DTPA0]Octreotide Versus Non Carrier Added 177Lu- [DOTA0,Tyr3]-Octreotate Efficacy in Patients With GEP-NET Treated Intra-arterially for Liver Metastases. Clin Nucl Med. 2016 Mar;41(3):194-200.
153. Kvols LK, Moertel CG, O'Connell MJ, Schutt AJ, Rubin J, Hahn RG. Treatment of the malignant carcinoid syndrome. Evaluation of a long-acting somatostatin analogue. N Engl J Med. 1986 Sep 11;315(11):663-6.
154. Oberg K, Norheim I, Theodorsson E. Treatment of malignant midgut carcinoid tumours with a long-acting somatostatin analogue octreotide. Acta Oncol. 1991;30(4):503-7.
155. Rinke A, Wittenberg M, Schade-Brittinger C, Aminossadati B, Ronicke E, Gress TM, et al. Placebo-Controlled, Double-Blind, Prospective, Randomized Study on the Effect of Octreotide LAR in the Control of Tumor Growth in Patients with Metastatic

Neuroendocrine Midgut Tumors (PROMID): Results of Long-Term Survival. Neuroendocrinology. 2017;104(1):26-32.
156. Chandrasekharan C. Medical Management of Gastroenteropancreatic Neuroendocrine Tumors. Surg Oncol Clin N Am. 2020 Apr;29(2):293-316.
157. Pavel M, Baudin E, Couvelard A, Krenning E, Oberg K, Steinmuller T, et al. ENETS Consensus Guidelines for the management of patients with liver and other distant metastases from neuroendocrine neoplasms of foregut, midgut, hindgut, and unknown primary. Neuroendocrinology. 2012;95(2):157-76.
158. Oberg K, Funa K, Alm G. Effects of leukocyte interferon on clinical symptoms and hormone levels in patients with mid-gut carcinoid tumors and carcinoid syndrome. N Engl J Med. 1983 Jul 21;309(3):129-33.
159. Detjen KM, Welzel M, Farwig K, Brembeck FH, Kaiser A, Riecken EO, et al. Molecular mechanism of interferon alfa-mediated growth inhibition in human neuroendocrine tumor cells. Gastroenterology. 2000 Apr;118(4):735-48.
160. Rosewicz S, Detjen K, Scholz A, von Marschall Z. Interferon-alpha: regulatory effects on cell cycle and angiogenesis. Neuroendocrinology. 2004;80 Suppl 1:85-93.
161. Pavel ME, Baum U, Hahn EG, Schuppan D, Lohmann T. Efficacy and tolerability of pegylated IFN-alpha in patients with neuroendocrine gastroenteropancreatic carcinomas. J Interferon Cytokine Res. 2006 Jan;26(1):8-13.
162. Schmidt C, Bloomston M, Shah MH. Well-differentiated neuroendocrine tumors: a review covering basic principles to loco-regional and targeted therapies. Oncogene. 2011 Mar 31;30(13):1497-505.
163. Rinke A, Muller HH, Schade-Brittinger C, Klose KJ, Barth P, Wied M, et al. Placebo-controlled, double-blind, prospective, randomized study on the effect of octreotide LAR in the control of tumor growth in patients with metastatic neuroendocrine midgut tumors: a report from the PROMID Study Group. J Clin Oncol. 2009 Oct 01;27(28):4656-63.
164. Caplin ME, Pavel M, Ruszniewski P. Lanreotide in metastatic enteropancreatic neuroendocrine tumors. N Engl J Med. 2014 Oct 16;371(16):1556-7.
165. Hall MN. An Amazing Turn of Events. Cell. 2017 Sep 21;171(1):18-22.
166. Zoncu R, Efeyan A, Sabatini DM. mTOR: from growth signal integration to cancer, diabetes and ageing. Nat Rev Mol Cell Biol. 2011 Jan;12(1):21-35.

167. Thomas GV, Tran C, Mellinghoff IK, Welsbie DS, Chan E, Fueger B, et al. Hypoxia-inducible factor determines sensitivity to inhibitors of mTOR in kidney cancer. Nat Med. 2006 Jan;12(1):122-7.
168. Yao JC, Phan AT, Chang DZ, Wolff RA, Hess K, Gupta S, et al. Efficacy of RAD001 (everolimus) and octreotide LAR in advanced low- to intermediate-grade neuroendocrine tumors: results of a phase II study. J Clin Oncol. 2008 Sep 10;26(26):4311-8.
169. Pietras K, Hanahan D. A multitargeted, metronomic, and maximum-tolerated dose "chemo-switch" regimen is antiangiogenic, producing objective responses and survival benefit in a mouse model of cancer. J Clin Oncol. 2005 Feb 10;23(5):939-52.
170. Raymond E, Dahan L, Raoul JL, Bang YJ, Borbath I, Lombard-Bohas C, et al. Sunitinib malate for the treatment of pancreatic neuroendocrine tumors. N Engl J Med. 2011 Feb 10;364(6):501-13.
171. Albertelli M, Dotto A, Nista F, Veresani A, Patti L, Gay S, et al. "Present and future of immunotherapy in Neuroendocrine Tumors". Rev Endocr Metab Disord. 2021 Sep;22(3):615-36.
172. Murray D, McEwan AJ. Radiobiology of systemic radiation therapy. Cancer Biother Radiopharm. 2007 Feb;22(1):1-23.
173. Desai S, Kobayashi A, Konishi T, Oikawa M, Pandey BN. Damaging and protective bystander cross-talk between human lung cancer and normal cells after proton microbeam irradiation. Mutat Res. 2014 May-Jun;763-764:39-44.
174. Saintigny Y, Roche S, Meynard D, Lopez BS. Homologous recombination is involved in the repair response of mammalian cells to low doses of tritium. Radiat Res. 2008 Aug;170(2):172-83.
175. Saintigny Y, Chevalier F, Bravard A, Dardillac E, Laurent D, Hem S, et al. A threshold of endogenous stress is required to engage cellular response to protect against mutagenesis. Sci Rep. 2016 Jul 11;6:29412.
176. Kumar C, Shetake N, Desai S, Kumar A, Samuel G, Pandey BN. Relevance of radiobiological concepts in radionuclide therapy of cancer. Int J Radiat Biol. 2016;92(4):173-86.
177. Howell RW. Radiation spectra for Auger-electron emitting radionuclides: report No. 2 of AAPM Nuclear Medicine Task Group No. 6. Med Phys. 1992 Nov-Dec;19(6):1371-83.
178. Krenning EP, Kooij PP, Bakker WH, Breeman WA, Postema PT, Kwekkeboom DJ, et al. Radiotherapy with a radiolabeled somatostatin analogue, [111In-DTPA-D-Phe1]-octreotide. A case history. Ann N Y Acad Sci. 1994 Sep 15;733:496-506.
179. de Jong M, Bakker WH, Krenning EP, Breeman WA, van der Pluijm ME, Bernard BF, et al. Yttrium-90 and indium-111 labelling, receptor binding and biodistribution of [DOTA0,d-Phe1,Tyr3]octreotide, a promising somatostatin analogue for radionuclide therapy. Eur J Nucl Med. 1997 Apr;24(4):368-71.

180. Bander NH, Milowsky MI, Nanus DM, Kostakoglu L, Vallabhajosula S, Goldsmith SJ. Phase I trial of 177lutetium-labeled J591, a monoclonal antibody to prostate-specific membrane antigen, in patients with androgen-independent prostate cancer. J Clin Oncol. 2005 Jul 20;23(21):4591-601.
181. Song H, Du Y, Sgouros G, Prideaux A, Frey E, Wahl RL. Therapeutic potential of 90Y- and 131I-labeled anti-CD20 monoclonal antibody in treating non-Hodgkin's lymphoma with pulmonary involvement: a Monte Carlo-based dosimetric analysis. J Nucl Med. 2007 Jan;48(1):150-7.
182. de Jong M, Breeman WA, Bakker WH, Kooij PP, Bernard BF, Hofland LJ, et al. Comparison of (111)In-labeled somatostatin analogues for tumor scintigraphy and radionuclide therapy. Cancer Res. 1998 Feb 1;58(3):437-41.
183. Reubi JC, Schar JC, Waser B, Wenger S, Heppeler A, Schmitt JS, et al. Affinity profiles for human somatostatin receptor subtypes SST1-SST5 of somatostatin radiotracers selected for scintigraphic and radiotherapeutic use. Eur J Nucl Med. 2000 Mar;27(3):273-82.
184. Forrer F, Uusijarvi H, Storch D, Maecke HR, Mueller-Brand J. Treatment with 177Lu-DOTATOC of patients with relapse of neuroendocrine tumors after treatment with 90Y-DOTATOC. J Nucl Med. 2005 Aug;46(8):1310-6.
185. Storch D, Behe M, Walter MA, Chen J, Powell P, Mikolajczak R, et al. Evaluation of [99mTc/EDDA/HYNIC0]octreotide derivatives compared with [111In-DOTA0,Tyr3, Thr8]octreotide and [111In-DTPA0]octreotide: does tumor or pancreas uptake correlate with the rate of internalization? J Nucl Med. 2005 Sep;46(9):1561-9.
186. Hammond PJ, Wade AF, Gwilliam ME, Peters AM, Myers MJ, Gilbey SG, et al. Amino acid infusion blocks renal tubular uptake of an indium-labelled somatostatin analogue. Br J Cancer. 1993 Jun;67(6):1437-9.
187. Janson ET, Westlin JE, Ohrvall U, Oberg K, Lukinius A. Nuclear localization of 111In after intravenous injection of [111In-DTPA-D-Phe1]-octreotide in patients with neuroendocrine tumors. J Nucl Med. 2000 Sep;41(9):1514-8.
188. Lubberink M, Wilking H, Ost A, Ilan E, Sandstrom M, Andersson C, et al. In Vivo Instability of (177)Lu-DOTATATE During Peptide Receptor Radionuclide Therapy. J Nucl Med. 2020 Sep;61(9):1337-40.
189. Kwekkeboom DJ, Teunissen JJ, Bakker WH, Kooij PP, de Herder WW, Feelders RA, et al. Radiolabeled somatostatin analog [177Lu-DOTA0,Tyr3]octreotate in patients with endocrine gastroenteropancreatic tumors. J Clin Oncol. 2005 Apr 20;23(12):2754-62.

190. Strosberg J, El-Haddad G, Wolin E, Hendifar A, Yao J, Chasen B, et al. Phase 3 Trial of (177)Lu-Dotatate for Midgut Neuroendocrine Tumors. N Engl J Med. 2017 Jan 12;376(2):125-35.
191. Baum RP, Kulkarni HR, Singh A, Kaemmerer D, Mueller D, Prasad V, et al. Results and adverse events of personalized peptide receptor radionuclide therapy with (90)Yttrium and (177)Lutetium in 1048 patients with neuroendocrine neoplasms. Oncotarget. 2018 Mar 30;9(24):16932-50.
192. Kunikowska J, Pawlak D, Bak MI, Kos-Kudla B, Mikolajczak R, Krolicki L. Long-term results and tolerability of tandem peptide receptor radionuclide therapy with (90)Y/(177)Lu-DOTATATE in neuroendocrine tumors with respect to the primary location: a 10-year study. Ann Nucl Med. 2017 Jun;31(5):347-56.
193. Bodei L, Kidd M, Paganelli G, Grana CM, Drozdov I, Cremonesi M, et al. Long-term tolerability of PRRT in 807 patients with neuroendocrine tumours: the value and limitations of clinical factors. Eur J Nucl Med Mol Imaging. 2015 Jan;42(1):5-19.
194. Cives M, Pelle E, Strosberg J. Emerging Treatment Options for Gastroenteropancreatic Neuroendocrine Tumors. J Clin Med. 2020 Nov 13;9(11).
195. Wild D, Fani M, Behe M, Brink I, Rivier JE, Reubi JC, et al. First clinical evidence that imaging with somatostatin receptor antagonists is feasible. J Nucl Med. 2011 Sep;52(9):1412-7.
196. Nicolas GP, Schreiter N, Kaul F, Uiters J, Bouterfa H, Kaufmann J, et al. Sensitivity Comparison of (68)Ga-OPS202 and (68)Ga-DOTATOC PET/CT in Patients with Gastroenteropancreatic Neuroendocrine Tumors: A Prospective Phase II Imaging Study. J Nucl Med. 2018 Jun;59(6):915-21.
197. Sandstrom M, Garske U, Granberg D, Sundin A, Lundqvist H. Individualized dosimetry in patients undergoing therapy with (177)Lu-DOTA-D-Phe (1)-Tyr (3)-octreotate. Eur J Nucl Med Mol Imaging. 2010 Feb;37(2):212-25.
198. Emami B, Lyman J, Brown A, Coia L, Goitein M, Munzenrider JE, et al. Tolerance of normal tissue to therapeutic irradiation. Int J Radiat Oncol Biol Phys. 1991 May 15;21(1):109-22.
199. Benua RS, Cicale NR, Sonenberg M, Rawson RW. The relation of radioiodine dosimetry to results and complications in the treatment of metastatic thyroid cancer. Am J Roentgenol Radium Ther Nucl Med. 1962 Jan;87:171-82.
200. Sundlov A, Sjogreen-Gleisner K, Svensson J, Ljungberg M, Olsson T, Bernhardt P, et al. Individualised (177)Lu-DOTATATE treatment of neuroendocrine tumours based on kidney dosimetry. Eur J Nucl Med Mol Imaging. 2017 Aug;44(9):1480-89.
201. Sandstrom M, Garske-Roman U, Granberg D, Johansson S, Widstrom C, Eriksson B, et al. Individualized dosimetry of kidney and bone

marrow in patients undergoing 177Lu-DOTA-octreotate treatment. J Nucl Med. 2013 Jan;54(1):33-41.
202. Hicks RJ, Kwekkeboom DJ, Krenning E, Bodei L, Grozinsky-Glasberg S, Arnold R, et al. ENETS Consensus Guidelines for the Standards of Care in Neuroendocrine Neoplasia: Peptide Receptor Radionuclide Therapy with Radiolabeled Somatostatin Analogues. Neuroendocrinology. 2017;105(3):295-309.
203. Galne A, Almquist H, Almquist M, Hindorf C, Ohlsson T, Nordenstrom E, et al. A Prospective Observational Study to Evaluate the Effects of Long-Acting Somatostatin Analogs on (68)Ga-DOTATATE Uptake in Patients with Neuroendocrine Tumors. J Nucl Med. 2019 Dec;60(12):1717-23.
204. Miller AB, Hoogstraten B, Staquet M, Winkler A. Reporting results of cancer treatment. Cancer. 1981 Jan 1;47(1):207-14.
205. Therasse P, Arbuck SG, Eisenhauer EA, Wanders J, Kaplan RS, Rubinstein L, et al. New guidelines to evaluate the response to treatment in solid tumors. European Organization for Research and Treatment of Cancer, National Cancer Institute of the United States, National Cancer Institute of Canada. J Natl Cancer Inst. 2000 Feb 2;92(3):205-16.
206. Eisenhauer EA, Therasse P, Bogaerts J, Schwartz LH, Sargent D, Ford R, et al. New response evaluation criteria in solid tumours: revised RECIST guideline (version 1.1). Eur J Cancer. 2009 Jan;45(2):228-47.
207. Forner A, Ayuso C, Varela M, Rimola J, Hessheimer AJ, de Lope CR, et al. Evaluation of tumor response after locoregional therapies in hepatocellular carcinoma: are response evaluation criteria in solid tumors reliable? Cancer. 2009 Feb 1;115(3):616-23.
208. Sundin A, Rockall A. Therapeutic monitoring of gastroenteropancreatic neuroendocrine tumors: the challenges ahead. Neuroendocrinology. 2012;96(4):261-71.
209. Choi H. Response evaluation of gastrointestinal stromal tumors. Oncologist. 2008;13 Suppl 2:4-7.
210. Wahl RL, Jacene H, Kasamon Y, Lodge MA. From RECIST to PERCIST: Evolving Considerations for PET response criteria in solid tumors. J Nucl Med. 2009 May;50 Suppl 1:122S-50S.
211. Meignan M, Gallamini A, Meignan M, Gallamini A, Haioun C. Report on the First International Workshop on Interim-PET-Scan in Lymphoma. Leuk Lymphoma. 2009 Aug;50(8):1257-60.
212. Oksuz MO, Winter L, Pfannenberg C, Reischl G, Mussig K, Bares R, et al. Peptide receptor radionuclide therapy of neuroendocrine tumors with (90)Y-DOTATOC: is treatment response predictable by pre-therapeutic uptake of (68)Ga-DOTATOC? Diagn Interv Imaging. 2014 Mar;95(3):289-300.

213. Strigari L, Konijnenberg M, Chiesa C, Bardies M, Du Y, Gleisner KS, et al. The evidence base for the use of internal dosimetry in the clinical practice of molecular radiotherapy. Eur J Nucl Med Mol Imaging. 2014 Oct;41(10):1976-88.
214. Gabriel M, Oberauer A, Dobrozemsky G, Decristoforo C, Putzer D, Kendler D, et al. 68Ga-DOTA-Tyr3-octreotide PET for assessing response to somatostatin-receptor-mediated radionuclide therapy. J Nucl Med. 2009 Sep;50(9):1427-34.
215. Haug AR, Auernhammer CJ, Wangler B, Schmidt GP, Uebleis C, Goke B, et al. 68Ga-DOTATATE PET/CT for the early prediction of response to somatostatin receptor-mediated radionuclide therapy in patients with well-differentiated neuroendocrine tumors. J Nucl Med. 2010 Sep;51(9):1349-56.
216. Chan DL, Pavlakis N, Schembri GP, Bernard EJ, Hsiao E, Hayes A, et al. Dual Somatostatin Receptor/FDG PET/CT Imaging in Metastatic Neuroendocrine Tumours: Proposal for a Novel Grading Scheme with Prognostic Significance. Theranostics. 2017;7(5):1149-58.
217. Titan AL, Norton JA, Fisher AT, Foster DS, Harris EJ, Worhunsky DJ, et al. Evaluation of Outcomes Following Surgery for Locally Advanced Pancreatic Neuroendocrine Tumors. JAMA Netw Open. 2020 Nov 2;3(11):e2024318.
218. Kwekkeboom DJ, Mueller-Brand J, Paganelli G, Anthony LB, Pauwels S, Kvols LK, et al. Overview of results of peptide receptor radionuclide therapy with 3 radiolabeled somatostatin analogs. J Nucl Med. 2005 Jan;46 Suppl 1:62S-6S.
219. Imhof A, Brunner P, Marincek N, Briel M, Schindler C, Rasch H, et al. Response, survival, and long-term toxicity after therapy with the radiolabeled somatostatin analogue [90Y-DOTA]-TOC in metastasized neuroendocrine cancers. J Clin Oncol. 2011 Jun 10;29(17):2416-23.
220. Ilan E, Sandstrom M, Wassberg C, Sundin A, Garske-Roman U, Eriksson B, et al. Dose response of pancreatic neuroendocrine tumors treated with peptide receptor radionuclide therapy using 177Lu-DOTATATE. J Nucl Med. 2015 Feb;56(2):177-82.
221. Breeman WA, Kwekkeboom DJ, Kooij PP, Bakker WH, Hofland LJ, Visser TJ, et al. Effect of dose and specific activity on tissue distribution of indium-111-pentetreotide in rats. J Nucl Med. 1995 Apr;36(4):623-7.
222. Marion-Audibert AM, Barel C, Gouysse G, Dumortier J, Pilleul F, Pourreyron C, et al. Low microvessel density is an unfavorable histoprognostic factor in pancreatic endocrine tumors. Gastroenterology. 2003 Oct;125(4):1094-104.
223. Takahashi Y, Akishima-Fukasawa Y, Kobayashi N, Sano T, Kosuge T, Nimura Y, et al. Prognostic value of tumor architecture, tumor-

associated vascular characteristics, and expression of angiogenic molecules in pancreatic endocrine tumors. Clin Cancer Res. 2007 Jan 1;13(1):187-96.
224. Wan C, Sun Y, Tian Y, Lu L, Dai X, Meng J, et al. Irradiated tumor cell-derived microparticles mediate tumor eradication via cell killing and immune reprogramming. Sci Adv. 2020 Mar;6(13):eaay9789.
225. Pfeifer AK, Gregersen T, Gronbaek H, Hansen CP, Muller-Brand J, Herskind Bruun K, et al. Peptide receptor radionuclide therapy with Y-DOTATOC and (177)Lu-DOTATOC in advanced neuroendocrine tumors: results from a Danish cohort treated in Switzerland. Neuroendocrinology. 2011;93(3):189-96.
226. Sabet A, Dautzenberg K, Haslerud T, Aouf A, Sabet A, Simon B, et al. Specific efficacy of peptide receptor radionuclide therapy with (177)Lu-octreotate in advanced neuroendocrine tumours of the small intestine. Eur J Nucl Med Mol Imaging. 2015 Jul;42(8):1238-46.
227. Schuchardt C, Kulkarni HR, Prasad V, Zachert C, Muller D, Baum RP. The Bad Berka dose protocol: comparative results of dosimetry in peptide receptor radionuclide therapy using (177)Lu-DOTATATE, (177)Lu-DOTANOC, and (177)Lu-DOTATOC. Recent Results Cancer Res. 2013;194:519-36.

Acta Universitatis Upsaliensis

Digital Comprehensive Summaries of Uppsala Dissertations from the Faculty of Medicine 1903

Editor: The Dean of the Faculty of Medicine

A doctoral dissertation from the Faculty of Medicine, Uppsala University, is usually a summary of a number of papers. A few copies of the complete dissertation are kept at major Swedish research libraries, while the summary alone is distributed internationally through the series Digital Comprehensive Summaries of Uppsala Dissertations from the Faculty of Medicine. (Prior to January, 2005, the series was published under the title "Comprehensive Summaries of Uppsala Dissertations from the Faculty of Medicine".)

Distribution: publications.uu.se
urn:nbn:se:uu:diva-492855

ACTA
UNIVERSITATIS
UPSALIENSIS
UPPSALA
2023